

B 1
R 8

Physics

Cole Memorial Library

MONTHLY NOTICES
OF THE
ROYAL ASTRONOMICAL SOCIETY

Volume 118 No. 1 1958



B 1
8

Published and Sold by the
ROYAL ASTRONOMICAL SOCIETY
BURLINGTON HOUSE
LONDON, W.1

Price £1 os. od.; in U.S.A. \$3

Annual Subscription for volume of six numbers: £5 5s. od. ; in U.S.A. \$16

ROYAL ASTRONOMICAL SOCIETY

Founded 1820

*A new international journal for the publication of
current geophysical research*

The

Geophysical Journal

of the

Royal Astronomical Society

Editors:

A. H. COOK, M.A., Ph.D.,
T. F. GASKELL, M.A., Ph.D.

The first part of Volume I, published in March 1958, contains the following new papers:

J. F. Evernden, Finite strain theory and the Earth's interior

K. E. Bullen and **T. N. Burke-Gaffney**, Diffracted seismic waves near the PKP caustic

A. H. Cook, The calibration of gravity meters by comparison with pendulums

H. M. Iyer, A study on the direction of arrival of microseisms at Kew Observatory

Leon Knopoff, Energy release in earthquakes

T. Obayashi and **J. A. Jacobs**, Geomagnetic pulsations and the Earth's outer atmosphere

E. Irving and **G. Green**, Polar movement relative to Australia

A. S. Merriweather, A seismic refraction shooting survey off the north coast of Cornwall

Harold Jeffreys, A modification of Lomnitz's law of creep in rocks

There are also reports on the proceedings of the Eleventh General Assembly of the International Union of Geodesy and Geophysics, held at Toronto in September, 1957.

Price (post free): £1 per part (\$3 in U.S.A.). Annual subscription for a volume of at least four parts, £3 (\$9 in U.S.A.).

Orders should be addressed to:

THE ASSISTANT SECRETARY

Royal Astronomical Society, Burlington House, London, W.1

MONTHLY NOTICES
OF THE
ROYAL ASTRONOMICAL SOCIETY

Vol. 118 No. 1

MEETING OF 1958 JANUARY 10

Dr W. H. Steavenson, President, in the Chair

The President announced that the Council had awarded the Gold Medal of the Society to Professor André Danjon for his contributions to astronomical photometry, to fundamental astronomy, and to the design of astronomical instruments.

The President announced that the Council had awarded the Eddington Medal to Professor H. W. Babcock for his work on the magnetic fields of early-type stars and of the Sun.

The election by the Council of the following Fellows was duly confirmed :—

George Eric Deacon Alcock, 55 Broadway, Farcet, Peterborough, Northants (proposed by G. Merton);

Hubert Roland Cooper, 118 Boness Road, Grangemouth, Stirlingshire (proposed by W. H. Marshall);

*Eric G. Forbes, Osservatorio Astrofisico, Firenze, Italy (proposed by G. Abetti);

David John Mercer, Carwoola Street, Bardon, Brisbane, Australia (proposed by D. J. Mercer);

Lloyd Motz, 815 West 181st Street, New York, U.S.A. (proposed by F. Benario);

James H. Parry, Physics Department, King's College, Newcastle-upon-Tyne (proposed by S. K. Runcorn);

Felix Arnold Edward Pirani, King's College, Strand, London, W.C.2 (proposed by B. Pagel);

*Richard Edward Small, 153 Rosebery Avenue, Manor Park, London, E.12 (proposed by C. W. Allen);

*Philip Henry Vince, 17 Stanley Hill Avenue, Amersham, Bucks. (proposed by A. W. Vince);

Gerald Thomas Webdale, 9 Northfield Avenue, Wells, Norfolk (proposed by S. K. Runcorn); and

Terence Woodhead, Guild of Undergraduates, 2 Bedford Street, Liverpool, 7 (proposed by A. Fletcher).

* Transferring from Junior Membership.

The election by the Council of the following Junior Members was duly confirmed :—

Frank Hedley Flinn, 25 Woodside Avenue, Beaconsfield, Bucks. (proposed by C. W. Allen);

John Sidney Griffith, 22 Vyne Road, Basingstoke, Hants. (proposed by C. W. Allen);

Ann Veronica Matthews, 11 Lake View, Edgware, Middx. (proposed by M. W. Ovenden); and
John William Owen, 21 Chambers Street, Crewe, Cheshire (proposed by F. Holden).

Fifty-nine presents were announced as having been received since the last meeting, including :—

R. H. Brown and A. C. B. Lovell : *The exploration of space by radio* (presented by the authors); and
W. Ley : *Rockets, missiles and space travel* (presented by Chapman & Hall Ltd).

ON THE QUANTITATIVE ANALYSIS OF STELLAR SPECTRA

*George Darwin Lecture delivered by Professor Albrecht Unsöld on
1957 November 8*

In a stellar spectrum we can measure the equivalent widths W_λ and in favourable cases also the profiles of the Fraunhofer lines as well as the energy distribution of the continuous spectrum. From these data we want to determine as far as possible the chemical composition of the star's atmosphere and the quantities determining its physical constitution. For the plane parallel static atmosphere—which for a long time was treated almost exclusively—these are the effective temperature T_e (giving by definition the correct total energy flux at the surface of the star $\pi F = \sigma T_e^4$) and the surface gravity g [cm sec^{-2}].

Until not so long ago it seemed legitimate to assume that all stellar atmospheres had practically the same chemical composition and that the two parameters T_e and g or spectral type and absolute magnitude completely determined the constitution of a star. However, more and more detailed analysis of stellar spectra revealed rotation of the stars, turbulence in their atmospheres, magnetic fields, shells and other features; so that, while the majority of stars indeed exhibit an almost surprising uniformity of chemical composition, we are quite sure nowadays that there are others with different abundances of the elements. The connection between these extra parameters, anomalies of chemical composition, the great problems of cosmogony and nuclear processes in the stars is still far from known. So it appears most desirable to have methods for analysing each star as an individual, i.e. to determine the composition *and* constitution of its atmosphere *directly* from spectroscopic (and eventually other) observations.

It is clear from the beginning that corresponding to the great diversity of stellar spectra our methods must be extremely flexible. Their general philosophy is essentially that of my famous countryman, Baron v. Münchhausen, who, the story tells, succeeded in pulling himself out of a swamp by his own pigtail! Mathematically speaking, we follow a procedure of successive approximations, beginning with rather crude assumptions and replacing these one by one, as far as the available observations allow, by more refined ones. Indeed the refinement of theory should always go hand in hand with the improvement of observation; otherwise we are very likely to thresh chaff.

The simplest useful approach to quantitative stellar spectroscopy is probably still the so-called "coarse analysis"—the "Grobanalyse", as we call it in German. I will not enter into the lengthy disputes about the relative merits of that method and the "method of curves of growth" and similar problems of "Weltanschauung", but simply deal with the application of theoretical common sense to stellar atmospheres.

Assuming—to begin with—grey radiative equilibrium, the temperature T as a function of the optical depth $\bar{\tau}$ for the Rosseland opacity $\bar{\kappa}$ (referring to total radiation) is given by

$$T^4 = \frac{3}{4} T_e^4 (\bar{\tau} + q(\bar{\tau})), \quad (1)$$

where the effective temperature T_e is connected with the total energy flux per cm^2 by the definition $\pi F = \sigma T_e^4$ and $q(\bar{\tau})$ is a well known function $\approx 2/3$. Besides

equation (1) we use the hydrostatic equation in a form connecting the gas pressure P_g with the optical depth $\bar{\tau}$:

$$\frac{dP_g}{d\bar{\tau}} = \frac{g}{\bar{\kappa}(P_g, T)} \quad (2)$$

where g , as already mentioned, is the surface gravity of our star. Now we make the assumption that within the layers of our atmosphere, which are essential for producing the spectrum, we can use constant average values for the temperature T , the gas pressure P_g , the electron pressure P_e (connected with P_g and T for a given mixture of elements by the theory of ionization), the opacity $\bar{\kappa}$ and its relation to the continuous absorption coefficient κ for a small wave-length range near λ . Integration of (2) then leads at once to

$$\bar{\kappa}(P_g, T) \cdot P_g = g \cdot \bar{\tau}, \quad (3)$$

which in connection with (1) determines T , P_e , P_g etc. for a given effective depth $\bar{\tau} = \bar{\tau}_0$.

The latter is determined by the theory of Fraunhofer lines or simply by asking how far we can look down into the atmosphere for a given wave-length region. The answer is, of course, essentially the same whether we use the theory of weight functions, Strömgren's average values or the Eddington-Barbier approximation.

For weak lines or the wings of strong lines the "centre of gravity" of the atmosphere is near an optical depth for the continuous spectrum $\tau_0 \approx 2/3$ or

$$\bar{\tau}_0 = \tau_0 \cdot \frac{\bar{\kappa}}{\kappa} = \frac{2}{3} \cdot \frac{\bar{\kappa}}{\kappa}$$

and all the atoms in the proper state of ionization and excitation down to optical depth τ_0 absorb corresponding to an average weight factor

$$\sim \left(\frac{d \ln B_\lambda}{d\tau} \right)_{\tau_0},$$

where $B_\lambda(\tau)$ means the Kirchhoff-Planck function. All these considerations presume that neither the excitation and ionization of the considered atoms nor the Kirchhoff-Planck function $B_\lambda(\tau)$ exhibit too violent and especially non-linear changes with τ . For a linear $B_\lambda \sim 1 + \beta\tau$ the above weight factor is simply $1/(1 + \frac{2}{3}\beta)$, changing quite slowly with β , so that within not too large ranges of wave-length it can even be considered as constant.

Within the frame of the approximations developed so far a stellar atmosphere with given T_e , g and chemical composition can be described by an average temperature T and pressure P_e respectively, P_g depending slightly on the wave-length region λ . The absorption lines are determined by an effective layer with a total number \overline{NH} of (all kinds of) atoms in a column of 1 cm^2 cross section.

Calculation of line profiles or equivalent widths is quite obvious for weak absorption. For stronger lines one uses just as easily the well known interpolatory approximation of the theory of line formation or the "general" curves of growth based on it.

The basic computations for atmospheres of the well known "standard composition" have been made in 1951 by Vitense*. The following graphs (taken from her paper) give $\log P_g$, $\log P_e$, and $\log \overline{NH}$ as functions of $\Theta_e = 5040/T_e$ and $\log g$ for the photographic region $\lambda \sim 4250 \text{ \AA}$. The \overline{NH} are indicated also for the red region $\lambda \sim 6380$; due to the increase of the continuous absorption coefficient they

* Vitense, E., *Zs. f. Astrophys.*, **29**, 73, 1951.

are there generally smaller than in the blue, in agreement with general spectroscopic experience. The accuracy of these calculations should of course not be overestimated but I think they are still quite useful for our orientation in the realm of stellar spectra.

One might ask: why should we still use these rather crude methods, having learned since how to treat the same problems much more accurately? There are two reasons. On the one hand we will see presently that *really* better accuracy can be obtained only by *simultaneously* introducing considerable refinements in *several* directions, so that already the analysis of a single spectrum becomes quite a lengthy procedure. On the other hand, general conclusions as well as new ideas will seldom be obtained by long and purely numerical methods. Here, too, more flexible, though somewhat less accurate, approximations are probably superior.

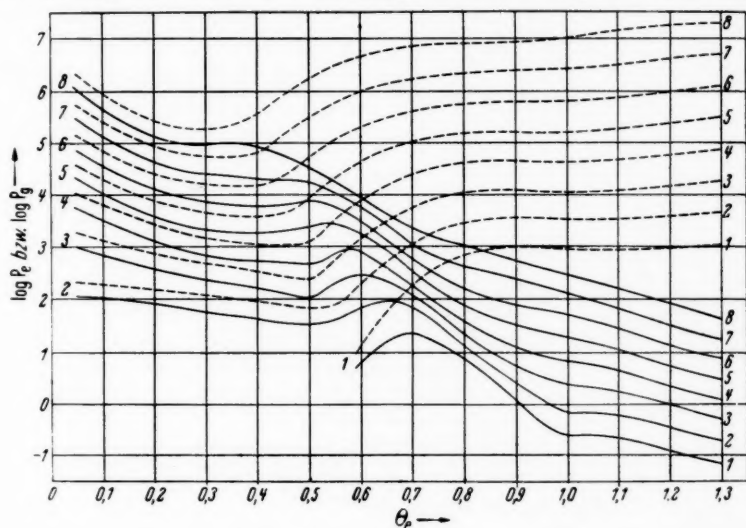


FIG. 1.— $\log P_g$ (---) and $\log P_e$ (—) as functions of $\theta_e = \frac{5040}{T_e}$ with $\log g$ as parameter. $\lambda = 4250 \text{ \AA}$.

As an example let me sketch the solution—in the sense of coarse analysis—of a problem which occurred to me in connection with my recent work at Mt Wilson and Lick Observatories: “How would the spectrum of a star be changed if the abundance ratios of Hydrogen, H : Helium, He : Heavy elements, R, were changed in a certain way?” (We presume for the moment that the ratios of the heavy elements among each other should not be changed). All the laborious calculations on ionization, continuous absorption, etc., have so far been made only for the well known standard mixture. Of course we might go to an electronic computer for just repeating these computations with different data. But upon entering we read the well known laconic sign: “Think!”. And we remember that the most difficult parts of our proposed task, namely the calculation of κ_ν and $\bar{\kappa}$ per gram of hydrogen, as well as the ionization of the heavy elements, remain the same as long as the continuous absorption is chiefly due to the atoms and negative ions of hydrogen and as long as we keep the *temperature* T and the *electron pressure* P_e constant.

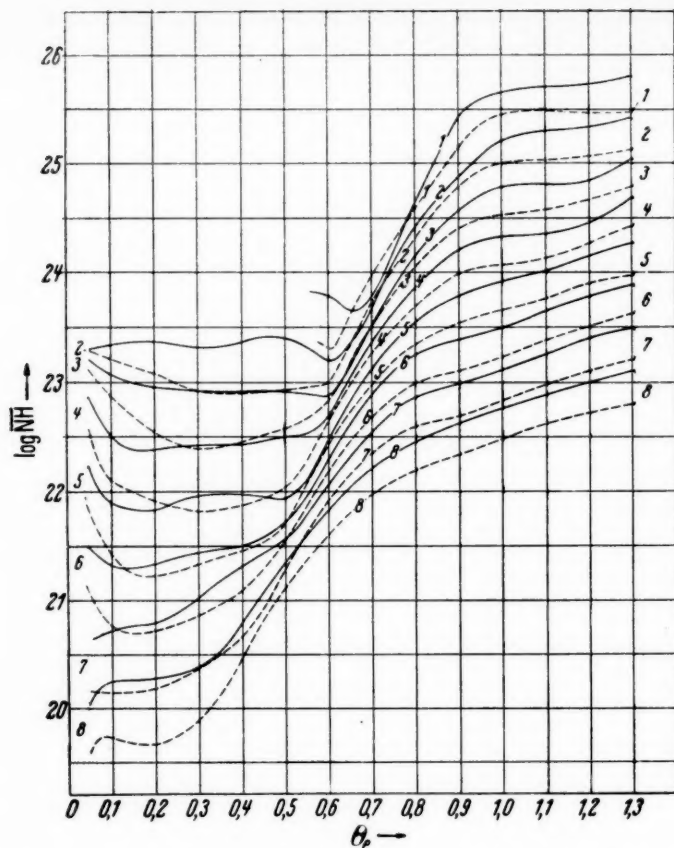


FIG. 2.—The effective number of absorbing atoms \overline{NH} as a function of $\theta_e = \frac{5040}{T_e}$ for $\lambda = 4250 \text{ A}$ (—) and $\lambda = 6380 \text{ A}$ (---) with $\log g_e$ as parameter.

Our trick will therefore be to compare stellar atmospheres with the same average values of the temperature T and the electron pressure P_e , but different $\text{H} : \text{He} : \text{R}$. The old and new ratios of gas pressure P_g to electron pressure P_e can be connected easily by applying Saha's formula just to H and eventually He. Then we can compare the densities and the absorption coefficients per gram matter (of whatever kind) and ask: how must we change the surface gravitation g of the star to obtain the old P_e for the same T_e with the new composition? And then we can write down straight away the change of the numbers of hydrogen, helium or heavy atoms in a 1 cm^2 column through the atmosphere.

As you know, some *subdwarfs* have been supposed by Chamberlain and Aller* to be stars with a particularly large abundance of hydrogen relative to the heavy elements (nothing being known so far about helium). Let us compare theoretically such a metal-deficient star with a normal star of the same temperature, but a surface gravity g changed in the calculated ratio. The result of our quite simple

* Chamberlain, J. W. and L. H. Aller, *Ap. J.*, **114**, 52, 1951.

calculations depends on whether the free electrons in the atmosphere originate mostly from hydrogen or from the heavy elements. In the first case (hotter stars), the hydrogen lines should remain unchanged, while the number NH of the metallic atoms above 1 cm^2 should decrease, roughly corresponding to their abundance. The changes in g , P_g , etc., should be only minor features. That picture might provide an explanation of spectra like HD 140283 on which Chamberlain and Aller did their pioneer work and which we are studying at present in detail, using a set of Mt Wilson Coudé plates. On the cooler stars (beginning about in the K's) the number of the absorbing atoms is still the same for hydrogen and reduced in the way described for the metals. But since free electrons now come only from the metals, the gas pressure (i.e. essentially the pressure of neutral hydrogen atoms) increases roughly in the same ratio as the effective number of metallic atoms decreases. So we should expect that the *faint* metallic lines on the linear part of the curve of growth are again considerably weakened. The equivalent widths of the *strong* metallic lines however depend on the number of atoms *times* the damping constant. The former behaves as before. The latter is mainly due to collisions with neutral hydrogen atoms and therefore proportional to the hydrogen pressure. So these strong lines should remain almost unchanged. A more detailed discussion should pay attention also to g -effects; these somewhat complicated matters however must be reserved for a special paper.

Dr A. H. Joy* kindly allowed me to compare under the Hartmann comparator some of his fine spectra of early M subdwarfs with corresponding main sequence dwarfs. The strong metallic lines, chiefly Fe I (all the lines which can be seen with the low dispersion used must be located on the damping branch of the curve of growth), do not exhibit any recognizable difference between subdwarfs and main sequence stars. In connection with our theoretical remarks, that does *not* imply that the ratio H:R is the same in both; it *could* indeed be just as different in the later spectral types!

Returning to more general problems we should now discuss the accuracy and possible pitfalls of the "coarse analysis" procedure. But we do that better in connection with the more progressive, but also much more complicated, "detailed analysis" of stellar spectra.

Our first problems will be of a deductive kind. We imagine a stellar atmosphere of given T_e , g and chemical composition (having obtained approximative values, e.g., from a coarse analysis). First we have to calculate the temperature T and the pressure as functions of the optical depth $\bar{\tau}$ for the total radiation or τ_λ for some particular wave-length. It has become customary in this connection to speak of "model atmospheres" although the term "model" originally had a rather different meaning in physics as well as astrophysics. In connection with the theory of the continuous spectrum as well as of the Fraunhofer lines it is essential to know T accurately for optical depths about 0.1 to 1.0; in some cases also smaller or larger depths are important. A good idea about the relative importance of the different $T(\tau)$ is obtained by plotting T not over τ itself but over a $3K_4(\tau) \approx e^{-\tau\sqrt{3}}$ scale which presents the whole atmosphere in the finite range between 0 and 1. Such a presentation exhibits at once the relative advantages or errors of using, for example, an average temperature T , a "grey" model with an average absorption coefficient for calculating $T(\tau)$, or a detailed "non-grey" model in which the variation of the absorption coefficient with wave-length and depth is taken into account.

* Joy, A. H., *Ap. J.*, 105, 96, 1947.

As an example we take an atmosphere with $T_e = 37\,450^\circ\text{K}$, $\log g = 4.45$, corresponding closely—according to Traving*—to the O9 V star 10 Lacertae:

Optical depth $\bar{\tau}$		0	0.1	0.5	1.0		
$e^{-\tau\sqrt{3}}$		1	0.84	0.42	0.18		
		$^{\circ}\text{K}$	$^{\circ}\text{K}$	$^{\circ}\text{K}$	$^{\circ}\text{K}$		
Radiative equilibrium temperature	{	grey, exact	30 400	32 200	36 300	39 800	
		non-grey, continuum only	27 700	33 500	39 800	43 500	
		non-grey, incl. Lyman lines	17 900	(difference disappears near $\tau \approx 0.01$).			

While the mean value and the range of temperatures between, for example, $\bar{\tau} = 0.1$ and 1.0 are $38\,500^\circ\text{K} \pm 5000^\circ\text{K}$, the difference between the non-grey model (for which these temperatures hold) and the exact grey model at $\bar{\tau} = 0.5$ is 3500°K . It is evident that a grey model offers very little advantage compared with a calculation using constant average values, where moreover the errors introduced by neglecting the variations both of temperature and pressure largely tend to cancel. Using a model atmosphere at all makes sense in general only if one computes at once a non-grey model with every possible refinement. That, by the way, is the reason why we have hesitated a long time in using model atmospheres.

If we are interested not only in the radiative transfer in general and the temperature distribution produced thereby but also in the continuous or line spectrum of certain wave-length regions, we must establish the relation between the τ_λ 's and our previously used $\bar{\tau}$. For illustration we note here at least the $\bar{\tau}$'s corresponding to the "centre of gravity" of the atmosphere $\tau_\lambda = 2/3$ for a few selected wave-lengths:

λ	6050	4340	3650+	Balmer limit	3650-	3300 A
$\bar{\tau}$	0.13	0.23	0.31		0.17	0.21

In the early-type stars, the essential "non-grey" features are connected with the jumps of κ , at the Lyman- and/or Balmer-limit of hydrogen. Only in connection with the central intensities of the hydrogen lines G. Traving noticed recently that for $\bar{\tau} < 0.01$ the radiation of the Lyman lines depresses the temperature in his late O star by fully $10\,000^\circ\text{K}$.

As an application of our model atmospheres, Fig. 3 shows the calculated energy distribution in the continuous spectrum of 10 Lac and a few other early-type stars. It emphasizes again how strongly these curves deviate from the black body distribution and how minute is the range of wave-lengths in which we are observing nowadays.

Since the calculation of non-grey models can—so far—be done only by successive numerical approximation and since these procedures are rather lengthy it is important to begin with a good, but not too clumsy, zero approximation. Following earlier work by Chandrasekhar on the blanketing effect in the solar atmosphere Hunger and Traving† have recently developed analytical formulae under the moderately schematic assumptions that the continuous absorption coefficient and the Kirchhoff-Planck function can both be split into one function depending on

* Traving, G., *Zs. f. Astrophys.*, **41**, 215, 1957.

† Hunger, K. and G. Traving, *Zs. f. Astrophys.*, **39**, 248, 1956.

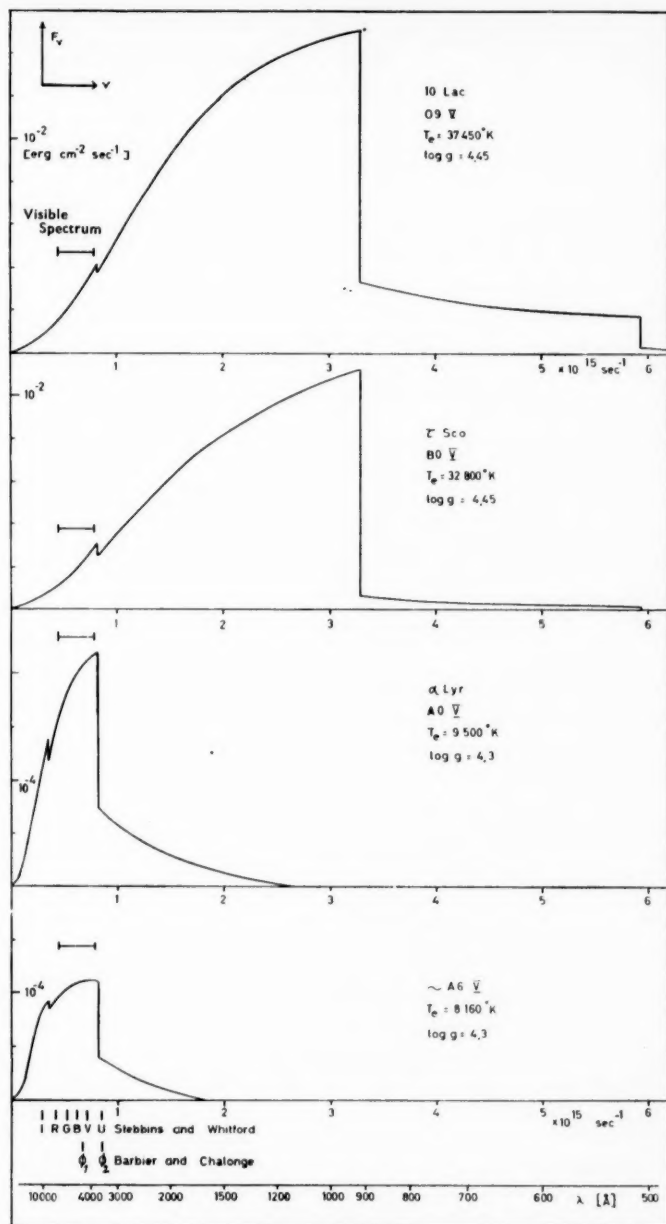


FIG. 3.—Calculated energy distributions.

the optical depth τ only *times* another function depending on wave-length or frequency only. Then they introduce, besides the well known Rosseland opacity, averaging $1/\kappa_\nu$, two more average values, $\bar{\kappa}_\nu$ and $\overline{1/\kappa_\nu^2}$, which emphasize the "peaks" and "holes" respectively of the continuous absorption coefficient. The zero approximation to the temperature distribution $T(\tau)$, which one obtains that way and which is in general already quite fair, is further checked and improved by applying combinations of the so called Λ - and flux-iteration procedures until the total energy flux as a function of depth is sufficiently constant. It should be remembered in this connection that—especially near the surface of an atmosphere—quite small changes in flux correspond to large changes in temperature.

Turning our attention toward the later type stars (so far only the Sun has been studied in some detail) the continuous absorption coefficient as a function of wave-length runs more smoothly, but here the many strong lines become important also in respect of the energy transfer and, what is much worse, we must take into account *convection*.

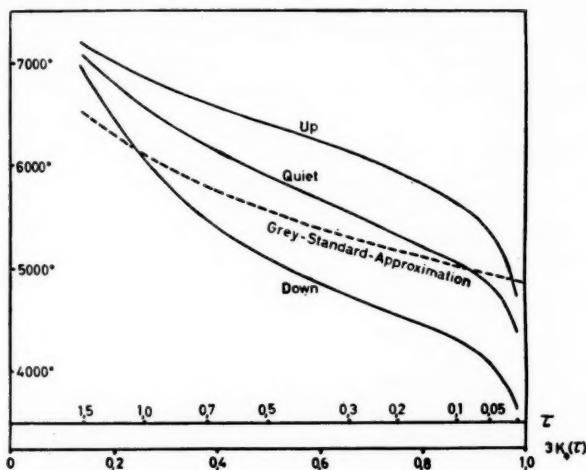


FIG. 4.—Grey model and Böhm's three-flux model of the solar atmosphere.

Theoretical studies* in agreement with modern photometric and spectroscopic observations of the solar granulation show that we have horizontal temperature differences of the order of $\pm 600^\circ\text{K}$. One can roughly incorporate these features into a model by dividing schematically the atmosphere into hot rising, cool down-going and also intermediate quiescent columns. Plotting, just for illustration, Böhm's† three-flux model over the rational $3K_4(\tau)$ scale (τ for 4050Å), and comparing it with the standard grey approximation, we notice that in many respects the drawbacks of taking a well-chosen average temperature relative to a homogeneous model are not much worse than those of the homogeneous relative to an inhomogeneous solar model! Recent studies by Adam, Voigt‡ and Schröter§ permit us to expect that such inhomogeneous models lead to an understanding of the asymmetry and the much-debated limb effect of solar lines. As

* Vitense, E., *Zs. f. Astrophys.*, **32**, 135, 1953.

† Böhm, K. H., *Zs. f. Astrophys.*, **35**, 179, 1954.

‡ H. H. Voigt, *Zs. f. Astrophys.*, **40**, 157, 1956.

§ E. H. Schröter, *Zs. f. Astrophys.*, **41**, 141, 1957.

to the detailed connection between motions and temperature differences, on the one hand in the photosphere and on the other hand in the higher layers of the chromosphere, much remains to be done. Concerning the theoretical aspects of that problem one should have in mind that the usual, I might say "militaristic", theory of shock waves is a rather poor guide to the magnetohydrodynamic plasma phenomena in an atmosphere where with strong density and temperature gradients. From the observational side, work on Fraunhofer lines and their centre-limb variation, as well as chromospheric observations with and without eclipse, looks quite hopeful.

In concluding my remarks on model atmospheres I should note that we know from observation at least two important phenomena which, as far as I know, we still do not understand at all. The one is the strong turbulence in early-type supergiant atmospheres where convective energy transfer should be altogether unimportant. The other is the mode of energy transfer e.g. in solar faculae which brings considerable amounts of energy into high layers of the atmosphere without affecting the deeper ones. The same mechanism seems to be at work in solar flares and in late-type stars, especially flare stars, T Tauri stars, etc.

Our next important topic, the calculation of *line profiles* or *equivalent widths* for a given atmosphere, can be treated briefly. For most lines atomic theory and astrophysical observation show plainly that the assumption of local thermodynamic equilibrium or true absorption—in Schwarzschild's terminology—satisfies every reasonable requirement. Concerning special investigations on the mode of radiative transfer in selected lines of simple atomic origin I am inclined to presume that at present the quantum theoretical treatment of the atomic problems is considerably safer than the required quite fine details of the atmospheric models. As to the method of actually calculating Fraunhofer lines we have mostly used the theory of weight functions for the "weak absorption" part of the line, the simple theory of central intensities for the "strong absorption" part, and interpolated in between using the well known formula essentially proposed first by Minnaert; and the "general" theory of the curve of growth. The possible errors of that procedure would certainly be much exaggerated by cutting off e.g. a "damping" line at depths of say 50 per cent or 20 per cent just horizontally or vertically. The equivalent widths W_λ which we would get then, instead of 100, are

Line profile cut off	at a depth of	
	50 per cent	20 per cent
vertically	114	157
horizontally	82	55

Systematic plus accidental errors of rather a similar order of magnitude seem to occur not infrequently in the literature!

It is obvious that concerning the interpretation of actual observations little is gained by using calculations, which have been made *mathematically* exact, for highly schematic models (e.g. M.E.-Model with linear Kirchhoff-Planck function etc.).

Aiming at higher accuracy one can use, with some slight restrictions, either Pecker's generalized curves of growth or—probably not much more complicated and free from any restrictions—just straightforward numerical quadrature. The fundamental formulae are, as you know, quite simple and the somewhat tedious computing will be taken over more and more by electronic machines. As to programming problems I would like to refer to the work done in Göttingen, Paris, Indiana, Michigan and other universities.

Quite recently Traving* has compared critically the work done on our old friend τ Scorpii, using coarse analysis by Unsöld, the standard curve of growth by Traving† and Pecker's generalized curves in connection with a slightly modified Traving model by Aller, Elste and Jugaku‡. Apart from systematic differences of the measurements, which as you know are still one of the most neuralgic points in stellar spectrophotometry, two generally important points came to light: (1) in former determinations of g , using "coarse analysis", I had not paid sufficient attention to the fact that, while all atoms contribute to the *weight* of a 1 cm^2 -column through the atmosphere, the atoms in the deeper layers contribute much less to the formation of the *Fraunhofer lines* than those of the higher layers. Consequently all the formerly determined g 's are systematically too large; and (2) the lines of high stages of ionization, like O III, originate almost wholly in rather deep layers, below $\tau_0 \approx 0.6$. So even an infinitely strong O III line could reach a central depth R_c only considerably smaller than e.g. a very strong O II line. That difference in the limiting central depths was taken into account automatically in the calculations of the Michigan group. It could and should have been introduced also using the standard curve of growth by shifting it in the 45-degree direction thus giving rise to a slight systematic change in the ionization equilibria.

But I should add a few words on the analysis of this or that individual star. All our information on it is contained in the more or less lengthy tape of a microphotometer record. In order to be able to determine the composition of the stellar atmosphere we must know also T_e and g . The temperature especially enters very delicately into the Boltzmann and Saha equations. We select different criteria—ionization ratios or quantities pertaining to hydrogen only—which are practically independent of the abundances but strongly dependent on either T_e or g . The straightforward method of finding a model fitting all these observational criteria by calculating a whole array of models with different T_e and g 's would be extremely lengthy. Having *one* good model which "hits" fairly well, it will mostly be just as accurate and much simpler to use *differentially* calculations following the much simpler procedure of coarse analysis. In some parts of the *Hertzsprung-Russell* diagram it is however quite difficult to find suitable criteria. Our problem of determining T_e and g is of course equivalent to that of two-dimensional spectral classification: the two pairs of (T_e , g) and (spectral-type, luminosity-class) are simply different coordinates covering the H.R. diagram. And it is well known that in certain parts of the H.R. diagram also the usual methods of spectroscopic parallaxes meet with essential difficulties.

I have mentioned already that two parameters are certainly not sufficient in all cases for labelling a star completely. The quantitative analysis of spectral peculiarities connected with population, age, etc., in rational terms will be one of the next important steps in the development of stellar spectroscopy. I hope however to have made clear also that even the most ordinary kinds of stellar spectra still demand much work and should by no means be neglected.

At present almost every spectrum which one analyses carefully brings some new surprise and we are still far from having anything like hard and fast methods that could be just applied more or less mechanically.

* Traving, G., *Zs. f. Astrophys.*, **44**, 142, 1958.

† Traving, G., *Zs. f. Astrophys.*, **36**, 1, 1955.

‡ Aller, L. H., G. Elste and J. Jugaku, *Ap. J. Suppl.*, Ser. No. 25, 1957.

What has been achieved so far? And what can we hope to achieve in the near future? This is not the place to collect tables on the chemical composition of stellar atmospheres. As to forming such average values I feel warned by Russell's well known story about the large pancake that was completely spoiled by just one bad egg that had not been examined individually! Within the present accuracy (very roughly $\Delta \log N \sim \pm 0.3$), which is still hampered by errors of measurement (especially systematic ones) as well as interpretation (transition probabilities, collision cross sections, accuracy of model atmospheres, etc.), we can say that among "ordinary" stars (main sequence, giants and super-giants earlier than $\sim K_5$) no significant differences in composition have been found. Quite a different type of investigation seems to show that also the planetary nebulae consist of the same material. On the other hand the so called helium stars, like HD 160 641, have almost certainly transformed most of their hydrogen into helium. Aller's preliminary analysis of HD 160 641 is at least compatible with the idea that the heavier elements have not been affected in the nuclear reactor of the star. There are a lot of other spectral peculiarities, some of which have been interpreted with more or less confidence as differences in chemical composition caused by some sort of nuclear processes. I should mention the differences in the isotopic ratio $C^{12}:C^{13}$, which are empirically well established. Then there are considerable differences between the various sequences of late type stars; a quantitative analysis of these molecular features would certainly require a great deal of preliminary work on normal and earlier type stars. But are the strong rare earth lines of the peculiar (magnetic) A stars really due to differences in composition? Also in the solar chromosphere the rare earth lines show very strange features (emphasized, e.g. by Menzel) which we cannot interpret, probably because our basic knowledge of the spectra, especially the second spark spectra, is very limited. And how about the too weak Ca II lines of the metallic line stars, which almost certainly are *not* due to differences in abundance, but which have so far defied explanation?

There are more and more indications that stars of the galactic halo, especially the aforementioned subdwarfs, have a ratio of metals to hydrogen smaller than the "normal stars" in the disk and the spiral arms of our galaxy. Hoyle, as you know, has attempted to explain this by the assumption that the heavy elements have been produced, at least partly, in connection with the evolution of succeeding generations of stars in the galaxy. Another possibility, indicated by M. Schwarzschild and R. Wildt, might be that hydrogen and heavy elements have been separated locally in the galaxy by more harmless physico-chemical processes. However that may be, it is quite clear that the quantitative analysis of stellar spectra will be a powerful tool for disentangling some of the most fundamental problems of stellar evolution. But that is not all. Two fundamental quantities of a star are its effective temperature and its bolometric magnitude. Both refer to the total energy flux and both can therefore not be measured directly because the Earth's atmosphere is transparent only within rather limited spectral ranges. Here again we can apply the "analytical boring machine" and at least for some types of stars these quantities and their relation to the directly measured colour temperatures and to the Fraunhofer spectra is, I think, fairly well known. On the other hand, recent work by Chalonge and his associates on the strange break in some stellar energy curves near $H\beta$ came just in time to prevent theorists from becoming too self-contented!

Also, in the permanent interaction between observation and theory which characterizes the modern development of stellar spectroscopy, the most fruitful attitude certainly is just:

"Quicquid nitet notandum".

ROCK CREEP, TIDAL FRICTION AND THE MOON'S ELLIPTICITIES

Harold Jeffreys

(Received 1957 November 25)

Summary

A law of creep under long continued stress proposed by C. Lomnitz makes the displacement in time t increase like $\log(at)$ with a constant. It is found that this rule does not account simultaneously for the sharpness of seismic pulses and the damping of the variation of latitude, but they can be accounted for by a law that makes the creep in time t proportional to $t^{0.17}$. The modified law accounts easily for the rotations of Mercury and the satellites of the Earth and Mars. It is consistent with the existence of the Moon's excess ellipticities.

In my recent papers (Jeffreys 1957*a, b*) on tidal friction I assumed a law of elastic afterworking such that a constant stress applied at $t = 0$ gives an initial elastic strain, but when it is maintained for a long time the strain increases asymptotically to a new constant value. The evidence for the inner planets and their satellites indicated that the limiting value is approached in a few weeks.

The law adopted was chosen mainly for simplicity and because it accounted for the more obvious features of the behaviour. However, many experimenters have claimed that the strain under small constant stress increases like $t^{1/3}$ or $\log t$, or some more complicated function. These rules were implausible as general statements since they would make the initial rate of strain infinite. C. Lomnitz (1956, 1957) has pointed out that this difficulty can be easily avoided, and proposes the law

$$\epsilon = \frac{P}{\mu} \{1 + q \log(1 + at)\} \quad (1)$$

when ϵ is the strain, P the stress, μ the rigidity, and q, a are positive constants. This gives satisfactory behaviour at $t = 0$. Experiments on rocks give values of q from 0.001 to 0.010. a is of the order of 1000 cycles/sec $\div 6 \times 10^3$ /sec. This is interesting because it implies heavy damping at audible frequencies and explains why most rocks do not ring when struck (phonolite and to some extent quartzites being exceptions).

I take the rather more general form

$$\epsilon = \frac{P}{\mu} \left[1 + \frac{q}{\alpha} \{(1 + at)^\alpha - 1\} \right] \quad (2)$$

which approximates to (1) for α small and at large and would give the $t^{1/3}$ law for $\alpha = \frac{1}{3}$.

Under variable stress, if the principle of superposition is applicable,

$$\begin{aligned} \epsilon &= \frac{1}{\mu} \int_{\tau=-\infty}^t \left[1 + \frac{q}{\alpha} \{(1 + a(t-\tau))^\alpha - 1\} \right] dP(\tau) \\ &= \frac{P}{\mu} + \frac{qa}{\mu} \int_{-\infty}^t P(\tau) \{1 + a(t-\tau)\}^{\alpha-1} d\tau. \end{aligned} \quad (3)$$

If $P(t) = \exp(i\gamma t)$ the integral is an incomplete factorial function, and the harmonic part after a long time is

$$\epsilon = \frac{e^{i\gamma t}}{\mu} + \frac{q}{\mu} \left(\frac{a}{\gamma}\right)^{\alpha} e^{i\gamma(t+1/\alpha)} \int_{\gamma/a}^{\infty} e^{-i\zeta} \zeta^{\alpha-1} d\zeta. \quad (4)$$

Since γ/a is small in our applications we can use the convergent expansion for the integral

$$\int_x^{\infty} e^{-i\zeta} \zeta^{\alpha-1} d\zeta = \frac{e^{-i\alpha\pi} \alpha! - x^{\alpha}}{\alpha} + \frac{1}{2! (\alpha+2)} x^{\alpha+2} - \frac{1}{4! (\alpha+4)} x^{\alpha+4} + \dots \\ + i \left(\frac{x^{\alpha+1}}{1! (\alpha+1)} - \frac{x^{\alpha+3}}{3! (\alpha+3)} + \dots \right) \quad (5)$$

and neglect all positive powers of x . Then

$$\epsilon \doteq \frac{1}{\mu} e^{i\gamma t} \left[1 + q \left(\frac{a}{\gamma}\right)^{\alpha} \left(\frac{e^{-i\alpha\pi} \alpha! - (\gamma/a)^{\alpha}}{\alpha} \right) \right]. \quad (6)$$

We are concerned chiefly with the lag η , which is approximately

$$\eta = \frac{1}{2} \pi \alpha! q \left(\frac{a}{\gamma}\right)^{\alpha}. \quad (7)$$

In Lomnitz's case ($\alpha=0$) this reduces to $\frac{1}{2} \pi q$; so long as γ/a is small the lag is almost independent of the period.

In the problems of the present paper the relevant constants are α and qa^2 ; we do not need separate determinations of q and a .

From the variation of latitude the lag for a period of 430 days is about $1/40$. We have further information from the sharpness of seismic pulses.

μ is effectively replaced by $\mu e^{i\eta}$; the form of a plane wave is

$$\exp(i\kappa x - i\kappa \beta t e^{i\eta}). \quad (8)$$

Write $\cos \frac{1}{2} \eta = c$, $\sin \frac{1}{2} \eta = s$; then a unit pulse would be modified to

$$\frac{1}{2} + \frac{1}{\pi} \int_0^{\infty} \sin \kappa (\beta t - cx) e^{-\kappa sx} \frac{d\kappa}{\kappa}, \quad (9)$$

which is equal to

$$\frac{1}{2} + \frac{1}{\pi} \tan^{-1} \frac{\beta t - cx}{sx}. \quad (10)$$

It rises from $\frac{1}{4}$ to $\frac{3}{4}$ when $\beta t - cx$ passes from $-sx$ to $+sx$. A unit pulse is therefore blunted, the scale of the blunting (in time) being given by $2sx/\beta$ or $2st$. Now if the lag was $1/40$ this would imply that a pulse taking 20 minutes to travel, as for S at about 80° , would be spread out over half a minute and be unreadable. If we take, as is reasonable, the spreading as having a scale of 2 seconds the lag must be about $1/600$ for periods near 6^s . This leads to the equation

$$\left[\frac{430^d}{6^s} \right]^{\alpha} = 15 \quad (11)$$

whence $\alpha = 0.17$ nearly, and $qa^2 = \frac{1}{40 \cdot \frac{1}{2} \pi \alpha!} \left(\frac{2\pi}{430^d} \right)^{\alpha}$.

The variation of latitude data can therefore be reconciled with the seismic ones by taking the creep under long-continued stress to increase like $t^{0.17}$, which is about midway between the logarithmic law and $t^{1/3}$.

With this value, at 430^d period, the amplitude is increased by about 10 per cent compared with that for perfect elasticity. This happens to agree with that for "short scale" elastic afterworking. This would be acceptable since the comparison between the observed and calculated periods of the variation of latitude is uncertain by about 10 per cent of the elastic effect.

For the logarithmic case, the magnification given by (6) approximates to

$$\frac{1}{\mu} e^{i\gamma t} \left[1 + q \left(\log \frac{a}{\gamma} - C \right) \right] \quad (12)$$

where C is Euler's constant. With $\frac{1}{2}\pi q = \frac{1}{40}$ and $a = 10^3$ cycles/sec the term in q is about 0.4. This would probably make the calculated period too long.

The following table gives some calculated lags. The first set is from (7); the second for elastic afterworking with $\tau = 17.0^d$, $\tau' = 18.7^d$; the third for elastic afterworking with $\tau = 251^d$, $\tau' = 276^d$. All are adjusted to make the lag 0.025 for a period of 430 days. The present law gives greater lag and therefore more damping than either of the previous ones, except for periods about 100^d for the short scale and about 1000^d for the long scale, and even there it is of the same order of magnitude. Since the smaller values of τ and τ' led to adequate tidal friction to account for the rotations of the smaller bodies there is no doubt that the present law is adequate.

Period (days)	(1)	(2)	(3)
0.25	0.0075	0.00022	0.000001
0.5	0.080	0.0044	0.00003
1	0.089	0.0088	0.00006
10	0.132	0.085	0.0058
100	0.196	0.450	0.057
1000	0.289	0.102	0.423
10000	0.428	0.0102	0.154
100000	0.634	0.0010	0.016
1000000	0.0939	0.00001	0.00016

The effect on the mean distance of Phobos would be about 20 times what was found on the short time scale. It still remains, however, much too small to account for the observed secular acceleration of Phobos, and similar considerations apply to Deimos.

For the Moon a similar correction indicates that something of the order of 20 per cent of the secular acceleration may be due to bodily tidal friction. A constant lag of 0.025 in the tide, irrespective of period, would account for nearly the whole amount and leave nothing for friction in the ocean to do.

Generally speaking, Lomnitz's law of creep does not explain the damping of the variation of latitude and the damping of seismic waves simultaneously, but a slightly modified form does so. The modified form also accounts satisfactorily for the rotations of Mercury, the Moon, Phobos and Deimos.

Subsidence of a surface inequality.—The initial conditions affect the subsidence to some extent. I take the problem in the form that a uniform incompressible gravitating sphere of radius b is loaded at time 0 with matter of equal density to a depth $b\epsilon_0 S_n$. The elastic displacement of the surface is then $b\epsilon_1 S_n$, where

$$\epsilon_1 \left(1 + \frac{nb\rho g}{(2n^2 + 4n + 3)\mu} \right) = - \frac{nb\rho g\epsilon_0}{(2n^2 + 4n + 3)\mu} \quad (13)$$

The total height of the surface above the mean sphere is then

$$b(\epsilon_0 + \epsilon_1)S_n.$$

We write

$$\epsilon_0 + \epsilon_1 = \epsilon'; \quad \frac{n}{2n^2 + 4n + 3} = N, \quad (14)$$

$$\{1 + Nb\rho g/\mu\}\epsilon' = \epsilon_0. \quad (15)$$

To adapt to creep we modify this to

$$\left(1 + \frac{Nb\rho g}{\mu}\right)\epsilon' + \frac{Nb\rho g}{\mu} \frac{q}{\alpha} \int_{\tau=0}^t \left[\left\{1 + a(t-\tau)\right\}^\alpha - 1\right] d\epsilon'(\tau) = \epsilon_0. \quad (16)$$

Since $a(t-\tau)$ is large, through most of the interval we can replace the integral by

$$\int_0^t a^\alpha (t-\tau)^\alpha d\epsilon'(\tau) = \frac{1}{p} a^\alpha \frac{\alpha!}{p^\alpha} p \bar{\epsilon}'(p) H(t) \quad (17)$$

where p is the Heaviside symbol and $\bar{\epsilon}'(p)H(t) = \epsilon'(t)$. Then

$$\epsilon' = \frac{\epsilon_0}{1 + \frac{Nb\rho g}{\mu} \left(1 + \frac{(\alpha-1)! q a^\alpha}{p^\alpha}\right)} H(t). \quad (18)$$

Expansion in negative powers of p gives a convergent expansion. For the Moon, with $n=2$, $Nb\rho g/\mu$ is about 0.01. If $t=10^8$ years,

$$q(\alpha-1)!(at)^\alpha \doteq 4.$$

Thus the second term will be about -0.04 of the first. Increasing t to 3×10^9 years gives about -0.07. Hence the changes of the Moon's ellipticities would have been small.

For very large t , ϵ' decreases like $t^{-\alpha}$, as is found by expanding in ascending powers of p . The leading term is

$$\epsilon' = \frac{\mu\epsilon_0}{Nb\rho g q(\alpha-1)! a^\alpha} p^\alpha H(t) = \frac{\mu\epsilon_0}{Nb\rho g q(\alpha-1)! (-\alpha)! (at)^\alpha}. \quad (19)$$

For the Moon this expansion is not required.

For the Earth, $Nb\rho g/\mu$ is about 0.3 for $n=2$. Thus the second term of the convergent expansion would be of the same order as the first for $t=10^8$ to 3×10^9 years. The terms of the expansion in negative powers of t will also decrease rather slowly, but the first will indicate an order of magnitude. We get $t=10^8$ years, $\epsilon' = 0.7\epsilon_0$; $t=3 \times 10^9$ years, $\epsilon' = 0.4\epsilon_0$. Thus a large fraction of the ellipticity of the equator and other low harmonics in the Earth's figure should have survived even if they were present originally.

For higher harmonics N is smaller and the flow accordingly less. The indications are therefore that no important part of isostatic adjustment can be attributed to linear creep, and fracture or flow near the elastic limit is presumably dominant.

160 Huntingdon Road,
Cambridge:
1957 November 4.

References

- H. Jeffreys 1957a, *M.N.*, **117**, 506-515.
H. Jeffreys 1957b, *M.N.*, **117**, 585-589.
C. Lomnitz 1956, *J. Geol.*, **64**, 473-9.
C. Lomnitz 1957, *J. Appl. Phys.*, **28**, 201-5.

THE PROFILES OF CHROMOSPHERIC $H\alpha$ AND D_3 FROM INTERFEROMETRIC OBSERVATIONS

S. V. M. Clube

(Communicated by the Director of the University Observatory, Oxford)

(Received 1957 November 8)

Summary

Five plates showing the chromospheric D_3 and $H\alpha$ lines as sets of interference fringes are analysed by Treanor's method (16). This reduction, for the lowest 3000 km in the chromosphere, gives a D_3 profile which shows no systematic change with height (intensities normalized) and an $H\alpha$ profile whose broadening decreases from 1.15 Å at 200 km to 0.795 Å at 3200 km. It is supposed therefore that the $H\alpha$ line is broadened in part by self-absorption, and a method of eliminating this is described. Assuming that the significant contributions to the $H\alpha$ and D_3 emissions come from the same regions in the chromosphere, it is deduced from a comparison of the resultant helium and hydrogen Doppler profiles that the turbulent velocity is about 16 km/sec and that, though the temperature cannot be accurately determined, it is probably higher than that of the photosphere.

Introduction.—Interest in the structure of the outermost layers of the Sun has led to considerable study of the chromosphere. This region, at one time observed only during eclipses (photography of the flash spectrum), is now the subject of 'out of eclipse' studies which, in spite of the difficulties of observation, are leading to a rapid accumulation of quantitative data.

Observations which have been at various times interpreted in support of either a low ($\sim 5000^\circ\text{C}$) or high temperature ($\sim 30\,000^\circ\text{C}$) in the chromosphere, are the high extension of the chromosphere, the emission of helium lines, and the great width of hydrogen and helium lines. There is a tendency however to prefer the hypothesis of a chromospheric temperature comparable to that of the photosphere, especially in view of the facts which suggest a lower temperature: the intensity of radio noise at $\lambda = 1\text{ cm}$; the ionization and excitation of metals; the intensity distribution in the Balmer continuum, and the Balmer discontinuity (see Van de Hulst (19)). Also, the theory of turbulence, as proposed by McCrea (7), has permitted a simple explanation of the high extension of the chromosphere, without recourse to the high temperature necessary to account for thermal support. This theory has not removed the difficulty in explaining the excitation of helium emission (Miyamoto has suggested that the He and He^+ lines are excited by coronal ultra-violet radiation (11)), though it can to a certain extent account for the observed widths of the hydrogen and helium lines. That there is still controversy over the temperature of the chromosphere, however, follows largely from the lack of precise observations of the hydrogen and helium lines and our ignorance of the physical processes giving rise to these lines.

In this paper the variation of the $H\alpha$ and D_3 emission line profiles with height in the chromosphere, are compared by a reduction and analysis of five plates taken out of eclipse by Dr Treanor. On these plates, the $H\alpha$ and D_3 lines appear as systems of interference fringes.

Section 1 of the paper describes the deduction of the chromospheric profiles; in Section 2, these are compared with other observations; and in Section 3, some calculations are made with a view to extracting values for turbulent velocity and kinetic temperature from the observations.

Section 1

1.1. *Chromospheric interferometry.*—Treanor's method of studying chromospheric line profiles is fully described in his investigation of the helium D_3 line (16). Here a summary of the method will suffice.

The optical arrangement for photographing the stronger emission lines of the chromosphere as systems of interference fringes was as follows: the 32 cm solar image produced by the Oxford 35 m telescope was formed on a screen containing a slot which passed light from a small region of the solar limb. A field lens, collimator, and ring lens system re-imaged this region on the slit, 0.02 mm in width, of a low dispersion spectrograph. By means of a guiding plate, it was arranged that the slit was tangential to the solar image while the base of the slit just contacted the limb. A Fabry-Perot etalon of high reflectivity and 0.5 mm spacer was placed between the collimator and ring lens, so producing a system of heterochromatic parabolic fringes at the focal plane of the spectrograph. These fringes were contributed to mostly by scattered photospheric light but also by the strongest chromospheric lines. (In Treanor's study of the D_3 line the plates were obtained with a 1 mm spacer. On these, successive orders overlapped considerably in the $H\alpha$ region so that separate profiles were not clearly distinguished. The etalon spacer of 0.5 mm used in conjunction with a slit width of 0.02 mm secures, however, a good separation of fringes at $H\alpha$ and D_3 .)

Besides the chromospheric interference spectrum, there was exposed on each plate:

- (1) an interference spectrum showing the $H\alpha$ line in absorption, taken at the centre of the Sun's disk;
- (2) an exposure of the solar centre through a calibrated rhodium-on-glass step wedge;
- (3) an exposure of the solar centre without the wedge to test for uniformity of illumination along the slit (exposure times were equalized by neutral filters to about 10 min); and
- (4) a cadmium lamp exposure superimposed on (3) which gave a set of sharp fringes serving as an adjustment check and as a means of calculating the centre of the fringe system (for the etalon was slightly tilted).

The following is a record of the plates taken and analysed in this paper:

TABLE I

Plate	Latitude of point of tangency	Date and time of exposure	Exposure time	Remarks
1956				
1	+20.4°	May 19.410	12 min	$H\alpha$
2	+44.8°	19.479	10	$H\alpha$ and D_3
3a	+3.0°	22.368	20	$H\alpha$ and D_3
3b	+14.1°	22.396	12	$H\alpha$ and D_3
4	+44.1°	22.480	5	$H\alpha$ and D_3 also $H\beta \rightarrow H10$.

2*

The fourth column records the lines suitable for measurement. It was eventually discovered that the H α and D $_3$ lines of plate 4 showed almost no intensity variation with height in the chromosphere. This, together with the appearance on the plate of further members of the Balmer series (up to H $_{10}$), suggested that a hot spot in the chromosphere was viewed and that the plate was exceptional.

Alongside the H α and D $_3$ fringes were then scratched by a dividing engine a series of marks 0.2 mm apart. Plate blackening for the profile and surrounding scatter intensity were found as a function of wave-length λ , and the chromospheric height h , by running the microphotometer (slit height = 0.35 Å approx.) across the fringe systems at and between each mark (i.e. at intervals of 0.1 mm) so that the profile blackening for each fringe was measured at some sixteen places. For the purposes of reduction, microphotometer traces were also obtained for the H α absorption interference pattern.

The programme for the reduction of the photometer traces to give real chromospheric profiles is described in Treanor's paper. Observed profiles for H α and D $_3$ were deduced according to this programme for the heights of 200, 800, 1400, 2000, 2600 and 3200 km in the chromosphere.

1.2. *Deduction of H α profile.*—It is found in non-eclipse observations that the H α profile displays a marked depression in the centre, especially for those profiles near to the solar limb (4, 5, 17), i.e. it has all the appearances of strong self-reversal. However, this depression can also be attributed to the superposition of the strong H α absorption line due to scattered photospheric light. Real chromospheric profiles can be deduced by the subtraction of the scattered absorption profile from the observed profiles:

$$I_c = I_0 - rI_s$$

where I_c = chromospheric intensity, I_0 = observed intensity, rI_s = residual intensity in the absorption profile and I_s = intensity of the scatter continuum in the region of H α . In this analysis an absorption profile for H α from the solar centre was deduced from the interference pattern and then, knowing the scatter intensity I_s corresponding to each observed chromospheric profile, real corresponding absorption profiles were constructed and the effect of the superposition of these on the chromospheric lines was eliminated by the above subtraction, to give the real chromospheric profiles.

de Jager (2) has shown that the H α absorption profile varies slightly across the solar disk, the central depression decreasing by about 6 per cent and the core becoming relatively less broad by about 10 per cent at the solar limb. It is clearly preferable to use a profile from the solar limb rather than the centre in the subtraction above but, in our analysis, such a variation gives rise to a change in the half-width of the chromospheric emission profile of < 0.02 Å and to a change in the central intensity of < 5 per cent. These relative differences in resultant profile do not alter its general appearance nor do they give rise to any significant difference in the measure of half-width (< 2 per cent). We are therefore justified in pursuing this analysis with a profile taken from the solar centre.

From the deduction of this profile in absorption we derive additional assurance as to the accuracy of the method, for the H α absorption profile compares favourably with the uncorrected profile in the Utrecht Atlas. In both cases

relatively high resolving power and great line width make the instrumental differences unimportant and the profiles are in substantial agreement (see Fig. 1).

In view of the known irregularities of the spicular structure of the chromosphere, considerable differences in profiles from plate to plate would not be remarkable, but since the chromospheric profiles now obtained displayed distinct similarities on four out of the five plates it was clearly meaningful to deduce 'mean profiles'. The exceptional one, plate 4, showing almost no intensity variation along the height of the chromosphere, was eliminated from this analysis. By normalizing all profile intensities to the total intensity beneath

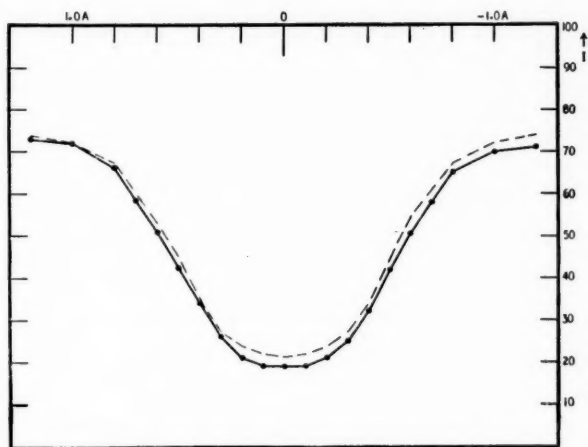


FIG. 1.—The observed $H\alpha$ absorption profile. The dashed curve shows that taken from the Utrecht Atlas.

the profile at 200 km above the solar limb, mean profiles were deduced for $H\alpha$ at each height up to 3200 km. These profiles, corrected for microphotometer slit pattern (width = 0.35 Å approx.) by Rayleigh's method for broad profiles, are shown in Fig. 2. The profile smearing produced by the interferometer resolving power ($\sim 45\,000$) was also examined and a correction was made for it, but since its pattern width was less than a quarter of that of the microphotometer, its effect proved to be almost negligible. The average r.m.s. error for any point on the profiles throughout the 3200 km region is ± 0.06 , the central intensity of the profile at 200 km being unity.

It is immediately apparent from these final profiles that the central depression of the observed $H\alpha$ profiles is contributed to mostly by scatter spectrum. The evidence for true self-reversal is only very slight. However, the profile half-width is decreasing with increasing chromospheric height up to 3200 km (see Table II), thus suggesting self-absorption as a cause of broadening of the line.

1.3. *Deduction of D_3 profile.*—Since there is no corresponding absorption line in the scatter spectrum at D_3 , the analysis is more straightforward. (A careful investigation of the effect of the absorption lines in the region of 5875.6 Å (as

recorded in the Utrecht Atlas), on the deduced chromospheric line, showed that the measured half-width needed no correction for these absorption lines in the scattered light). As for the H α line, mean D₃ profiles were drawn at each height up to 3200 km in the chromosphere (excluding the exceptional plate). It was

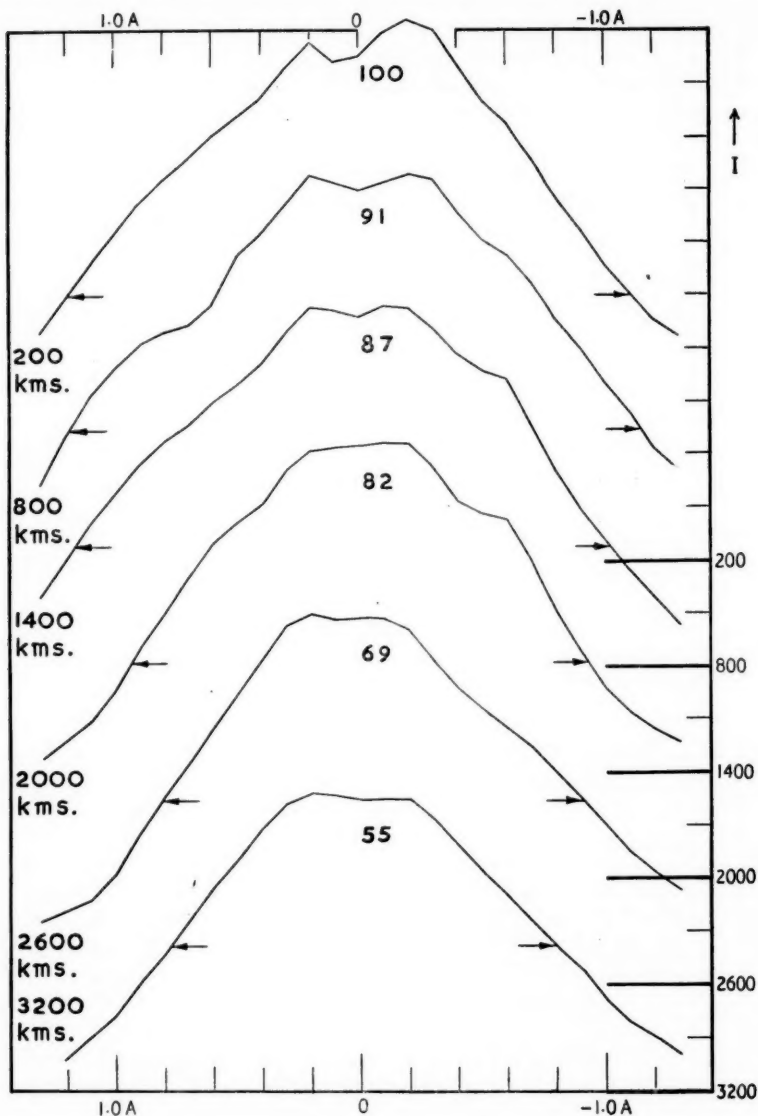


FIG. 2.—Deduced H α emission profiles at six successive heights in the chromosphere, from 200 km (highest in the figure) to 3200 km. The zero intensity marks for each profile are shown on the right hand side of the figure, and the central maximum intensity (= 100 at 200 km) marked at the peak of each profile.

18
nat
he
ght
was

noticeable that the profile shape did not vary systematically with increasing height in the chromosphere. A mean profile for the region up to 3200 km was therefore deduced: this was approximately Gaussian in appearance and after correction for microphotometer slit width and interferometer resolving power and for the presence of a satellite line, as in Treanor's paper, it gave a true Doppler profile at 5875.6 Å (see Fig. 3).

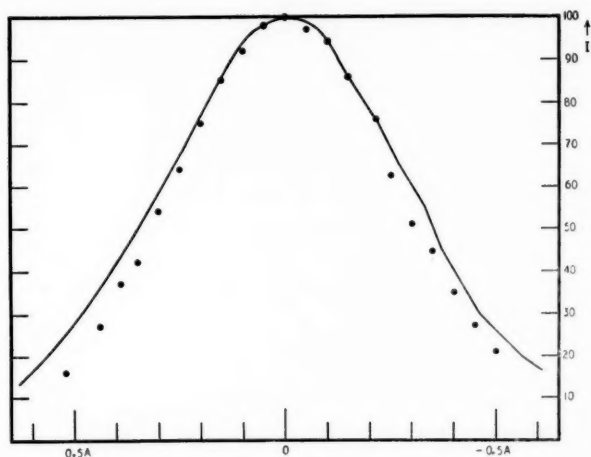


FIG. 3.—The observed D_3 emission profile, uncorrected for the presence of a satellite line, for the region 200–3200 km in the chromosphere. The dots are Treanor's observed points for a similar region.

1.4. *Summary of results.*—Table II presents a summary of the resultant profiles. By $\Delta\lambda_{1/2}$ is meant $\frac{1}{2}$ (total width at half maximum intensity):—

TABLE II

Chromospheric height	$\Delta\lambda_{1/2}$	
	He, 5876	H α , 6563
200 km		1.15 \pm 0.04 Å
800		1.21
1400		1.08
2000	0.32 \pm 0.04 Å	0.925
2600		0.865
3200		0.795

The adopted height scale depends on a precise location of the solar limb on the plates. Since the solar image was guided so that the tangential slit just failed to contact the solar limb, the absence of this latter from our plates gives rise to some uncertainty in the determination of heights. But the fact that our $\log(\text{intensity})/\text{height}$ curves for both the H α and D_3 profiles are similar to those of other observers confirms that there is no serious discrepancy between the various height scales. Following the custom of representing chromospheric intensity distributions by the form $I = I_0 \exp(-\beta h)$, we find for the region 0–2000 km:

$$\begin{aligned} \beta &= 0.075 \times 10^{-8} \text{ cm}^{-1} & \text{for H}\alpha & \quad (\beta^{-1} = 13\,300 \text{ km}) \\ \beta &= 0.078 \times 10^{-8} \text{ cm}^{-1} & \text{for D}_3 & \quad (\beta^{-1} = 12\,800 \text{ km}) \end{aligned}$$

with a tendency thereafter for β to increase. Qualitatively this is confirmed by other studies of these lines (1, 6, 10), while de Jager and Prokof'eva (12) have found the value of $0.1 \times 10^{-8} \text{ cm}^{-1}$ for the case of H α in the lowest 3000 km of the chromosphere. Since however our curves could not be corrected for scintillation effects, these must be regarded as limiting values for β .

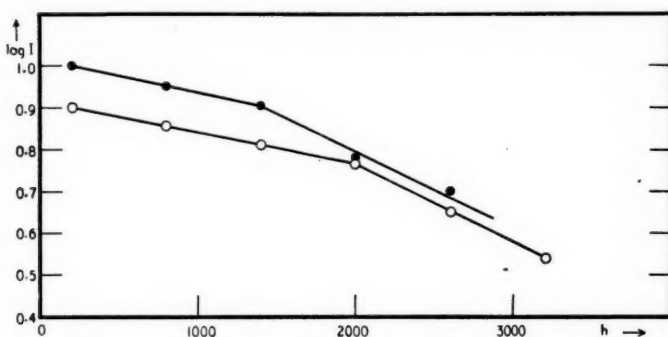


FIG. 4.—Curves of \log (total intensity) against h . Unfilled circles are those for H α ; the filled for D $_3$.

Section 2

It is instructive to compare our results with those of other observers and in the table below are recorded some of the relevant data in various studies of the chromospheric D $_3$ line:

TABLE III (D $_3$)

Name	Number of plates examined	$\Delta\lambda_{1/2}$ in A	height (km)	I_c/I_s	t
Clube	4	0.315 ± 0.04	0-3000	1/4	10 min
Treanor (16)	7	0.285 ± 0.02	0-4000	1/5	1-2 min
Melnikov and Peripelkin (8)	8	0.315 ± 0.04	0-3000	1	20 sec
Unsold (17)		0.265	1500	1	
Krat and Krat (6)	2	0.260 ± 0.03	0-4000	1	~ 1 sec
Michard (10)	2	0.22 at $\rightarrow 0.31$ at	1000 6000	2.5	~ 1 sec
Redman (14)	1	0.260	2500	eclipse	~ 1 sec

In the fourth column of Table III is recorded the approximate ratio of chromospheric intensity to the scattered light intensity. In the fifth column are shown the various exposure times. The random errors of observations are, when known, recorded in column 3.

At first sight it is encouraging to note the consistency in the values for $\Delta\lambda_{1/2}$ but one must be surprised at the difference with the results of Michard, obtained as they were under exceptionally good seeing conditions. Michard suggests, as have Redman and Suemoto on other grounds (14), an increase in profile width with height in the chromosphere; reasons for this discordance have been sought. The use of a tangential slit can lead to apparent variations with height in the chromosphere, which in fact arise from variations along the limb of the Sun. Alternatively, Michard's observations are restricted to the pole of the Sun,

which could suggest that they are a local effect—the more organized appearance of spicules in this region possibly lends credence to this idea. The lower level of scattered light in Michard's work from ours suggests that our profiles may be altered by some superimposed absorption line (as in $H\alpha$) but the absorption profiles in the D_3 region have been shown to have a negligible effect on the observed profile. Perhaps a more significant factor is the difference in exposure times, suggesting that the longer exposures in our spectra render more likely a smearing over a considerable height in the chromosphere.

For the $H\alpha$ line, comparable studies are few in number. From measurements of four plates, Keenan (4) has shown that $\Delta\lambda_{1/2}$ changes from 0.95 Å at 200 km to 0.75 Å at 3000 km, while Michard's observations on individual spicules (10) above 5000 km (7 plates) have shown that $\Delta\lambda_{1/2}$ is changing from 0.45 to 0.25 Å at 8000 km. Menzel and Cillié determined that $\Delta\lambda_{1/2} = 1.25$ Å at the solar limb but de Jager's values for $\Delta\lambda_{1/2}$ of 0.9 Å at 3000 and 5000 km seem to be exceptional. Save for the latter, these observations form a consistent picture with our own of a profile decreasing rapidly in width with height in the chromosphere (see Table IV). Recently, Krat and Krat (6) have published an extensive study of chromospheric lines including measures of the $H\alpha$ line and from two plates they deduce that $\Delta\lambda_{1/2} = 0.29$ and 0.36 Å, a value that hardly changes over the region 1500–7000 km. Their profiles are probably seriously in error, however, due to the subtraction of an incorrect absorption profile from the observed $H\alpha$ profiles. (Since the $H\alpha$ absorption profile has wings that extend to some 20 Å on either side of the centre, the assumption that the continuum level is reached at about 2 Å from the centre leads to an incorrect profile.)

TABLE IV ($H\alpha$)

Height in chromosphere 0 km	Menzel and Cillié 1.25	Observed values of $\Delta\lambda_{1/2}$			
		Keenan	Clube	Michard	de Jager
200		0.95	1.15		
1000		0.90	1.15		
3000		0.75	0.80		0.90
5000				0.45	0.90
8000				0.25	

Section 3

3.1. *Analysis of the $H\alpha$ and D_3 profiles.*—If the profiles of $H\alpha$ and D_3 had both been Doppler profiles, it would have been immediately possible to separate out the contributions of turbulent and kinetic temperature motions in the chromosphere, since the measured widths would have been connected with the turbulent velocity v , and kinetic temperature T , according to McCrea's relation for Doppler width:

$$\Delta\lambda_D = (\lambda/c)\sqrt{v^2 + 2RT/\mu} \quad (1)$$

where μ is the gram molecular weight. The use of formula (1) for the interpretation of our observations assumes that the significant contributions to the $H\alpha$ and D_3 emissions come from the same height in the chromosphere. Bishop's work (1) on the chromospheric $H\alpha$ and D_3 lines, shows that the observed emission

intensity rises to a peak near the solar limb and then dies away exponentially with height in the chromosphere. That this peak occurs at the same height in the chromosphere for both lines to within 100 km, reveals that the H α and D $_3$ light is emitted from much the same regions in the chromosphere and that the assumption above is unlikely to be seriously in error. In any case, various smearing processes on observations conspire to give us average values for v and T for regions of the chromosphere rather than specific values for certain heights. These smearing processes are (a) the unavoidable integration of emissions along the line of sight and (b) the blurring which arises out of the conditions of guiding and seeing.

The rapid variation of the H α profile width with no distinct change in the D $_3$ profile indicates however that self-absorption is another broadening factor in the H α line (though not in the D $_3$ line) and that our observations do not extend to a sufficient height to eliminate this effect. However, the assumption of self-absorption suggests an alternative way of analysing our profiles.

3.2. *Theory of self-absorption in the chromosphere.*—Pannekoek's expression for the monochromatic intensity due to a tangential column 1 cm square through the chromosphere, and in the line of sight, distant h from the solar limb, is:

$$I_{\lambda}(h) = B_{\lambda} [1 - \exp \{ -N(h) \alpha e^{-(\Delta\lambda/\Delta\lambda_D)^2} \}] \quad (2)$$

where B_{λ} = the source function in the column, $N(h)$ = (for the Balmer series) the total number of Balmer ground level atoms in the column, and $\alpha = \pi e^2 \lambda^2 f / mc^2 \Delta\lambda_D$, where f is the oscillator strength for the line transition and the other symbols have their usual meaning.

It should be noted that in the deduction of this formula it is necessary to assume that the source function remains constant in the tangential column. If a small height range of the chromosphere, where the temperature remains approximately constant, contributes most to the formation of the Balmer lines (e.g. the lowest 3000 km in the chromosphere), this is not an unreasonable assumption. Put another way, any analysis of profiles with Pannekoek's formula which shows a rapid variation of $\Delta\lambda_D$ (and therefore temperature) with height in the chromosphere contradicts the basic assumptions in its deduction.

We reduce equation (2) for $\Delta\lambda = 0$ at the central maximum intensity, and $\Delta\lambda = \Delta\lambda_{1/2}$ at half maximum intensity, and get:

$$\left(\frac{\Delta\lambda_{1/2}}{\Delta\lambda_D} \right) = \left[-\log_e \frac{-\log_e \{ 1 - \frac{1}{2}(1 - e^{-\alpha N}) \}}{\alpha N} \right]^{1/2}. \quad (3)$$

This equation presents Pannekoek's expression in a form suitable for a discussion of our measures of the half-width of the H α line.

3.3. *A preliminary determination of T .*—For a preliminary investigation, values of $N(h)$ as given by Thomas (15) for various heights in the chromosphere were used in conjunction with our measured values of $\Delta\lambda_{1/2}$ to determine the Doppler width of the H α line at these heights. For example, at 1500 km $N(h) = 0.25 \times 10^{16}$ according to Thomas, while $\Delta\lambda_{1/2} = 1.0 \text{ \AA}$ from our measures: these on substitution in equation (3) give $\Delta\lambda_D = 0.37 \text{ \AA}$. Similarly, for further out in the chromosphere at 3000 km ($N(h) = 0.063 \times 10^{16}$, $\Delta\lambda_{1/2} = 0.8 \text{ \AA}$), it is found that $\Delta\lambda_D = 0.33 \text{ \AA}$. Taking these in conjunction with the observed Doppler

width of the helium D_3 line ($\Delta\lambda_D = 0.38 \text{ \AA}$), the kinetic temperature was found to be -8000°C and -12500°C at these heights. The dominating influence of the turbulent velocity term in the Doppler width naturally gives rise to considerable uncertainty in the determination of temperature but an extreme experimental error of 10000°C hardly removes these meaningless negative temperatures. In addition to this anomaly, there is a marked tendency for $\Delta\lambda_D$ to decrease with height in the chromosphere, which is a disturbing discovery so far as our theory goes. This all indicates either the failure of the self-absorption theory or that Thomas's values for $N(h)$ are incorrect.

Thomas calculated values for $N(h)$ from eclipse observations of the Balmer decrement, assuming an emission mechanism of cascade transitions and strong self-absorption in the higher members of the Balmer series ($n > 10$). These assumptions, as he has shown, can only be reconciled with a high temperature chromosphere. Kawaguchi (3) has preserved these values of $N(h)$ but, by assuming that coherent scattering of photospheric light is the chief cause of chromospheric emission, he has argued in favour of a low temperature chromosphere. Miyamoto (11) also has preserved Thomas's value for $N(h)$ at 1500 km in order to interpret Redman's profiles of the $H\beta$, $H\gamma$ and $H\delta$ lines as the result of self-absorption on the Doppler profile for 5700°C , but both he and Kawaguchi have neglected the contribution of turbulent velocity to the kinetic temperature term which appears in the expression for self-absorption.

Since, however, it is quite likely that both the above mechanisms (i.e. cascade transitions and coherent scattering) are responsible for chromospheric emission, it would seem that there are too many unknown parameters to determine $N(h)$ from the Balmer decrement. In view of the fact also that Thomas's results depend rather critically on intensity measures from a region of the spectrum ($\sim 3800 \text{ \AA}$), whose continuum level is difficult to measure because it is crossed by many absorption lines, we must regard them as suspect.

We now describe a determination of $N(h)$ which is based on half-width measurements and which is therefore independent of the mechanism producing the total intensity of the Balmer lines.

3.4. *A redetermination of $N(h)$ at 1500 km.*—It is assumed that the theory of self-absorption is accurate, so that equation (3) is acceptable. In Table V are shown some observed values for the half-widths of the first four members of the Balmer series at a height of 1500 km in the chromosphere. Now from equation (1) we see that for a given region of the chromosphere ($\Delta\lambda_D/\lambda$) is constant for all members of the Balmer series; preserving this constancy, a reasonable choice of $N(h)$ can be made which, on substitution in the term αN (see equation (3)), gives values for $\Delta\lambda_{1/2}$ which are in close accord with the observed values. The lack of observational data does not allow us to determine N absolutely by this method, though its order of magnitude is established. In Table V are also shown calculated values of $\Delta\lambda_{1/2}$ for various choices of $N(h)$: we select $N(h) = 0.75 \times 10^{14}$ as the most probable value to give a close fit to the observed values of $\Delta\lambda_{1/2}$.

Confirmation of this approximate magnitude can be obtained from two sources. Redman and Suemoto (14), interpreting their 1952 eclipse observations of the later members of the Balmer series ($H7$ – $H31$) on rather similar lines to the above analysis, made empirical corrections for Stark effect and self-absorption,

and deduced a mean value over all the resultant Doppler profiles, for $\Delta\lambda_D/\lambda$ of 0.75×10^{-4} at about 1000 km height in the chromosphere. This compares favourably with our deduced value of 0.76×10^{-4} at 1500 km but their value for $N(h)$ of about 10^{12} is probably less exact than our own for the broadening becomes less sensitive to changes in $N(h)$ higher in the Balmer series. Menzel and Cillié (9) have concluded from their measures of the emission gradients

TABLE V
Observed values of $\Delta\lambda_{1/2}$ at 1500 km.

Name	H α	H β	H γ	H δ
Redman (13)		0.39	0.29	0.29
Keenan (4)	0.87	0.45		
Clube	1.03			
Mean value	0.5	0.42	0.29	0.29

Calculated values of $\Delta\lambda_{1/2}$ at 1500 km.

H α	H β	H γ	H δ	Chosen value of $N(h)$	($\Delta\lambda_D/\lambda$)
0.76	0.47	0.36	0.29	6.3×10^{14}	0.48×10^{-4}
0.87	0.47	0.32	0.26	1.6	0.63
0.94	0.44	0.32	0.28	0.75	0.76
0.87	0.42	0.33	0.30	0.19	0.86
0.70	0.43	0.39	0.37	0.06	1.04

The final column shows that value of $\Delta\lambda_D/\lambda$ which, when taken in conjunction with the chosen value of $N(h)$, gives the closest fit between observed and calculated $\Delta\lambda_{1/2}$'s.

and absolute intensities of the lower members of the Balmer series at the 1932 eclipse that $N(h)$ at the base of the chromosphere has the value of 10^{14} . Also, Woltjer's observations of spicule intensities in H α , give a value of 10^{13} at 4000 km, without any special assumptions about temperature in the chromosphere (20).

Now, assuming our deduced value for $N(h)$ at 1500 km, it is immediately possible to obtain from our observations of the H α line (i) an approximate distribution of $N(h)$ with height in the chromosphere, and (ii) having found $\Delta\lambda_D$ for the H α profiles, a determination of the contributions of turbulent velocity and kinetic temperature.

3.5. *Variation of $N(h)$ with height.*—Taking $\Delta\lambda_{1/2} = 1.0 \text{ \AA}$ and $N(h) = 0.75 \times 10^{14}$ at 1500 km from our measures, we find from equation (3) that $\Delta\lambda_D = 0.55 \text{ \AA}$. Using this value in conjunction with the observed half-widths for H α (Table II) at various heights, we deduce that:

$N(h) = 2.85 \times 10^{14}$	at	500 km
1.20		1400
0.44		2000
0.31		2600
0.22		3200

On account of profile smearing, this set of values must be regarded as lying on a minimum slope. If we suppose that the number of emitting atoms per cm^3 in the chromosphere decreases exponentially with height, $n = n_0 e^{-h/H}$, then it

follows that $N(h_0) = n_0 \sqrt{(2\pi RH)}$ where n_0 is the number per cm^3 at height h_0 above the limb. This gives, from our measures, values of n_0 decreasing from 46.5×10^3 at 500 km to 3.6×10^3 per cm^3 at 3000 km.

3.6. *Calculation of turbulent velocity and temperature.*—The advantage of this method of analysis is that no assumptions as to chromospheric temperature have had to be made. We now substitute in equation (1) for the $H\alpha$ line, $\Delta\lambda_D = 0.55 \text{ \AA}$; and we have already found for the D_3 line, $\Delta\lambda_D = 0.38 \text{ \AA}$. Using these figures, we find:

$$\begin{aligned} \text{turbulent velocity,} & \quad v = 17 \pm 2 \text{ km/sec,} \\ \text{kinetic temperature,} & \quad T = 20\,000^\circ\text{C} \pm 15\,000^\circ\text{C.} \end{aligned}$$

As indicated before, the dominating influence of the turbulent velocity precludes any possibility of a precise determination of T —the large error arises out of 4 per cent random errors in the measures of $\Delta\lambda_D$ for the two lines and the possible 20 per cent error in our measure of $N(h)$.

It is interesting to make a further calculation, using a mean value for $\Delta\lambda_D/\lambda$ taken from all the measures on the Balmer series, and one for $\Delta\lambda_D/\lambda$ taken from all the measures on the D_3 line. These give respective Doppler widths for $H\alpha$ and D_3 of 0.50 \AA and 0.347 \AA , from which we deduce:

$$v = 15.6 \text{ km/sec,} \quad T = 17\,000^\circ\text{C.}$$

Conclusion

It appears that there are four possible causes of the broadening of the Balmer lines in the chromospheric spectrum:

- (a) Doppler broadening due to kinetic temperature;
- (b) Doppler broadening due to turbulent motions;
- (c) Self-absorption;
- (d) Stark effect.

For the early members of the Balmer series, the effect of (c) is considerable low down in the chromosphere, whereas (d) is insignificant. For the later members, however, (c) becomes progressively less important while (d) predominates. The elimination of both (c) and (d) from the observed profiles leaves hydrogen line profiles which, when compared with observed helium line profiles, reveal that (b) contributes most to the Doppler broadening.

The cumulative effect of the smearing processes on observations, the use of the self-absorption formula, and the order of magnitude calculation of $N(h)$ in Section 3, has obscured without a doubt many details of chromospheric structure, but this comparison of the $H\alpha$ and D_3 lines has established an approximate value for the density of Balmer ground level atoms at 1500 km of 10^4 per cm^3 , a value of about 16 km/sec for the turbulent velocity, and though the temperature cannot be accurately determined, it may well be higher than that of the photosphere.

Acknowledgments

In conclusion, the author wishes to express his gratitude to Dr Treanor for his guidance throughout the course of this work; to Dr Hindmarsh for his

suggestion that a comparison between the $H\alpha$ and D_3 lines would yield a measure of chromospheric temperature; and to the D.S.I.R. for a maintenance grant which enabled this work to be pursued.

University Observatory,
Oxford:

1957 November 1

References

- (1) Bishop, R. O., *M.N.*, **116**, 593, 1956.
- (2) de Jager, C., Thesis, Rech. Astr. Obs. Utrecht, Vol. 13, 1952.
- (3) Kawaguchi, I., *Pub. Astr. Soc. Jap.*, **3**, 171, 1951.
- (4) Keenan, P. C., *Ap. J.*, **75**, 277, 1932; **76**, 134, 1932.
- (5) Krat, T. V., *Izv. Glavn. Astr. Obs. Pulkova* (No. 152), **19**, 20, 1954.
- (6) Krat, T. V. and Krat, V. A., *Izv. Glavn. Astr. Obs. Pulkova* (No. 153), **19**, 1, 1955; (No. 155) **20**, 2, 1956.
- (7) McCrea, W. H., *M.N.*, **89**, 718, 1929; **95**, 80, 1935.
- (8) Melnikov, O. and Peripelkin, E. J., *Obs. Bull. Pulkova* (No. 122), **14**, 5, 1935.
- (9) Menzel, D. H., and Cillié, G. G., *Harv. Circ.*, **410**, 1935.
- (10) Michard, R., *Ann. d'Ast.*, **19**, 1, 1, 1956; **20**, 1, 1, 1957.
- (11) Miyamoto, S., *Mem. Coll. Sci. Kyoto*, **25**, 31, 1947; *Pub. Ast. Soc. Jap.*, **3**, 67, 1951.
- (12) Prokof'eva, I. A., *Izv. Glavn. Astr. Obs. Pulkova*, (No. 152), 40, 1955.
- (13) Redman, R. O., *M.N.*, **102**, 140, 1942.
- (14) Redman, R. O. and Suemoto, Z., *M.N.*, **114**, 524, 1954.
- (15) Thomas, R. N., *Ap. J.*, **111**, 165, 1950.
- (16) Treanor, P. J., *M.N.*, **117**, 22, 1957.
- (17) Unsöld, A., *Zs. f. Astrophys.*, **46**, 782, 1928.
- (18) Utrecht Atlas.
- (19) Van de Hulst, H. C., *The Sun* (ed. Kuiper), Ch. 5, 1953.
- (20) Woltjer, L., *B.A.N.*, **12**, 165, 1954.

STELLAR PARALLAXES DETERMINED PHOTOGRAPHICALLY AT THE CAPE OBSERVATORY (TWENTIETH LIST)

J. B. G. Turner

(Communicated by H.M. Astronomer at the Cape)

(Received 1957 November 11)

Summary

Newly determined relative parallaxes are given for 18 stars, 11 of them not previously observed at the Cape, and relative proper motions in declination for 408 stars whose relative parallaxes and proper motions in right ascension have already been published.

The material given in this paper was collected together by Mr Turner shortly before his unexpected death brought to a halt, at least temporarily, the parallax work which has been carried on continuously at the Cape since it was started by Sir Harold Spencer-Jones in April 1926.

The first section is in exactly the same form as previous lists and gives the newly-determined relative parallaxes for 11 stars. The units in the last five columns are 0".001. Two values of the proper motion in right ascension are given. The first (as also the proper motion in declination) is absolute and is derived from meridian observations or other sources; the second is the relative value obtained from the parallax plates. The two values of probable error entered in the last column refer respectively to the parallax and to the photographic relative proper motion in right ascension. The observations for the short period variable star AI Velorum extend only over a period of three years. For the other stars, the time interval between the first and last plates ranges between seven and fifteen years.

The second section refers to stars which have been previously observed at the Cape and which have now been re-observed. In each case, a completely new series of plates has been used for the second determination though a few of the best plates of the earlier series have usually been re-measured and incorporated. In the case of No. 1580 a fresh selection of reference stars was used for the second determination. For each star, the results of the original determination are given on the first line, of the new determination on the second, and the weighted mean of both determinations on the third line.

The third section of this paper gives the relative annual proper motions in declination for the 408 stars for which the relative parallaxes and proper motions in right ascension were given in the Seventh, Eighth, Ninth, Tenth and Eleventh Lists published in the *Monthly Notices (M.N.* 96, 115, 1935; 97, 79, 1936; 98, 81, 1937; 99, 52, 1938; 100, 128, 1939). The numbers given in the first column of the table refer to these lists while those in the second column refer to the 1952 Yale General Catalogue of Trigonometric Stellar Parallaxes. The

proper motions given in the third column are relative to the combined motion of the parallax reference stars. Each was determined from measurements made on two plates, the first selected from the earliest plates of the regular parallax series and the second taken fairly recently especially for this purpose. The measures were corrected for the effect of parallactic displacement, using the parallax as determined at the Cape. Due to the comparatively long interval between the two plates measured, the formal probable error of the derived proper motion rarely exceeds $\pm 0''.003$. The only exceptions are for the second set of plates for Canopus (No. 767) and both sets of plates for Sirius (No. 770) for which the probable errors are $\pm 0''.008$, $\pm 0''.006$ and $\pm 0''.008$. The special 10-magnitude filter used for these sets of observations deteriorated after use and it was not possible to get recent plates. Consequently the proper motions given depend on plates which are separated by a time interval of only five years. The weighted mean of the observed proper motions is $+0''.012$ for Canopus and $-1''.204$ for Sirius. In the case of Sirius, the measures were corrected for the effect of orbital motion using the orbit given by Volet (*Bulletin Astronomique* 7, 30, 1931) and assuming that the ratio of the mass of the faint component to the brighter is 0.47.

No.	Name and D.M. No.	Mag. Vis. Phot.	Type	R.A., Dec. (1900.0) h m s	Proper Motion R.A.	Dec.	P.E. Unit Weight	Parallax	P.E.
1801	ξ Sculptoris GC 1229	5.57 6.57	Ko	0 56 38 -39° 27'.4	+ 75 + 31	+ 56	± 22	+ 29	± 7 ± 3
1802	ZC 745 -40° 394	8.4 9.6	Ma	1 31 16 -40° 21'.0	+ 63 + 29	+ 40	± 34	- 20	± 11 ± 4
1803	FS 464 -47° 502	... 10.9	Mo	1 35 33 -47° 00'.9	+ 20 + 4	- 76	± 19	+ 62	± 6 ± 2
1804	GC 8195 -22° 1389	8.39 9.1	Ko	6 17 20 -22° 09'.7	+ 6 + 16	- 232	± 27	+ 31	± 7 ± 3
1805	AI Velorum -44° 4192	Var.	Fo	8 10 48 -44° 16'.2	+ 19 + 28	+ 34	± 21	+ 30	± 5 ± 4
1806	α Corvi GC 16586	4.18 4.52	F2	12 03 15 -24° 10'.3	+ 83 + 143	- 48	± 28	+ 79	± 8 ± 3
1807	FS 14660 CAZ -51° 479	... 11.7	K5	16 13 37 -51° 05'.1	- 279 - 259	+ 15	± 26	+ 12	± 6 ± 2
1808	ZC 15411 -50° 10865	9.5 9.0	Go	16 44 50 -50° 57'.3	- 148 - 136	- 155	± 17	+ 29	± 4 ± 1
1809	FS 17523 CPD -41° 8353	... 12.0	K5	17 47 10 -41° 34'.2	- 63 - 77	- 212	± 21	+ 2	± 5 ± 2
1810	ZC 18128 -50° 12453	9.0 9.4	F8	19 15 33 -50° 14'.2	- 77 - 91	- 204	± 22	+ 25	± 6 ± 2
1811	FS 19728 CAZ -43° 69	... 12.6	K7	21 52 22 -42° 39'.6	- 162 - 174	- 162	± 23	+ 8	± 8 ± 2

Second determinations

No.	Name and D.M. No.	Mag. Vis. Phot.	Type	R.A., Dec. (1900) h m s	P.M. in R.A.	P.E.	Relative Parallax	P.E.	
1128	FS 5128 -46° 47'07	... 10.8	Mo	8 50 04 -41° 04'.8	+ 27 + 33 + 33	± 7 ± 2 ± 2	+ 6 + 17 + 13	± 11 ± 9 ± 7	(1) (2) Mean
965	γ Virginis	3.65 3.93	Fo	12 36 36 - 0° 54'.1	-592 -588 -589	± 8 ± 4 ± 4	+129 +102 +118	± 10 ± 12 ± 8	(1) (2) Mean
		3.68 3.96	Fo		-591 -583 -585	± 10 ± 5 ± 4	+119 + 46 + 91	± 12 ± 15 ± 9	(1) (2) Mean
1269	FS 11145 -46° 87'23	... 12.3	Mo	13 27 56 -46° 45'.0	+ 37 + 46 + 46	± 6 ± 1 ± 1	- 12 + 29 + 8	± 7 ± 7 ± 5	(1) (2) Mean
1453	FS 12725 -46° 97'85	... 12.2	Mo	14 59 15 -46° 23'.1	- 83 - 84 - 84	± 4 ± 2 ± 2	+ 23 + 35 + 30	± 7 ± 6 ± 5	(1) (2) Mean
1580	GC 21104 -44° 103'33	8.90 8.84	Ao	15 35 59 -44° 37'.3	-180 -174 -179	± 3 ± 8 ± 3	+ 8 + 19 + 14	± 6 ± 8 ± 5	(1) (2) Mean
1477	FS 18398 -48° 128'18	... 13.7	m	18 51 33 -48° 23'.7	+149 +147 +148	± 1 ± 1 ± 1	+ 93 + 88 + 91	± 4 ± 6 ± 3	(1) (2) Mean
1478	FS 18543 CAZ -48° 192	... 13.5	M	19 08 47 -47° 26'.3	- 49 - 37 - 41	± 3 ± 2 ± 2	+ 28 + 6 + 17	± 8 ± 8 ± 6	(1) (2) Mean

Proper motions in declination

RAS Number	Yale		RAS Number	Yale		RAS Number	Yale	
751	26	+0.007	928	192	-0.188	931	378	+0.176
837	36	-0.188	929	246	+0.590	659	387	-0.340
923	54	+1.187	602	253	+0.293	660	399	-0.153
752	64	-0.483	839	259	-0.314	844	406	-0.221
753	69	+0.344	654	261	+0.099	603	411	+0.268
924	97	+0.007	655	264	+0.111	845		+0.177
925	119	-0.092	930	267	-0.473	932	428	+0.037
838	120	+0.449	840	269	-0.238	933	430	+0.070
651	128	+0.058	656	282	-0.463	661	438	-0.342
601	141	+0.160	841	286	-0.222	754	441	+0.373
926p	146	-0.069	842p	352	-0.007	755	480	+0.068
926f	146	-0.103	842f	352	+0.050	934	488	-0.033
652	154	+0.221	657	358	+0.048	756	512	-0.135
653	166	-0.197	843	363	-0.017	846		-0.331
927	171	-0.086	658	365	+0.880	662	529	-0.263

Proper motions in declination—cont.

RAS Number	Yale		RAS Number	Yale		RAS Number	Yale	
847	537	-0°241	676	1121	-0°615	618	1662	+0°390
604	546	+0°136	608	1147	-0°015	868	1686	+0°194
605	560	+0°055	861	1148	-0°128	948	1712	+0°225
663	563	-0°215	609	1150	+0°312	687	1714	-0°247
606	570	+0°242	764	1164	+0°105	688p	1739	+0°154
848	586	-0°588	862	1170	-0°255	688f	1739	+0°139
935	618	+0°206	863	1186	-0°201	949	1756	+0°399
936	619	-0°027	677	1186	-0°204	869	1766	+0°085
849	633	-0°062	678	1211	+0°142	689	1792	+0°120
850	636	+0°256	942	1242	-0°822	773	1807	-0°261
851	665	+0°404	679	1246	-0°087	774	1809	-0°252
664	675	+0°298	864	1257	-0°465	950	1846	-0°206
937	690	-0°096	680	1265	+0°001	690	1853	-0°300
938	692	-0°045	865	1296	+0°295	691	1859	-0°224
665	712	-0°782	866	1338	-0°360	692	1860	-0°097
607	734	-0°268	681	1339	+0°077	693	1879	+0°117
852	742	+0°005	682	1341	+1°236	775	1888	-0°260
853	750	-0°206	683	1346	-0°660	951	1935	+0°219
666	763	-0°194	610	1350	+0°400	619	1945	-0°071
757	771	-0°332	943	1360	-0°432	620	1948	-0°631
667	788	+0°758	765	1370	+0°148	870	1947	-0°339
854	827	-0°547	944	1386	-0°052	871	1960	-0°166
668	831	+0°080	684	1416	+0°354	694	1995	+0°003
758	841	-0°029	945	1422	+0°006	776	1998	-0°010
759	841	-0°020	946	1456	-0°219	872	2041	-0°034
669	851	+0°109	766	1457	-0°795	695	2049	-0°002
855	873	-0°154	611	1481	+0°011	621	2060	-0°010
856	878	-0°103	612	1492	+0°406	696	2077	-0°088
857	903	-0°349	767	1497	+0°010	952	2096	-0°047
670	906	+0°106	767	1497	+0°028	697	2145	+0°095
858	917	+0°295	685	1509	-0°663	777	2158	+0°658
760	948	-0°140	613	1518	-0°346	953	2157	-0°054
671	957	-0°194	686	1519	-0°263	778	2160	-0°010
859	956	+0°243	768	1552	-0°214	698	2199	+0°149
761	993	-0°173	769	1576	+0°303	699	2226	+0°307
672	994	-0°258	770	1577	-1°195	700	2233	+0°274
860	1006	+0°138	770	1577	-1°215	701	2242	-0°564
939	1028	-0°166	614	1606	+0°001	779	2244	-0°083
940	1034	-0°131	771	1608	+0°225	954	2247	+0°071
941	1048	-0°077	615	1635	-0°602	622	2267	+0°053
762	1052	+0°160	867	1638	+0°021	873	2268	+0°070
673	1053	+0°003	616	1641	+0°609	702	2272	+1°245
763	1054	-0°026	772	1652	+0°002	955	2293	-0°057
674	1058	-0°181	947	1655	-0°033	703	2320	+0°024
675	1108	+0°229	617	1662	+0°383	704	2358	+0°213

Proper motions in declination—cont.

	RAS Number	Yale		RAS Number	Yale		RAS Number	Yale	
390	705	2361	-0.479	963	2812	+0.425	734	3334	-0.438
194	956	2368	+0.028	883	2820	-1.011	735	3359	-0.030
225	623	2387	+0.093	722	2851	+0.263	736	3386	-0.476
247	780	2399	+0.251	723	2864	-0.113	890	3391	-0.243
154	957	2414	+0.316	724	2867	-0.075	799	3438	-0.483
139	958	2419	-0.011	725	2880	-0.143	891	3439	+0.145
399	959	2422	+0.338	884	2887	-0.054	737	3458	-0.081
085	624	2426	-0.149	787	2888	-0.255	800	3487	-0.091
120	706	2431	+0.102	626	2889	-0.324	801	3504	+0.048
261	707	2446	-0.070	964	2904	-0.709	892	3515	-0.118
252	781	2453	-0.281	726	2914	+0.346	893	3515	-0.133
206	874	2481	0.000	965p	2924	+0.030	970	3521	+0.003
300	782	2485	-0.047	965f	2924	+0.071	738	3564	-0.198
224	708	2489	-0.017	627	2941	+0.036	739	3566	-0.004
097	709	2502	-0.111	727	2954	-0.233	894	3572	-0.103
117	960	2509	-0.109	628	2974	+0.198	971	3613	-0.114
260	710	2515	+0.155	728	2975	-0.025	740	3619	-0.182
219	783	2521	+0.197	885	2985	-0.130	802	3629	-0.011
071	875	2538	+0.010	788	2988	-0.151	803	3632	-0.142
631	711	2562	+0.137	886	3012	-0.324	972	3638	-0.179
339	876	2569	-0.020	629	3016	-0.303	895	3652	+0.344
166	784	2598	-0.264	729	3017	-0.141	632	3687	-0.498
003	712	2606	-0.190	789	3021	-0.133	804	3708	-0.491
010	713	2608	-0.045	730	3039	-1.064	896	3730	-0.344
034	961p	2618	-0.733	790	3041	-0.040	805	3741	-0.025
002	961f	2618	-0.737	887	3044	-0.104	633	3766	0.000
010	877	2621	+1.178	966	3053	+0.106	634	3767	-0.699
088	714	2623	-0.030	967	3077	-0.146	973	3773	-0.314
047	715	2644	-0.004	888	3081	-0.462	635	3823	-0.261
095	625	2647	-0.062	731	3097	-0.146	897	3838	-0.314
658	878	2657	+0.073	630	3111	0.000	741	3842	-0.021
054	716	2681	-0.859	889	3143	-0.559	974	3844	-0.913
010	879	2707	-0.007	631	3145	-0.096	806	3853	+0.235
149	880	2708	-0.004	732	3154	-0.488	975	3884	+0.592
307	881	2709	-0.554	733	3161	-0.292	898	3906	-0.416
274	882	2710	+0.011	791	3162	-0.049	742	3909	-0.221
564	717	2716	-0.351	792	3211	-0.648	899	3935	-0.216
083	718	2725	+0.418	793	3247	-0.191	807	3952	-0.036
071	719p	2727	-0.146	968	3255	-0.116	976	3981	+0.476
053	719f	2727	-0.143	794	3263	-0.257	977p	3991	-0.190
070	720	2764	-0.259	795	3281	-0.383	977f	3991	-0.220
245	785	2773	+0.023	796	3298	-0.275	636	4005	-0.151
057	721	2791	-0.414	797	3306	-0.323	743	4011	+0.005
024	962	2790	+0.042	798	3313	-0.234	744	4011	+0.006
213	786	2803	+0.026	969	3328	-0.374	978	4047	-0.197

Proper motions in declination—cont.

RAS Number	Yale		RAS Number	Yale		RAS Number	Yale	
900	4050	—0"189	909	4561	—0"293	822	5258	—0"299
979p	4054	+0"003	643	4582	—0"186	916	5262	—0"291
979f	4054	+0"001	910	4635	—0"334	823	5272	—0"300
808	4078	+0"006	911	4734	—0"862	994	5278	—0"233
901	4087	—0"021	912	4734	—0"865	995	5299	—0"388
809	4098	+10"383	913	4737	—0"252	996	5336	—0"118
902	4129	—0"173	985	4736	—0"354	824	5352	—0"641
637	4133	—0"315	644	4745	—0"364	825	5379	—0"785
903	4149	—0"202	914	4754	—1"144	997	5400	—0"090
745	4172	—0"169	815	4758	—0"232	917	5410	—0"368
810	4188	—0"009	986	4808	—0"215	826	5432	—0"812
904	4197	—0"128	746	4817	+0"258	827	5448	—0"138
980	4199	—0"162	747	4840	—0"434	918	5471	—0"105
811	4242	+0"003	987	4908	—0"017	919	5486	—0"024
905	4249	—0"183	748	4911	+0"487	828	5561	—0"046
906	4249	—0"177	816	4916	—0"265	920	5565	—0"159
638	4267	—0"654	749	4919	—0"250	829	5566	—0"238
907	4301	—0"670	915	5015	—1"148	830	5566	—0"242
981	4303	—0"205	817	5089	—0"677	998	5593	+0"001
982	4305	—0"151	818	5100	—1"090	831	5602	—0"080
639	4312	—0"500	988	5111	—0"183	832	5614	—0"408
983	4324	—0"193	989	5118	+0"089	833	5631	—1"186
640	4362	—0"358	990	5119	+0"002	645	5642	—0"100
641	4365	—0"365	750	5152	+0"814	834	5680	—0"033
812	4397	—0"261	819	5189	—0"102	835	5700	—0"043
813	4461	—0"372	991	5194	—0"037	646	5726	—0"035
814	4462	—0"036	992	5195	+0"004	647	5743	—0"137
908	4465	—0"177	820	5196	—0"100	921	5746	+0"052
984	4470	—0"297	821	5211	—0"279	648	5756	—0"214
642	4477	—0"434	993	5222	+0"005	836	5769	—0"831

Royal Observatory,
Cape of Good Hope:
1957 November 2.

MODELS FOR MAIN SEQUENCE STARS

Joyce M. Blackler

(Received 1957 June 28)

Summary

Computations for main sequence models have been made using the method of Haselgrove and Hoyle (1) for uniform compositions ranging from 76 per cent to 99 per cent hydrogen (by mass). Early stages of the evolution of the models with initial composition of 85 per cent hydrogen are also discussed, and finally a model for the Sun with initial composition 76.2 per cent hydrogen is given.

1. *Introduction.*—Recent papers by Haselgrove and Hoyle (1) have discussed a method of solving the equations of stellar structure, using an electronic computer. Their work was chiefly concerned with the evolution of a star of mass 1.25 solar units and initial composition of 93 per cent hydrogen so as to infer the age of the globular cluster M3. In this paper an account is given of subsequent work at the Cambridge University Mathematical Laboratory to find a theoretical main sequence by similar methods. The work of Haselgrove and Hoyle involved finding solutions for stars of constant mass but with changing composition (the composition becoming non-uniform as hydrogen was converted to helium by thermo-nuclear energy generation processes) whereas the problem for the main sequence, since it is essentially a mass sequence, was to find solutions for stars of uniform composition and different mass values. Models have been computed for uniform compositions with hydrogen content ranging from 76 per cent to 99 per cent, all with carbon-nitrogen concentration 0.25 per cent and the remaining material helium. Hence if low metal content does correspond to Type II stars then these may be considered to be Type II models, although in any case the metal content has little effect on the solutions discussed in this paper (Hoyle and Schwarzschild (2)).

Preliminary work for the main sequence was carried out on the EDSAC 1, using almost exactly the same procedure as Haselgrove and Hoyle, although some modifications were made to their original programme to include large stars where radiation pressure becomes important. However, the results given in this paper were obtained (or re-checked) using the new computer at the Cambridge University Mathematical Laboratory, the EDSAC 2, while it was in its temporary prototype stage known as the EDSAC 1½. This machine, which had a simple control system giving operation facilities similar to those of EDSAC 1, was an engineers' machine designed to test the components of the EDSAC 2 before the complicated controls of the final machine were built in. Although the EDSAC 1½ was only available for a short time, the fact that it had twice the storage space of the EDSAC 1 and was usually run at a speed 30 times as fast as the old machine (and sometimes at twice this speed) made the project worthwhile. The large store made it possible to compute a whole main

sequence range of models automatically, which was a great advantage for this type of problem.

2. *Variables and equations.*—Following the notation of Haselgrove and Hoyle, the main variables for each solution are:—

M , the mass inside a spherical surface within the star,

R , the radius of this spherical surface,

L , the energy flux across this spherical surface,

P , the total pressure at radius R ,

T , the temperature at radius R , and

X , the fraction by mass at radius R consisting of hydrogen (constant for the main sequence).

M_s , R_s and L_s are the total mass, radius and luminosity of a solution, and P_c and T_c are the central pressure and temperature. Subsidiary variables are the density ρ , the rate of energy generation U , the opacity K and Γ the adiabatic exponent.

If spherical symmetry is assumed (which implies that magnetic and rotary effects are neglected) and the star is in hydrostatic equilibrium, the mathematical problem (taking M as the independent variable) is to solve the following differential equations:

$$\frac{dR}{dM} = \frac{1}{4\pi R^2 \rho} \quad \text{the equation of continuity,}$$

$$\frac{dP}{dM} = -\frac{GM}{4\pi R^4} \quad \text{the equation for hydrostatic equilibrium,}$$

$$\frac{dL}{dM} = U \quad \text{the energy generation equation,}$$

$$\frac{dT}{dM} = -\frac{3KL}{64\pi^2 ac \rho T^3 R^4} \quad \text{for radiative transfer of energy,}$$

provided that $\left| \frac{dT}{dM} \right| \leq \frac{\Gamma-1}{\Gamma} \frac{T}{P} \left| \frac{dP}{dM} \right|,$

otherwise, $\frac{dT}{dM} = \frac{\Gamma-1}{\Gamma} \frac{T}{P} \frac{dP}{dM}$ for convective transfer of energy.

In computing the subsidiary variables ρ , Γ , and U , the same formulae as those of Haselgrove and Hoyle were used. For the energy generation, U , however, only the contribution from hydrogen (both the "proton chain" and the "carbon-nitrogen cycle" processes) was required, as the contributions from other elements or from gravitational contraction are irrelevant to the main sequence. From more recent information, Hoyle gives $[-113.4]$ instead of $[-112.1]$ for the "carbon-nitrogen cycle" constant in their equation (12). The revised value was used for the main sequence calculations. For K_{rad} the following equation was used instead of equation (20) of Haselgrove and Hoyle;

$$K_{rad} = 0.19(1+X)\rho \left\{ 1 + \frac{10^{27}\rho}{T^4} \right\}.$$

This equation gives a slightly better agreement with the values of Keller and Meyerott (3), although both equations give the correct value for electron scattering, which is the main source of opacity for massive stars.

For the starting point of the inward run of the solutions, the temperature $T=10^5$ deg. K was used for the models discussed in this paper. From trial runs with different values of P it was found that ρ/T^3 is a slowly varying function of M in the outer parts of main sequence stars, and so equations (32) and (33)

TABLE I
Models of uniform composition

Hydrogen content	Mass (Solar units)	$\text{Log}_{10} R_s$	$\text{Log}_{10} L_s$	$\text{Log}_{10} P_c$	$\text{Log}_{10} T_c$	T_{eff}	m_{bol}
per cent 76	1	10.832	33.495	17.201	7.122	5,560	4.95
	2	10.928	34.939	17.274	7.316	11,420	1.34
	4	11.109	36.105	16.985	7.402	18,150	— 1.57
	8	11.301	37.082	16.665	7.469	25,540	— 4.02
	16	11.484	37.917	16.378	7.524	33,460	— 6.10
	32	11.629	38.596	16.168	7.565	41,800	— 7.80
	64	11.743	39.146	16.050	7.591	50,390	— 9.18
	128	11.838	39.600	15.991	7.608	58,640	— 10.31
85	1	10.861	33.235	17.065	7.058	4,590	5.60
	2	10.930	34.750	17.296	7.291	10,220	1.82
	4	11.103	35.948	17.034	7.386	16,730	— 1.18
	8	11.294	36.949	16.714	7.455	23,850	— 3.68
	16	11.481	37.808	16.417	7.513	31,520	— 5.83
	32	11.636	38.516	16.190	7.556	39,660	— 7.60
	64	11.754	39.088	16.058	7.585	48,100	— 9.03
	128	11.849	39.549	15.989	7.603	56,210	— 10.18
93	1	10.896	33.010	16.946	7.004	3,900	6.17
	2	10.936	34.584	17.298	7.265	9,220	2.23
	4	11.098	35.811	17.075	7.372	15,510	— 0.83
	8	11.288	36.833	16.756	7.444	22,460	— 3.39
	16	11.478	37.712	16.453	7.503	29,930	— 5.59
	32	11.640	38.446	16.213	7.549	37,900	— 7.42
	64	11.762	39.034	16.066	7.580	46,200	— 8.90
	128	11.861	39.517	15.991	7.600	54,410	— 10.10
99	1	10.917	32.851	16.863	6.966	3,480	6.56
	2	10.945	34.464	17.283	7.241	8,520	2.53
	4	11.095	35.714	17.102	7.362	14,720	— 0.59
	8	11.284	36.751	16.787	7.435	21,530	— 3.19
	16	11.475	37.643	16.480	7.496	28,860	— 5.42
	32	11.642	38.395	16.231	7.543	36,710	— 7.30
	64	11.768	38.998	16.074	7.576	44,910	— 8.80
	128	11.868	39.485	15.991	7.596	53,000	— 10.05

R_s in cm; L_s in ergs per sec; P_c , the central pressure in dynes per cm^2 ; T_c , the central temperature and T_{eff} , the effective surface temperature in deg. K.

of Haselgrove and Hoyle (which neglect the derivative of ρ/T^3) were used to determine the starting value of P at the temperature of 10^5 deg. K. Hence it was necessary to specify only the total radius R_s and total luminosity L_s for the beginning of the inward runs, and also the central pressure and temperature, P_c and T_c , for the start of the outward runs.

3. *Procedure for finding solutions.*—It is not possible to integrate the equations the whole way from the surface of the star to the centre, or from the centre to the surface, because errors become too large and the necessary boundary conditions cannot be satisfied. An iterative process of searching for a solution has to be used, as described by Haselgrove and Hoyle, by estimating values of R and L at the surface and of P and T at the centre and integrating in both directions to an assigned mass value, and thereafter, if the first values are reasonably close, adjusting the values of R_s , L_s , P_c and T_c until the values of the variables are the same at the meeting point. This gives the required solution for all the variables throughout the star. The EDSAC 1½ was programmed to find a solution automatically by adjusting the values of the parameters R_s , L_s , P_c and T_c , using a first-order iterative process, and, having printed out one solution, to increase the mass value, interpolate new starting parameters and search for the next solution. In this way successive models were computed, proceeding along the main sequence track, having provided the machine with data for the first solution only. The iterative process only converges if the initial values of the parameters are reasonably good, so this automatic method was a great advantage. It was possible to double the mass in six steps. The computing time for a sequence of 2 to 128 solar masses was about four hours, whereas, partly because the problem could not be handled as a whole, it took six hours of computation to find a single solution on the EDSAC 1. For models with mass between 1 and 2 solar units it was necessary to provide full data for each solution as the interpolation process was not sufficiently sensitive—the reason for this is evident from the results discussed in the next section.

4. *Results for main sequence models.*—Models for the main sequence have been obtained for compositions of 99 per cent, 93 per cent, 85 per cent and 76 per cent hydrogen, all with carbon-nitrogen content 0.25 per cent and the remaining material helium. Table I gives the values determined for masses of 1, 2, 4, 8, 16, 32, 64 and 128 solar units. Full tables of the solutions have been deposited with the Society. Fig. 1 shows the main sequence for the massive stars with 76 per cent and 99 per cent hydrogen, illustrating that an increase in helium content places the star higher up the original main sequence track and slightly below it (equal mass values are joined), although the actual line of the main sequence track is almost the same for all four values of the composition. Fig. 2 shows the mass-luminosity relation, also for 76 per cent and 99 per cent hydrogen. Fig. 3 shows the behaviour of the four main parameters R_s , L_s , P_c and T_c , in the case of 76 per cent hydrogen, for all the mass values considered. The maximum in P_c between 1 and 2 solar masses occurs at the mass which first possesses a central convective core (all the solutions for the solar mass are radiative throughout). The solutions were particularly difficult to find in this region, and had to be handled with special care. The central convective core increases in size and mass with increasing total mass of the star. At 2 solar units, the convective core contains about one-tenth of the total mass and has a radius of approximately three-twentieths of R_s while at 128 solar units the core has increased to contain almost two-thirds of the total mass in approximately eleven-twentieths of the total radius. At the bottom of the main sequence the material of the star is concentrated towards the centre of the star, while for large masses the star becomes more distended. For masses above about 128 solar units it was found that the maximum density was no longer at the centre, due to the effect of

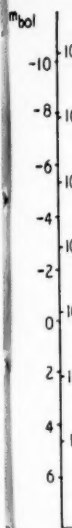


FIG. 1
99 per cent
indicate the
position in

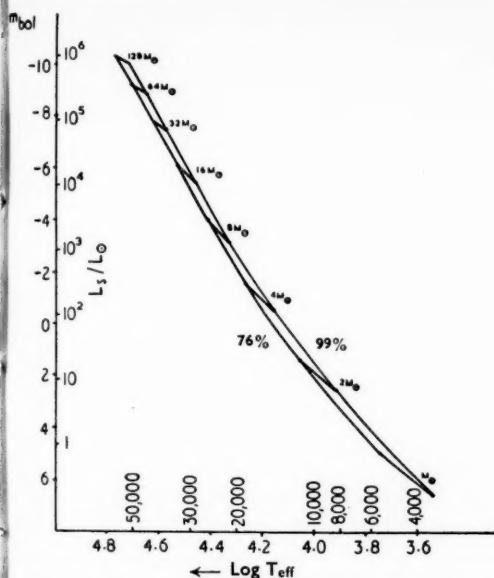


FIG. 1.—The main sequence determined for 76 per cent and 99 per cent hydrogen content. Equal mass points are joined to indicate the position on the diagram for a given mass with composition in this range.

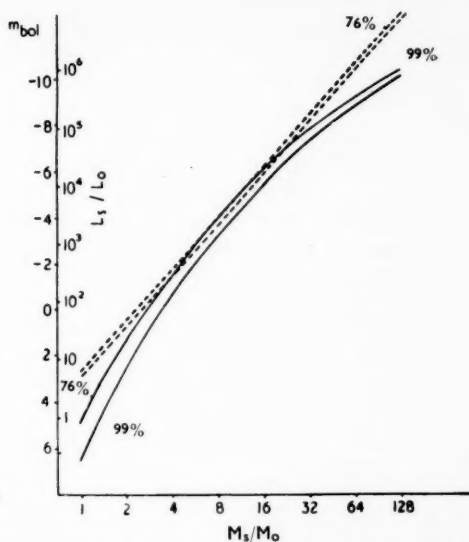


FIG. 2.—The mass-luminosity relation for 76 per cent and 99 per cent hydrogen content. For comparison, the dotted lines give the values for the relation $L_s = 8 L_0 M_s^3 / (1 + X) M_0^3$.

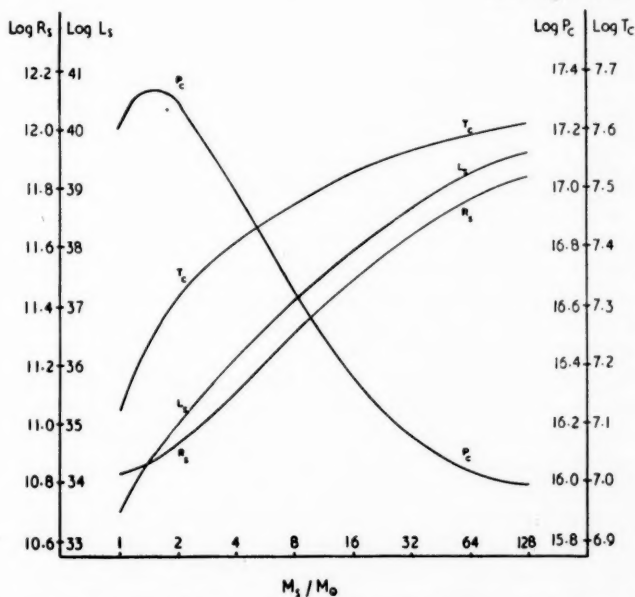


FIG. 3.—The diagram shows the behaviour of the four parameters R_s , L_s , P_c and T_c for 76 per cent hydrogen content over the range of masses considered. The scales for $\log R_s$ and $\log L_s$ are given on the left hand side, and for $\log P_c$ and $\log T_c$ on the right.

radiation pressure. It seems unlikely that models much heavier than 128 solar masses can exist, as radiation pressure becomes so large that the surface layers become gravitationally unstable. The masses at which these phenomena occur vary only slightly for the different compositions considered, although increasing the hydrogen concentration causes the convective core to appear at a slightly smaller mass. The appearance of the convective core also coincides with the mass at which the energy generation by the "carbon-nitrogen cycle" becomes equally important with that by the "proton chain" process.

5. *Early stages of evolution.*—Starting with the main sequence models for 85 per cent hydrogen and following the method of Haselgrove and Hoyle, models have been computed through the first stages of the evolution (due to the conversion of hydrogen into helium), where it can be considered that gravitational contraction makes negligible contribution to the energy generation. As in the work of Haselgrove and Hoyle, it is assumed that the convectively unstable regions are well mixed (and hence of uniform composition) but that elsewhere the mixing is negligible. Tables of the results have been deposited with the Society for masses of 2, 4, 8, 16, 32, 64 and 128 solar units. The EDSAC 1½ was programmed to proceed automatically along the evolutionary track, and the runs were stopped when the hydrogen concentration at the centre of the star had fallen to between 25 per cent and 20 per cent. This corresponds approximately to stage 7 of the results given by Haselgrove and Hoyle in their second paper. The results must be regarded as preliminary, as again the simple form of the surface condition had to be used, but running the programme of the EDSAC 1½ was valuable experience for handling the problem on a high speed computer. It is hoped to carry out further more extensive computations through later stages of evolution when the EDSAC 2 is available.

The evolutionary tracks are shown in Fig. 4. For the mass values of 4, 8 and 16 solar units the swing to the right is more evident at first than that for the stars of small and large mass which tend to "climb" the main sequence before swinging off to the right on the diagram. This phenomenon seems to bear a relation to the central pressure which has a maximum for 2 and 4 solar masses just as the swing right occurs, is steadily decreasing for 8, 16 and 32 solar masses, has a minimum for 64 solar masses at the maximum for T_{eff} , and is steadily increasing for 128 solar masses. (This excludes the last step where P increases in most cases, probably because the hydrogen concentration is getting very low.) Similar tracks were obtained for 76 per cent and 93 per cent concentration for masses of 4 and 64 solar units, but there was not sufficient machine time available to complete all the runs for these compositions.

The total times of evolution along the plotted tracks are, starting with two solar masses: 3×10^{16} , 5×10^{15} , 1.2×10^{15} , 4.5×10^{14} , 2×10^{14} , 1.4×10^{14} and 10^{14} seconds respectively. The time is longer than might have been expected for the large masses because the large convective cores allow the new helium formed to be dispersed further through the stars.

6. *The Sun.*—Several models were computed for the solar mass with different uniform compositions, but it was not possible to find a model with both the solar radius and solar luminosity. This is evident from the main sequence models given for 76 per cent and 85 per cent hydrogen. Some trial evolutionary runs were then made with different initial compositions to find a model with both the solar radius and luminosity. The models computed for an initial composition

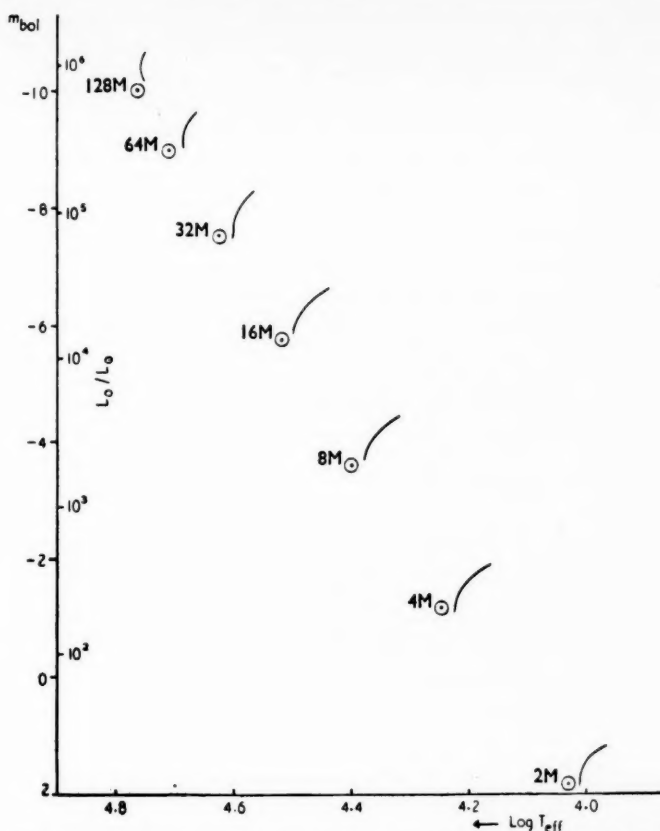


FIG. 4.—Evolutionary tracks for the main sequence models with initial content 85 per cent hydrogen. The times of evolution along the tracks are (starting with $2M_{\odot}$): 3×10^{16} , 5×10^{15} , 1.2×10^{15} , 4.5×10^{14} , 2×10^{14} , 1.4×10^{14} , and 10^{14} seconds respectively.

TABLE II

Evolutionary models for the solar mass, with hydrogen concentration 76.2 per cent. Time step between solutions = 10^{16} secs.

Solution	$\text{Log}_{10} R_s$	$\text{Log}_{10} L_s$	$\text{Log}_{10} P_c$	$\text{Log}_{10} T_c$	$\text{Log}_{10} T_{\text{eff}}$	m_{bol}
1	10.833	33.484	17.196	7.119	3.742	4.98
2	10.834	33.494	17.208	7.123	3.744	4.95
3	10.835	33.505	17.219	7.127	3.746	4.93
4	10.836	33.516	17.231	7.131	3.748	4.90
5	10.837	33.528	17.244	7.135	3.751	4.87
6	10.838	33.539	17.257	7.140	3.753	4.84
7	10.839	33.551	17.270	7.145	3.755	4.81
8	10.840	33.564	17.284	7.149	3.758	4.78
9	10.842	33.577	17.299	7.154	3.760	4.75
10	10.843	33.590	17.314	7.160	3.763	4.71

of 76.2 per cent hydrogen are given in Table II. Solution 10 corresponds almost exactly to the solar values, and occurs after a time of about 9×10^{16} seconds. This gives the surprisingly low age for the Sun of approximately 3×10^9 years. This model, which has no convective core, will need reconsideration when a more accurate surface procedure and an improved opacity formula is possible, but nevertheless gives a much more likely model for the Sun than any model with uniform composition. The necessity of taking non-uniform models for the Sun was pointed out by Bondi (4).

7. *Acknowledgments.*—It is a pleasure to acknowledge the help and encouragement I have received from Mr F. Hoyle and Dr C. B. Haselgrove, particularly in making their method and programmes available to me, and to thank the Director of the University Mathematical Laboratory, Cambridge, for the use of the EDSACs and the laboratory facilities. I am indebted to the Department of Scientific and Industrial Research for the award of a maintenance grant during the tenure of which this work was started, and to the Electors to the Isaac Newton Studentships for an award during the tenure of which the work was completed.

Girton College,
Cambridge:
1957 June 26.

References

- (1) C. B. Haselgrove and F. Hoyle, *M.N.*, **116**, 515 and 527, 1956.
- (2) F. Hoyle and M. Schwarzschild, *Ap. J. Supp.*, **1**, No. 5, 121, 1954.
- (3) G. Keller and E. Meyerott, *Ap. J.*, **122**, 32, 1955.
- (4) H. Bondi, *M.N.*, **110**, 606, 1950.

ON THE VELOCITY DISTRIBUTION OF 743 STARS WITHIN 20 PARSECS OF THE SUN

R. v. d. R. Woolley

(Received 1957 November 5)

Summary

The velocities of 743 stars within 20 parsecs of the Sun, as given in Gliese's catalogue, are analysed in various ways. The mean motion relative to the Sun is $u_0 = 11$ km/sec (towards the galactic centre) $v_0 = -17$ km/sec (tangential to the galactic centre) and $w_0 = -7$ km/sec North (perpendicular to the galactic plane and northward) or 21.4 km/sec away from R.A. $18^h 13^m$ and Dec. $= +30^\circ 5'$. The median motion in the v coordinate shows a weak correlation with spectral type. In spectral types M and K the median tangential velocity is larger, compared with the median radial velocity, than random sampling would allow, and the distribution of tangential motion is far from Gaussian, suggesting that the sample is prejudiced in favour of large proper motion. The stars are grouped according to the eccentricity of their galactic orbits, and the vertex of the velocity ellipse is shown not to differ significantly from the direction of the galactic centre in the groups with small eccentricity. The quantity $(B-A)/B$ formed from the Oort constants A and B is found to have a value near 3.1 . Dispersion of the velocities perpendicular to the galactic plane shows a clear correlation with high eccentricity in the galactic plane. The dispersion in $(v-w_0)$ remains constant when the stars are grouped according to mass, which is to say that equipartition is completely absent.

1. *Introduction.*—Analysis of the space motions of the stars has proceeded along lines which are of course well known to students of the subject, Schwarzschild's conception of the velocity ellipsoid having superseded the earlier star-stream conception, which is described very clearly in Eddington's *Stellar Movements and the Structure of the Universe*. The object of the present paper is to discuss the data on stars nearer than 20 parsecs newly provided by Gliese's catalogue, with a view to testing current theories of stellar dynamics in a rotating galaxy.

The Schwarzschild ellipsoidal hypothesis can rest as an empirical representation of the statistics of stellar motion, or it can to some extent be based on a theory of stellar motions. In the first or empirical view the hypothesis suffers from the fact, a well-known one, that in one coordinate (tangential to the galactic motion) the distribution of stellar velocities is highly asymmetrical; and from the second or theoretical point of view a weakness is that the hypothesis is a consequence of equilibrium of some sort. Now it is thought that the time of relaxation of stellar motions in this part of the galaxy is at least 10^{12} years, whereas the stars themselves have not existed in their present form for much more than 10^{10} years. The motions are therefore not relaxed and no doubt reflect very much indeed the original condition of motion. Present stellar motions may be the debris of a limited number of star streams or extended open clusters, rather than a distribution to be arrived at by an application of Liouville's theorem.

If this view is correct, it is not necessarily very helpful to classify stars according to their spectral type and then look for characteristic mean velocities and velocity dispersions. An open cluster such as the Pleiades or Hyades contains stars in a wide range of spectral types, yet they have a common motion. If we were able to do so, we should classify the stars according to their ages, or to their common membership of an old open cluster. We are not able to do this; but with the help of a little theory we can classify the stars according to the eccentricities of their galactic orbits. Those with practically circular orbits may show some statistical features indicating a different age or different place of origin from those of stars whose present orbits take them, for example, half-way in to the centre of the galaxy. This procedure enables us to construct colour-luminosity diagrams of some interest that are the subject of a later paper.

With the foregoing general considerations in mind, a number of analyses have been made of the best available collection of velocities of local stars, namely Gliese's *Katalog der Sterne näher als 20 Parsek für 1950.0**. Gliese himself has already analysed the material†, but the analyses here attempted are quite different from and complementary to his.

The *Katalog* lists 1094 stars of which the parallax is supposed by Gliese to be $0''.050$ or greater. In 742 cases the radial velocity, proper motion and parallax are known and are combined to give three rectangular coordinates of the velocity, relative to the Sun, in kilometres per second. If we add to these the Sun itself we have 743 velocities for discussion. The axes chosen by Gliese are the u axis, directed away from the centre of the galaxy, or longitude 148° ; the v axis in the plane of the galaxy tangential to the circular motion in the direction in which it takes place, or longitude 58° ; and the w axis perpendicular to the plane of the galaxy, or latitude $+90^\circ$.

2. *Solar motion*.—We start by examining the solar motion or, what comes to the same thing, by using the material to set up a local frame of reference. We can define the solar velocity in the u coordinate, u_0 , for example, in three ways, as follows.

(a) From the simple mean of the stellar velocities $(u_0)_1$ defined by

$$\sum\{u - (u_0)_1\} = 0.$$

In forming this mean, the convention is adopted of counting two components of a double star as separate if they are so listed by Gliese: for example 4A and 4B count separately, and so do 60A, 60B and 60C. If, as in the last-mentioned case, Gliese only shows one set of velocities u, v, w (in this case for 60A) the same velocities are supplied to the remaining components.

(b) By weighting the velocities with the best available masses of the stars, that is to say finding $(u_0)_2$ defined by

$$\sum\mu(u - (u_0)_2) = 0.$$

The masses μ are found from the absolute magnitudes given by Gliese, using Eggen's tables‡. In the case of stars fainter than $10^m.0$ the conventional mass $\mu = 0.40 \odot$ was used. For two bright stars outside the range of Eggen's tables,

* *Astronomisches Recheninstitut in Heidelberg: Mitteilungen*, Serie A, Nr. 8, 1957.

† *Zs. f. Ap.*, 39, 1, 1956.

‡ O. J. Eggen, *Lick Observatory Bulletin*, 544; *A.J.*, 61, 361, 1956.

masses were used as follows:

$$\alpha \text{ Lyr} \quad \mu = 4.50 \odot,$$

$$\alpha \text{ Boo} \quad \mu = 4.00 \odot.$$

(c) The median velocity $(u_0)_3$ may be found such that the number of stars (with the same convention as in (a)) with velocities more positive than $(u_0)_3$ is equal to the number with velocities more negative than $(u_0)_3$.

In the u and w coordinates the results of using these three methods on all 743 stars agree within one kilometre per second, but in the v coordinate differences amounting to 5 km/sec arise.

If we adopt

$$u_0 = +11 \text{ km/sec}$$

$$v_0 = -17 \text{ km/sec}$$

$$w_0 = -7 \text{ km/sec}$$

the following residuals are obtained by analysis, using the methods (a), (b) and (c):

$$(u_0)_1 - u_0 = +0.6 \text{ km/sec}$$

$$(u_0)_2 - u_0 = +0.95 \text{ km/sec}$$

$$(u_0)_3 - u_0 = +0.2 \text{ km/sec}$$

$$(v_0)_1 - v_0 = -5.0 \text{ km/sec}$$

$$(v_0)_2 - v_0 = -3.7 \text{ km/sec}$$

$$(v_0)_3 - v_0 = +0.4 \text{ km/sec}$$

$$(w_0)_1 - w_0 = -0.1 \text{ km/sec}$$

$$(w_0)_2 - w_0 = +0.1 \text{ km/sec}$$

$$(w_0)_3 - w_0 = -0.2 \text{ km/sec}.$$

We adopt $u_0 = +11$ km/sec, $v_0 = -17$ km/sec and $w_0 = -7$ km/sec in the remainder of this paper. The solar motion is then 21.4 km/sec directed towards $\alpha = 18^h 13^m.2$ and $\delta = +30^\circ.5$, but this vertex cannot have any galactic significance: nor can the solar motion, if we cannot refer it to a coordinate system of galactic significance (e.g. relative to a point moving in an invariable plane of symmetry of the galaxy, at a constant distance from the centre of the galaxy and with the circular velocity about that centre).

3. *Analysis according to spectral type.*—A conventional analysis of the grouping of the velocities according to spectral type was made and the results are shown in Table I. In each case the dispersion σ is calculated from the median value

TABLE I

Analysis of velocities (in km/sec) when the stars are grouped according to spectral type

No. of stars	Type	Medians			Solar motion from spectral type	Dispersions			
		u_0	v_0	w_0		σ_u	σ_v	σ_w	σ_u/σ_v
292	M	+7	-16	-7	18.4	40	24	18	1.65
190	K	+15	-19	-9	26.1	37	20	16	1.83
136	G	+16	-20	-7	26.5	38	24	19	1.53
84	F	+10	-12	-6	16.4	29	16	13	1.87

of (the velocity *minus* the median velocity of the spectral type) from the formula which assumes that the distribution is Gaussian, namely

$$\sigma = 1.483 \times \text{median}.$$

The median is preferred to any other characteristic of a Gaussian distribution, as it avoids giving high weight to exceptionally large velocities.

It should not be forgotten in discussions of stellar velocities that the distribution in v is *never* Gaussian but is always highly unsymmetrical however the stars are grouped, large negative values of v occurring more frequently than equally large positive values. This well-known fact weakens the significance of σ_v .

For what it is worth, however, the analysis of Table I shows that the value of σ_u/σ_v varies irregularly with spectral type. The mean value of σ_u^2/σ_v^2 weighted according to the number of stars of each spectral type is 2.91.

The correlation between v_0 and σ_v shown by the Gliese stars is weak. A correlation between these quantities is expected in ellipsoidal theory (cf. Smart, *Stellar Dynamics*, Sections 12.21 and 12.22) and has been given some observational support. However, the figures given by Strömberg, *Ap. J.*, 104, 12, 1946, only really show a difference between type F and later types*, which is indeed to be seen in Table I. Strömberg's axes (longitudes 339° and 69°) are not quite the same as Gliese's but the results are generally comparable. In the Strömberg list (also of stars within 20 parsecs of the Sun) there are 83 F stars, 104 G stars, 108 K stars and 98 M stars, and the Gliese stars give generally smaller values of σ . This is no doubt due to the addition by Gliese of stars within 20 parsecs of the Sun with small proper motion. The effect of selection due to the use of large proper motions in the search for stars of measurable parallax is discussed in the next section.

4. *Selection effects.*—Some parallax programmes have been drawn up using large proper motion as a criterion to decide whether to observe the parallax of a star or not. It is therefore to be expected that a catalogue of stars having measured parallaxes greater than some limit will be biased, and will contain more large transverse motions relative to small transverse motions than would be shown by a sample unbiased by selection through proper motion. This may be tested by examining the median transverse motions and the median radial motions, as it may be supposed that few, if any, stars were placed on parallax programmes because of large radial velocity.

If the motions of the stars were isotropic, and exponential in every component so that the number $n(v) dv$ of velocities between v and $v + dv$ was given by

$$n(v) = \text{const.} \times e^{-j^2 v^2}$$

in every direction, then the root-mean-square radial velocity \bar{R} would be given by

$$(\bar{R})^2 = \int_0^\infty x^2 e^{-j^2 x^2} dx / \int_0^\infty e^{-j^2 x^2} dx$$

or

$$j\bar{R} = 1/\sqrt{2}$$

while the root-mean-square tangential velocity \bar{T} would be given by

$$(\bar{T})^2 = \int_0^\infty \int_0^\infty (x^2 + y^2) e^{-j^2(x^2 + y^2)} dx dy / \int_0^\infty \int_0^\infty e^{-j^2(x^2 + y^2)} dx dy$$

or

$$j\bar{T} = 1$$

so that

$$\bar{T}/\bar{R} = \sqrt{2}.$$

* His ellipsoid for A-type stars is based on only 26 stars.

The ratio is disturbed if the distribution of velocities is ellipsoidal. If

$$n(u) = e^{-j^2 u^2}, \quad n(v) = e^{-\lambda^2 j^2 v^2}, \quad n(w) = e^{-j^2 \lambda^2 w^2}$$

where u, v, w are velocities in any three mutually perpendicular directions, then (for $\lambda > 1$)

$$(\bar{T}/\bar{R})^2 = \frac{(\lambda^2 - 1)^{1/2} + \lambda^2 \tan^{-1}(\lambda^2 - 1)^{1/2}}{\lambda \tanh^{-1}(1 - 1/\lambda^2)^{1/2}}.$$

If $\lambda = \sqrt{3}$, which may be taken as a rough approximation to the actual distribution,

$$(\bar{T}/\bar{R})^2 = \frac{\sqrt{2+3} \tan^{-1} \sqrt{2}}{\sqrt{3} \tanh^{-1} \sqrt{\frac{2}{3}}} = 2.156.$$

Radial and transverse motions were corrected by adjusting for the solar motion and then grouped according to spectral type. The medians were then found, and are shown in Table II. Table II shows that transverse velocities predominate

TABLE II

Mean radial and transverse velocities, corrected for the solar motion

Spectral type	No. of stars	Median radial velocity	Median transverse velocity	T^2/R^2
		R	T	
M	292	14	32	5.2
K	190	16	27½	3.0
G	136	15	26	2.9
F	84	12	18	2.6

over radial velocities and do so by a large relative number in the later types. We may interpret this as being due to the fact that a high proportion of M stars have been put on parallax programmes on account of their large proper motion, and we may therefore suppose that a considerable number of M-type stars have parallaxes greater than $0''.050$, but have not got large proper motions, because the velocity is small or because the motion is directed mainly in the line of sight. That the effect is smaller in F-type stars probably arises because main sequence F-type stars within 20 parsecs are so bright in apparent magnitude that they have mostly been examined for parallax whatever their proper motion. The distribution of the M-star transverse velocities is very far from being Gaussian, as compared with which it is very deficient in low velocities. One can attribute this to observational selection*.

A separate analysis was made of 209 M stars brighter than 11^m.0 absolute visual magnitude, and the median differences from the solar motion were found to be 15 km/sec radial and 34 km/sec tangential, in close agreement with the result for all M stars, including very faint ones.

Table III shows comparisons between the observed distributions of radial and tangential velocities of 292 M stars and various Gaussian distributions. It is not implied that the "true" distribution (i.e. the distribution which would be shown by a complete catalogue of velocities of M stars within 20 parsecs) is necessarily Gaussian: but the comparison is instructive.

The Gaussian (1) distribution has a median velocity (without regard to sign) of 14 km/sec, and the fit with the observed radial velocity distribution is tolerable, although there are too many fast stars observed for a good fit. The Gaussian (2)

* Cf. e.g. Wehlau, *A.J.*, 62, 169, 1957. Mrs Wehlau uses quite large factors to correct an ellipsoid for this effect.

distribution has a median velocity of $32\frac{1}{2}$ km/sec, which is the same as that of the observed distribution. It is quite clear that far too few M stars with low velocities have been detected. The Gaussian (3) distribution is an entirely conjectural one with 584 stars and a median velocity of $14 \times \sqrt{2 \cdot 156}$, or 20.5 km/sec. It fits the middle range of the observed distribution, but there are too many very fast stars observed to give a good fit, and of course the number of slow ones is conjectural.

TABLE III

Comparison of radial and tangential velocity distributions of 292 M stars with Gaussian distributions

Velocity range km/sec	Corrected radial velocity		Corrected tangential velocity		
	Observed	Gaussian (1)	Observed	Gaussian (2)	Gaussian (3)
0 to 9	116	113	19	45	143
10 to 19	74	84	40	46	136
20 to 29	31	53	50	42	112
30 to 39	23	27	63	37	79
40 to 49	21	11	48	32	53
50 to 59	27	4	19	26	31
60 to 69			18	20	16
70 to 79			10	15	8
80 to 89			3	10	3
90 to 99			3	7	1
over 100			19	19	1

It seems certain, however, that the catalogue of M star velocities is greatly affected by observational selection, so that the observed dispersion in M star velocities is too high. This point is of first-class importance if one wishes to investigate variation of velocity dispersion with spectral type.

5. *Classification of stars according to galactic orbits.*—Following in principle the researches of Lindblad, approximate galactic orbits may be constructed for individual stars, from their present positions and velocities. If the velocity is not very different from the circular velocity, the eccentricity of the galactic orbit is small and an explicit formula for the orbit may be written down. It will differ from an ordinary ellipse if the field is not an inverse square field. Since the departure from the inverse square field is reflected in the values of the Oort constants, the approximate orbit involves a parameter related to these Oort constants. The purpose of the present section is merely to develop useful formulae for setting up a classification system of stars according to their velocities U and V in the galactic plane, relative to the circular velocity, the quantity found being equal to the eccentricity if this is small.

If the attracting force function $\mu(u)$ as a function of the inverse distance u is linear, that is to say if

$$\mu(u) = \mu_1 + (u - u_1)\mu' \quad (5.1)$$

then the orbit in coordinates with origin at the galactic centre is*

$$u = \frac{\mu_0}{h^2} (1 + e \cos n\theta) \quad (5.2)$$

where $n^2 = 1 - \mu'/h^2$ and $\mu_0 = (\mu_1 - u_1\mu')/n^2$.

* R. v. d. R. Woolley, *M.N.*, **114**, 193, 1954. This is equivalent to orbits given in a moving coordinate system by Lindblad. See Smart, *Stellar Dynamics*, § 12.14.

The quantity e in (5.2) is called the eccentricity of this orbit, in this paper, although the orbit is not a closed ellipse. The equation (5.2) is accurate if the condition (5.1) is accurate, which will not in general be the case, so that the orbit (5.2) is only a good approximation if e is small and the star moves only through a small range of values of u .

The Oort constants A and B are defined in terms of the circular velocity V and distance from the centre R by

$$\begin{aligned} 2A &= V/R - dV/dR \\ 2B &= -V/R - dV/dR \end{aligned}$$

and can be expressed in terms of $\mu(u)$ and u . Since $\mu = V^2 R$ and $\mu' = -R^2(dV/dR)$ we have

$$-\frac{\mu'}{V^2 R^2} = 1 + 2 \frac{R}{V} \frac{dV}{dR}$$

so that in the limiting case where e is small and the constant of areas h differs from VR by a quantity of order e^2 we have, neglecting e^2 ,

$$n^2 = 4B/(B - A).$$

The motion (5.2) may be described by a kind of epicycle if the square of the eccentricity is neglected. In the notation of Smart's *Stellar Dynamics*, Chapter 12, ϖ is the distance from the centre of the galaxy and Θ_c the circular velocity, positive in the direction of increasing galactic longitude (whereas the circular velocity V is always taken positive). If a point C , the epicentre, is allowed to move at a constant distance ϖ_1 from the centre with the circular velocity Θ_c , and fixed rectangular axes $C\xi, C\eta$ are set up with the instantaneous position of C as origin and such that $C\xi$ is the line from the centre of the galaxy to C produced and $C\eta$ is in the direction of increasing longitude, then the coordinates of a point on (5.2) are (neglecting e^2)

$$\left. \begin{aligned} \xi &= -e\varpi_1 \cos n\theta \\ \eta &= \frac{2e}{n} \varpi_1 \sin n\theta \end{aligned} \right\} \quad (5.3)$$

(These are equivalent to Smart's equations 12.15, (5) and (6), but may be derived from equation (5.2) in an elementary manner.)

If the velocity of a point P on (5.2) is (Π, Θ) in fixed axes whose origin is the instantaneous position of the epicentre C , then

$$\left. \begin{aligned} \Pi &= \Theta_c e n \sin n\theta \\ \Theta &= \Theta_c (1 + e \cos n\theta) \end{aligned} \right\} \quad (5.4)$$

but it is more useful to obtain expressions for the velocities U and V in axes whose directions are fixed but whose origin moves with the circular velocity of the star. Then

$$\left. \begin{aligned} U &= -Cen \sin n\theta \\ V &= \frac{2B}{B-A} Ce \cos n\theta \end{aligned} \right\} \quad (5.5)$$

where now C is the circular velocity at the position of the star, considered positive, and V is counted positive in the direction in which the galaxy (near the Sun) rotates. Equations (5.5) are equivalent to Smart's equations (2) and (6) of

Section 12.16. (Note that Smart's $\dot{\eta}$ is measured in rotating axes, and that $\dot{\eta} = 2(\dot{\Theta} - \dot{\Theta}_c)$.)

We add for completeness that the coordinates of the epicentre, (x, y) relative to the star as origin are $(-\xi, +\eta)$ as the sense of the tangential axis has been reversed (i.e. it is now positive in the direction in which motion takes place). Then

$$\left. \begin{aligned} x &= eR \cos n\theta \\ y &= 2eR/n \sin n\theta \end{aligned} \right\}. \quad (5.6)$$

Further,

$$\frac{x}{V} = -\frac{y}{U} = -\frac{1}{2B}. \quad (5.7)$$

Lastly, the eccentricity e can be found from U and V by

$$\left(\frac{B}{B-A}\right) U^2 + V^2 = C^2 e^2 \left(\frac{2B}{B-A}\right)^2 = 4B^2 e^2 R^2 \quad (5.8)$$

formula (5.8) being equivalent to Smart's 12.16, (7). (The equivalence of the formulae given here to those in Smart's *Stellar Dynamics* can be checked by the relations $n^2 = g^2/\omega^2$ and $e^2 \pi_1^2 = c^2$.)

By the use of (5.8) the individual stars can be grouped according to the eccentricity of their orbits, identifying U with $(u-u_0)$ and V with $(v-v_0)$. Exact values of the eccentricity can only be determined if $B/(B-A)$ and the circular velocity C (or radius R) are known, and they cannot be supposed known with any certainty. However, by adopting definite values one can set up a classification system which does grade the orbits according to an eccentricity criterion and does so well for small values of the eccentricity.

Since

$$\frac{B}{B-A} = \frac{1}{\lambda^2} = \frac{\sigma_v^2}{\sigma_u^2}$$

(see Smart's *Stellar Dynamics*, Section 12.12) a value of $B/(B-A)$ equal to $(1.70)^{-2}$ or 0.346 was adopted, having regard to the results shown in Table I, and the quantity

$$S^2 = 0.346(u-u_0)^2 + (v-v_0)^2$$

was formed for each star. The stars were grouped in six grades according to the value of S , as shown in Table IV. The division points a, b correspond to $e=0$,

TABLE IV

Orbits classified according to eccentricity

Class	Limits of S , km/sec	No. of stars	Average mass ($\odot = 1$)	Mean value of $v-v_0$, in km/sec	
				unweighted	weighted
a	$0 \leq S \leq 14$	159	0.94	+ 1.3	+ 1.7
b_1	$14 < S \leq 21$	151	0.82	+ 2.5	+ 2.9
b_2	$21 < S \leq 28$	137	0.79	+ 4.8	+ 6.7
c	$28 < S \leq 42$	155	0.72	- 3.2	- 2.7
d	$42 < S \leq 56$	70	0.64	- 13.9	- 15.0
e	$56 < S \leq 70$	30	0.75	- 63.8	- 20.6
e^+	$70 < S$	41	0.66	- 41.9	- 76.1

$e=0.1$, $e=0.2$, etc.*, if $C=210$ km/sec: but the precise value of these division points is uncertain and not of vital importance. (It must be remembered that e^2 has been neglected in comparison with unity.) The well-known increase of $\overline{v-v_0}$ with velocity, first known as a result of Oort's researches, is shown very plainly. The quantity $\overline{u-u_0}$ varies irregularly over a range of ± 4 km/sec, except for group *d* where it is $+10.5$ km/sec (unweighted). This irregularity may be supposed to show that there is still considerable streaming of stars, in various groups, in the u -coordinate, due perhaps to the circumstances of formation of groups of stars in the past. The quantity $\overline{w-w_0}$ is much steadier (see Table VI).

6. *Rotation of the axes of the ellipsoid.*—In this section we consider the rotation of the axes of the various eccentricity classes. We consider only rotation in the (u, v) plane and suppose that one axis of the velocity ellipsoid passes through the galactic pole: but we enquire whether the u and v axes are indeed the major and minor axes of the velocity ellipse formed by the intersection of the ellipsoid with the galactic plane.

It may be shown† that if the velocity distribution is ellipsoidal and if components in one plane are considered and the quantities

$$\begin{aligned}\Sigma(u-u_0)^2 &\equiv [U^2], & \Sigma(u-u_0)(v-v_0) &\equiv [UV], \\ \Sigma(v-v_0)^2 &\equiv [V^2]\end{aligned}$$

are formed for any group of stars, and if λ is a root of the quadratic equation

$$\begin{vmatrix} [U^2] - \lambda & [UV] \\ [UV] & [V^2] - \lambda \end{vmatrix} = 0 \quad (6.1)$$

then the major axes of the velocity ellipse are displaced an angle θ from the (u, v) axes where

$$\tan \theta = \frac{\lambda - [U^2]}{[UV]}. \quad (6.2)$$

From the explicit solution of the quadratic equation (6.1) it can be seen that the displacement vanishes when the sum of the products $[UV]$ vanishes: and changes sign with $[UV]$ when $[UV]$ is small.

The explicit solution of (6.1) is in fact

$$2\lambda = [U^2] + [V^2] \pm \{([U^2] - [V^2])^2 + 4[UV]^2\}^{1/2}$$

and if $[UV]$ is small

$$2\lambda = [U^2] + [V^2] \pm ([U^2] - [V^2])(1 + 2[UV]^2/([U^2] - [V^2])^2)$$

so that

$$\lambda = [U^2] + [UV]^2/([U^2] - [V^2])$$

or

$$\lambda = [V^2] - [UV]^2/([U^2] - [V^2]).$$

The first solution gives $\tan \theta = [UV]/([U^2] - [V^2])$ a small displacement changing sign with $[UV]$. The second solution gives an axis at right angles to the first.

The results of applying this analysis are shown in Table V. A single star (Gliese Nr. 451: $+38^\circ 2285$) has $u = -263$, $v = -151$ and therefore makes a contribution of $+36716$ to the sum of the products $\Sigma(u-u_0)(v-v_0)$. This is

* Group *b* was found to contain a large number of stars and was broken into two groups b_1 and b_2 .

† E.g. Trumpler and Weaver, *Statistical Astronomy*, Chapter 3.3.

enough to change the sign of the tilt of the *e* group and indeed alters the tilt of the ellipse for all stars by $1^{\circ} \cdot 1$ in the positive direction. This striking example shows that the tilt from the direction of the galactic centre of the axis of the velocity ellipse has not very much significance, and indeed the tilt apparently changes sign from one group to another of the stars with orbits of small eccentricity, to which alone the theory of the orbits applies.

Although many investigations have given quite large deviations of the vertex of the velocity ellipse from the galactic centre, Hins and Blaauw* found a vertex for faint low latitude stars which coincides approximately with the galactic centre. They remark that "this is what we have to expect from simple dynamical considerations. No explanation of the large difference between this result and the longitude found by Schwarzschild's methods was attempted. . . . It was, however, considered as an indication that the latter were not conclusive."

Table V includes entries for groups *d* and *e* obtained by correcting stars in these groups with the mean values of v_0 given in Table IV, instead of the general mean value. This procedure alters the tilt slightly and also alters the values of $\Sigma(u-u_0)^2/\Sigma(v-v_0)^2$. If we omit groups *d* and *e* on account of this uncertainty, and also because the theoretical connection with the constants of galactic rotation only holds for small eccentricities, we find a mean value of $\Sigma(u-u_0)^2/\Sigma(v-v_0)^2$, weighted according to the number of stars in the group†, is $3 \cdot 08$. According to theory‡ this quantity is equal to the ratio between the Oort constants $(B-A)/B$.

TABLE V
Rotation of axes of velocity ellipse

Eccentricity class of star	No.	$\Sigma(u-u_0)^2$	$\Sigma(v-v_0)^2$	$\Sigma(u-u_0)(v-v_0)$	θ	$\frac{\Sigma(u-u_0)^2}{\Sigma(v-v_0)^2}$
<i>a</i>	159	18402	7784	+ 790	+ $4^{\circ} \cdot 2$	2.36
<i>b</i> ₁	151	76812	18402	+ 485	+ $0^{\circ} \cdot 6$	4.17
<i>b</i> ₂	137	123074	36844	- 9151	- $6^{\circ} \cdot 0$	3.34
<i>c</i>	155	255917	103210	- 30313	- $10^{\circ} \cdot 8$	2.48
<i>d</i>	70	229718	84818	- 28651	- $10^{\circ} \cdot 8$	2.71
<i>e</i>	71	540069	386833	+ 13114	+ $4^{\circ} \cdot 8$	1.40
all stars	743	1243992	637891	- 53726	- $1^{\circ} \cdot 6$	1.95
<i>d</i> ₁ ($v_0 = -31$): 70			71630	- 19237	- $7^{\circ} \cdot 3$	3.21
<i>e</i> ₁ ($v_0 = -62$): 71			245538	+ 8686	+ $1^{\circ} \cdot 7$	2.20

The values of the Oort constants have been discussed recently by Schmidt§. He gives $A = 19.5$ km/sec/kpc and $B = -6.9$ km/sec/kpc as best values. Accordingly $(B-A)/B = 3.8$. However, the mean error of B is given as ± 2 km/sec/kpc from determinations by Oort|| and by Morgan and Oort¶, and if we suppose that A is better determined than B , the values $A = +19.5$ km/sec/kpc, $(B-A)/B = 3.1$ give $B = -9.3$ km/sec/kpc, which is quite reasonable.

* B.A.N., 10, 365, 1948: No. 391.

† If we merely sum $(u-u_0)^2$ and $(v-v_0)^2$ over all groups and divide, group *e* receives a disproportionately high weight.

‡ cf. Smart, *Stellar Dynamics*, section 12.12.

§ B.A.N. 13, 15, 1956, No. 468.

|| *Colloques Int. du Centre National de la Rech. Sc.*, 25, 60, 1950.

¶ B.A.N. 11, 379, 1951: No. 431.

On the other hand Gascoigne and Eggen* consider that the value of A should be as low as $17\frac{1}{2}$ km/sec/kpc, from a discussion of the nearer cepheid variable stars. With $(B-A)/B=3.1$, the corresponding value of B is -8.3 km/sec/kpc, well within the range quoted by Schmidt.

From a discussion of faint low latitude stars in certain selected areas Hins and Blaauw† find the square of the velocity ratio to be 4.2, substantially higher than the value found here from the nearby stars. It may be noted that the mean value of σ_u^2/σ_v^2 from Table I is 2.9.

7. *Motions perpendicular to the galactic plane.*—The mean motion perpendicular to the galactic plane or w -velocity coordinate shows considerable stability in the sense that no substantial variations in the mean value can be seen whether the results for all stars are examined by weighted or unweighted means, or by medians (Section 1) or by classifying the stars according to spectral type (Table I). The same stability of w_0 is shown when the stars are grouped according to orbit ellipticity, as shown in Table VI. The dispersion of $w-w_0$ increases from

TABLE VI

Class	Correction to w_0 weighted for stellar mass	km/sec unweighted	Dispersion ($w-w_0$) km/sec
<i>a</i>	-1.1	-0.5	9
<i>b</i>	-0.0	+0.3	14
<i>c</i>	-0.2	-1.0	22
<i>d</i>	-0.1	+0.1	23
<i>e</i>	+0.1	+0.1	36
All stars	+0.11	-0.13	16.3

class *a* to class *e*. This was calculated in each case from the median assuming a Gaussian distribution. The dispersion in u for all stars is 37 km/sec. The *e* stars therefore move in and out of the galaxy much more freely than they do perpendicular to it, and should not be considered as "halo" stars.

Equipartition of energy among the stars was deduced from observations of stellar motion by Halm‡ in 1911, and remained a more or less generally accepted idea for at least thirty years. There is an interesting discussion in a Report to the Council of this Society by Bok§ in 1946, to which the reader is referred. Generally speaking, the evidence in favour of equipartition is the increase in average velocity, relative to the mean of the (main sequence) stars in the neighbourhood of the Sun, with spectral type, from A to M. This is, generally speaking, the evidence as shown in Table I, of an increase in σ from type F to type M.

It appears likely that part of this increase is due to the selection of M stars on parallax programmes by large proper motion, as discussed in Section 4. A further difficulty in accepting the data as evidence of equipartition is one of interpretation: as the circular velocity must be added to v , before it is squared,

* M.N., **117**, 430, 1957.

† B.A.N., **10**, 365, 1948. No. 391.

‡ M.N., **71**, 634, 1911.

§ M.N., **106**, 66, 1946.

to obtain the kinetic energy relative to axes fixed in the galaxy*. Rather than attempt to resolve the complicated question of what is meant by equipartition of energy in the (u, v) plane in the presence of galactic rotation, it seems better to examine the w motion perpendicular to the galactic plane. It also seems better to classify the stars according to mass (as in Section 2) rather than to classify by spectral type and then rely on a connection between spectral type and mass. This has been done and the results are shown in Table VII.

TABLE VII

Range of mass, $\odot = 1$	No. of stars	Median velocity $ w - w_0 $ km/sec
< 0.49	178	$11\frac{1}{2}$
0.50 to 0.59	47	11
0.60 to 0.69	46	12
0.70 to 0.79	35	13
0.80 to 0.99	35	11
1.00 to 1.19	41	9
1.20 to 1.59	37	12
All stars	419	$11\frac{1}{2}$

Double and multiple stars (shown as such by Gliese) were excluded from the counts. Table VII shows no evidence at all of a systematic decrease of median velocity with increasing mass: on the contrary, the median remains remarkably constant. This analysis is therefore completely unfavourable to the hypothesis of equipartition of energy.

8. *Colour-luminosity diagrams.*—Colour-luminosity curves of the stars classified into the ellipticity groups *a* to *e* (but with a modification depending on the position of the epicentre) form the subject of a separate paper by Dr O. J. Eggen and the present writer.

The analyses reported in this paper represent the results of a large amount of computing carried out with nothing more elaborate than desk machines. I have been helped by a number of vacation students working at Herstmonceux, notably Miss J. Crampin (London University), Miss M. Hodgkinson (Manchester) and Mr M. E. Dixon (Oxford); and by my professional assistant, Miss L. Mather.

Royal Greenwich Observatory,
Herstmonceux:
1957 October.

* It is clear from Table IV that some contribution to the appearance of equipartition is made by the correlation between large negative values of $(v - v_0)$ and small mass. Relative to fixed axes, the stars of large negative $(v - v_0)$ have less energy than those with $v = v_0$.

COLOUR-LUMINOSITY ARRAYS OF NEARBY STARS

R. v. d. R. Woolley and O. J. Eggen

(Received 1957 November 5)

Summary

Colour-luminosity arrays are constructed for nearby stars taken from Gliese's Catalogue of stars within 20 parsecs of the Sun, but restricted to those stars for which two independent trigonometric parallaxes have been measured. The stars are classified according to the closeness with which they approach the centre of the galaxy. There is a steady progression from class A with nearly circular galactic orbits, which shows a comparatively "new" array like that of the Pleiades, to the extreme class E+ whose orbits penetrate deeply towards the centre of the galaxy. These show an array suggesting that of the "very old" cluster M 67.

In a recently published paper (Woolley 1958) one of us has classified the nearby stars in Gliese's (1957) catalogue of stars within 20 parsecs of the Sun according to the eccentricities of the galactic orbits. It occurred to us that a similar classification might be adopted with advantage in setting up colour-luminosity arrays for nearby stars, and when this was done differences appeared between the stars of low eccentricity and those with high eccentricity. It was thought, however, that more significance could be attached to distance from the centre of the galaxy at pericentre than to eccentricity as such, and the stars were regrouped according to this feature.

The galactic orbit of a star, in the notation of Paper I, can be represented by

$$u = \mu/h^2(1 + e \cos n\theta) \quad (1.1)$$

where n is related to the Oort constants A and B by

$$n^2 = 4B/(B - A).$$

This equation is only approximate and remains valid for small values of e such as keep the orbit within radial limits within which the attracting force of the galaxy is a linear function of the distance from the centre: in other words limits within which $B/(B - A)$ does not vary appreciably. We, however, adopt this equation as a means of setting up a classification of stellar orbits according to minimum distance from the galactic centre. Systematic errors in the cases where e is large will make the actual galactocentric distances of the dividing points inexact without, presumably, disturbing the classification.

Consider a star at a point where the circular velocity is C , having peculiar velocities U and V relative to axes moving with velocity C , the U axis being directed away from the centre of the galaxy and the V axis lying in the plane of the galaxy, perpendicular to the U axis and positive in the direction in which the galactic motion takes place.

The motion given by equation (1.1) can be represented by an elliptical epicycle, of which the epicentre moves on a circular deferent. The rectangular coordinates of the epicentre, referred to the star as origin, are (x, y) , where

$$\frac{x}{V} = -\frac{y}{U} = -\frac{1}{2B} \quad (1.2)$$

the x axis being directed radially outwards from the centre of the galaxy and y measured positive in the direction in which galactic rotation takes place. As the Oort constant B has a negative value, the epicentre is outside the present position of the star if V is positive, and inside if V is negative. The closest approach to the centre of the galaxy is a distance eR inside the epicentre, where R is the radius of the deferent. This is found from equation (1.1) and neglecting e^2 .

From the definition of the Oort constants, whose values are now supposed taken at the epicentre, we have

$$\Theta_e = R(B - A)$$

where Θ_e , the circular velocity at the epicentre, is positive in the direction of increasing longitude.

The distance from the closest approach to the centre of the galaxy, or pericentre, from the present position of the star, is $(-x + eR)$. Now, from (1.1), the components U and V of the velocity of the star in fixed rectangular axes whose origin is the instantaneous position of the star are

$$\Pi = \Theta_e e \times \sin n\theta$$

$$\Theta = \Theta_e(1 + e \cos n\theta)$$

so that $\Pi^2 + n^2(\Theta - \Theta_e)^2 = \Theta_e^2 e^2 n^2$. From this we can derive

$$U^2 B / (B - A) + V^2 = 4B^2 e^2 R^2, \quad (1.3)$$

and from (1.2) and (1.3) we get

$$-x + eR = -\frac{1}{2B} [-V + \{V^2 + U^2 B / (B - A)\}^{1/2}]. \quad (1.4)$$

The stars were classified into five groups A, B, C, D and E, according to the value of $v = -V + \{V^2 + U^2 B / (B - A)\}^{1/2}$ as follows:

Class	km/sec
A	$v = 0$ to 9
B	$v = 10$ to 29
C	$v = 30$ to 59
D	$v = 60$ to 99
E	$v = 100$ to 129
E +	$v > 130$

In computing v , the value $B/(B - A) = 0.346$ was used.

If we assume the rough values $B = -0.010$ km/sec/pc and $R = 10$ kpc, then $-2BR = 200$ km/sec and we get the following very approximate figures for the division points:

v (km/sec)	Fraction of radius inwards ($e-x/R$)	Distance of pericentre inwards from Sun's present position (kpc)
10	0.05	0.5
30	0.15	1.5
60	0.30	3.0
100	0.50	5.0
130	0.65	6.5

Stars in class E + pass within 3.5 kpc of the centre of the galaxy, and so on. Since the theory of the orbit (1.1) assumes that e is small, however, these division points are doubly uncertain—because e is not small for the higher division points,

and because B and R are uncertain. Nevertheless, the classification from class A to class $E+$ represents a gradation of increasingly close pericentric approach to the centre of the galaxy.

The 743 stars in Gliese's catalogue for which all three velocity components are available, were classified into groups A , B , C , D , E and $E+$ according to the procedure set out in the preceding section, and their colours and luminosities were collected from photoelectric observations given by various observers (Eggen 1955*a, b*; 1956*a, b*; Kron 1956; Mumford 1956; Johnson 1955; Evans, Menzies and Stoy 1957). They were all reduced to the $(P-V)_E$ system. Stars were discarded from the list unless the mean parallax was greater than $0''.050$ as determined by at least two trigonometric parallaxes, on the grounds that the luminosity is uncertain unless this condition is fulfilled. Double stars were rejected because of the difficulty of separating the luminosities of the two components, unless (i) the magnitude difference is less than $0^m.5$, in which case the mean luminosity and colour were used, or (ii) the magnitude difference was greater than $2^m.5$, in which case the observed magnitude and colour were assigned to the bright star and the faint star was rejected. Finally, a number of stars were removed from the list because photoelectric magnitudes and colours were not available. Stars with trigonometric parallaxes greater than $0''.05$ from at least two determinations but not plotted in Fig. 1 are listed in Table II.

TABLE I
Grouping of 743 nearby stars according to closest approach to the centre of the galaxy

Class	Gliese	Omitted in Fig. 1						Plotted
		(a)	(b)	(c)	(d)	(e)	(f)	
A	259	65	17	1	13	19	42	102
B	220	42	9	0	8	21	39	101
C	108	19	3	4	4	9	17	52
D	102	10	2	1	4	9	18	58
E	27	1	0	2	0	3	3	18
E+	27	5	0	0	0	4	1	17
Total	743	142	31	8	29	65	120	348

(a) Only one trigonometric parallax available

(b) No trigonometric parallax

(c) Trigonometric parallax less than $0''.050$

(d) Magnitude difference unsuitable

(e) No photoelectric colour available

(f) Faint companions

Table I shows the extent to which the material available can be considerably strengthened by further observations of trigonometrical parallaxes, and to a lesser extent colours, of known nearby stars. It should also be noted that 362 stars in Gliese's list lack radial velocities and that an unknown but presumably comparable number of stars await discovery of large trigonometric parallaxes. Intensive observation of nearby stars can therefore double, approximately, the amount of material available for discussion. Observational programmes designed to strengthen the material will be undertaken at the Royal Greenwich Observatory. An investigation similar to this one of stars with parallaxes down to $0''.020$ is also planned. As these later parallaxes are smaller, errors in parallax determination are more serious and the main sequence will be ill-defined, but some classification of giants may be possible.

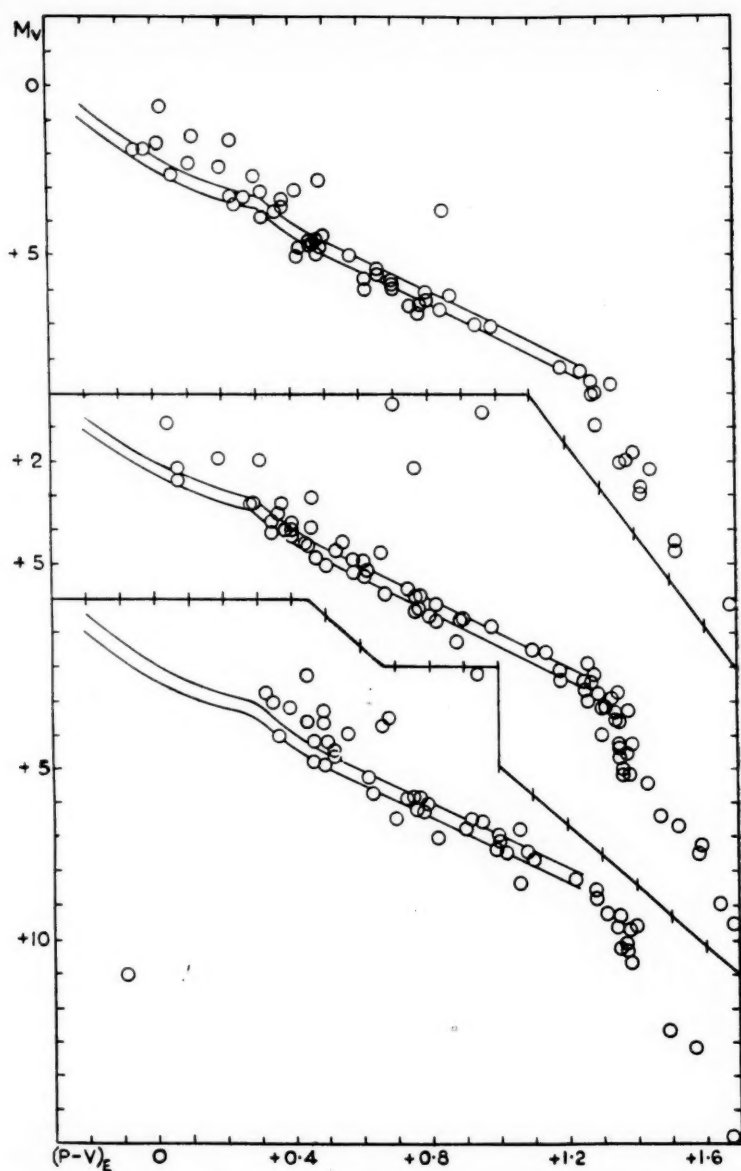


FIG. 1 (a)—Colour-luminosity arrays for class A, B and C stars (top to bottom) for which the trigonometric parallax, from at least two determinations, is greater than $0''.05$. The order A, B, C represents decreasing pericentric distance of the star's galactic orbit from the galactic centre.

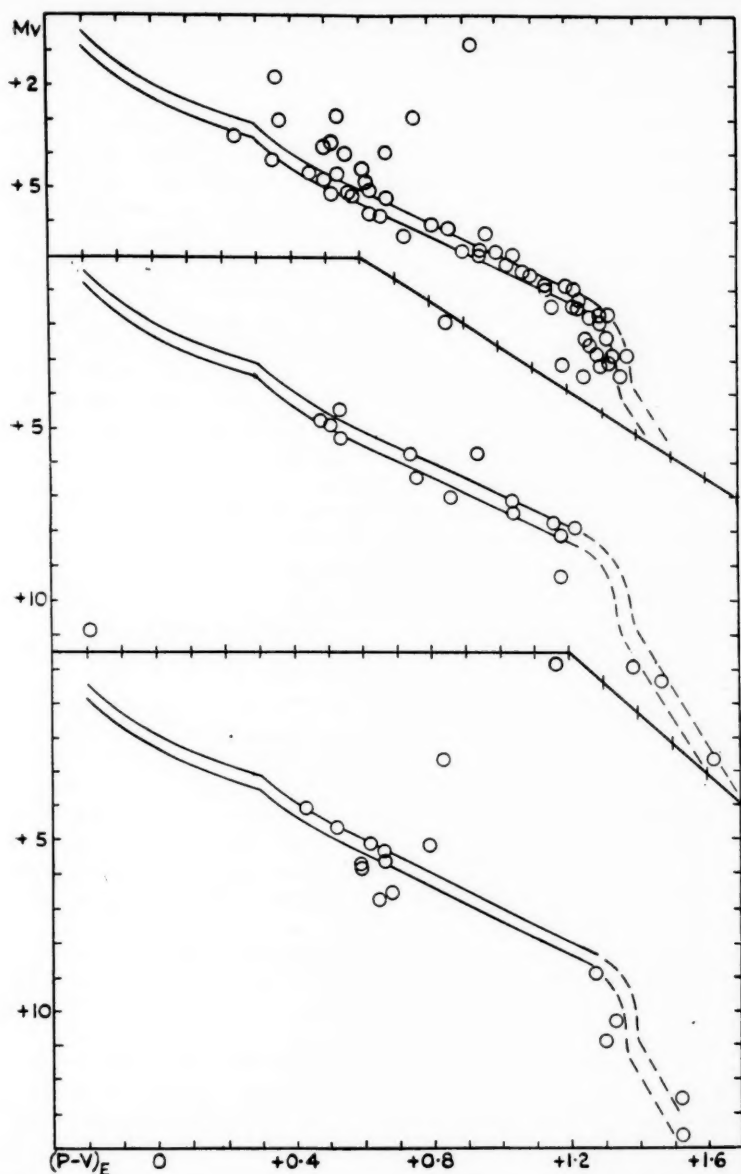


FIG. 1 (b)—Colour-luminosity arrays for class D, E, and E+ stars (top to bottom) for which the trigonometric parallax, from at least two determinations, is greater than $0''.05$. The order D, E, E+ represents decreasing pericentric distance of the star's galactic orbit from the galactic centre.

Colour-luminosity arrays for the six classes are shown in Fig. 1. The following features are pointed out:

(a) The colour of the mean of the four bluest stars both on and above the main sequence moves systematically from blue to yellow as we pass from class A ($0^m.00$) and class B ($+0^m.09$) through class C ($+0^m.36$), class D ($+0^m.33$) to class E ($+0^m.52$) and class E+ ($+0^m.53$).

(b) The percentage of subdwarfs appears to increase from class A to class E. Although one or two apparently subluminous stars in classes A and B have well-determined distances, the presence of uncertain parallaxes in the material prevents us from drawing any conclusions about a sharp separation between dwarf and subdwarf sequences. However, in class C and later the subdwarfs stand off conspicuously from the main sequence and in class E+ the subdwarfs, giants and subgiants outnumber the main sequence stars.

(c) A large number of subdwarfs in class D fall near the intersection of the dwarf and subdwarf sequences. A few of these stars have ultra-violet colours, U , available, and where this is the case they show an ultra-violet excess compared with main sequence dwarfs of the same $(P-V)_E$; in agreement with a previous conclusion (Eggen 1955b) that M-type subdwarfs are approximately two-tenths of a magnitude brighter in the ultra-violet than main sequence dwarfs.

(d) A fairly conspicuous feature of Fig. 1 is the apparent gap between $(P-V)_E \sim +1^m.0$ to $+1^m.2$ in the main sequence of class A stars. This gap is still apparent, but not so conspicuous, in class B and is perhaps visible in class C; but it is completely filled in class D. This may be an effect of deficiency in slow moving K4 and K5 dwarfs due to selection by proper motion in preparing parallax programmes, but the analysis of radial and tangential velocities in K-type stars (Paper I, Table II) suggests that this selection is much greater in M-type than in K-type stars.

The arrays shown in Fig. 1 can be related to current evolutionary theory. The arrangement shown by the stars in classes A and B is similar to that shown by such clusters as the Hyades and Praesepe, that is to say, there is a well-defined main sequence of stars later than type F0, or colour index $\sim 0^m.2$, but having most of the bluer stars above the main sequence*. The early type main sequence shown in Fig. 1 is that defined by such "young" clusters as the Pleiades, or Perseus. In these "young" clusters the giant stars are blue, whereas in class A and especially in class B, as in the Hyades and Praesepe clusters, there is a scattering of yellow giants.

In terms of the evolutionary theory, classes A and B are old enough to have lost their O- and B-type stars and to have raised their A-types above the main sequence, but not old enough to have experienced any effects in later type main sequence stars.

Turning to classes C and D, the A-type stars have disappeared and later types, of F in class C and late G in class D, are raised above the main sequence—or are beginning to show age. Classes E and E+ are not well represented in the available material, and are probably not well represented in the total stellar population near the Sun. The colour-luminosity array of class E+, however, as far as it goes, suggests that derived from the "very old" cluster M67 (Johnson and Sandage 1956). The sequence from class A to class E+ is

* The single star δ Eridani in class A (colour, $+0^m.85$, $M_V = +3^m.6$) does not fit into the scheme

TABLE II

Stars not plotted in Fig. 1

No.	M_V	Sp	No.	M_V	Sp	No.	M_V	Sp
A.			m			m		
47	+10.2	dM3	195B	+13.0	M5	738A	+3.9	GoV
125	+9.4	M3	221	+8.9	K5	B	+6.0	—
185	+8.7	dM1	234B	+16.8	—	752B	+19.2	dM5
206	+11.0	dM4	294A	+4.4	F8	795A	+6.9	—
244B	+11.5	DA5	B	+8.8	—	B	+7.9	—
250B	+10.4	M2	C	+12.2	—	871B	+8.7	M1
271B	+7.0	dK6	314A	+4.1	—	D.		
274B	+11.4	—	B	+5.6	—	22A	+10.3	dM3
277A	+10.3	dM4	324B	+11.8	M5	B	+12.1	M4
B	+11.6	dM4	327	+5.5	dG3	26	+10.7	dM4
280B	+13.1	DF:	331B	+9.9	—	90	+5.6	dK4
290	+5.6	dG8	C	+10.2	—	166C	+12.5	dM4
335B	+6.7	—	349	+7.0	dK5	200B	+13.0	M2:
348B	+7.5	Ko	352A	+10.9	dM4	226	+10.6	M3
351A	+2.7	—	B	+11.0	dM4	228A	+10.6	—
B	+3.4	—	361	+9.6	dM2	B	+12.6	—
356B	+13.2	—	387B	+10.2	M1	318	+10.5	DA
420B	+10.6	—	414A	+8.0	dM1	354B	+12.1	—
428A	+7.2	—	B	+9.7	dM2	367	+10.7	M4
B	+8.3	—	429A	+4.9	dKo	412B	+16.0	dM5
512A	+7.6	dKo	B	+6.0	dK5	421A	+9.2	dM1
B	+10.8	dM4	505B	+9.3	dM2	B	+8.3	dM1
540	+9.5	M1	586A	+5.6	dK1	C	+12.0	M5
559A	+4.4	G2V	B	+7.1	dK5	544A	+6.1	KoV
B	+5.8	dK5	599B	+12.7	DA	B	+13.0	M6
566A	+5.5	G8V	621	+7.2	dK2	635B	+5.6	KoV
B	+7.7	dK5	702B	+7.4	K5V	771B	+10.7	M3
666B	+9.1	Mo	748	+11.1	dM4	781	+10.7	dM3
667A	+6.8	K3	765B	+11.9	—	800A	+9.5	dM2
B	+8.3	K4	819A	+5.8	dK1	B	+13.1	—
684A	+4.3	GoV	B	+8.7	Mo	815A	+9.6	M2
B	+7.1	Mo	849	+10.6	dM3	B	+11.6	—
704B	+7.3	—	860A	+11.8	dM3	886	+5.9	K4V
710	+8.7	dM1	B	+13.4	dM4	E.		
773	+7.8	dM1	C.			328	+8.8	dM1
799A	+11.1	dM4	48	+10.2	dM4	369	+9.3	dM2
B	+11.4	dM4	79	+8.1	dM1	392B	+11.0	—
806	+10.8	dM3	301A	+8.5	—	529	+7.7	dK6
859A	+4.8	dG2	B	+9.5	—	783B	+12.7	M5
B	+4.9	dG1	416	+7.7	dMo	914B	+8.3	—
909B	+11.6	Mo	491B	+11.3	—	E +		
B.			507A	+9.6	Mo	38	+10.0	dM2
2	+10.3	dM	B	+12.0	M3	465	+11.8	dM4
105B	+12.5	M4	549B	+10.	M3	861	+12.	sdK6
142	+7.3	dMo	695B	+10.7	M4			
161	+6.5	dK2	C	+11.1	M4			
195A	+9.3	dM1	716	+5.8	dKo			

therefore a sequence of increasing age. This is not unreasonable if one considers that the stars in class A are now in orbits which do not penetrate much into the centre of the galaxy, and that for this reason the stars, at least statistically, have always been at the same distance from the centre, and must have originated at this distance from the centre. On the other hand, stars in class E+ all go more than halfway into the centre of the galaxy at some point in their orbit and it may well be supposed that most of them were formed much nearer to the centre of the galaxy than their present position. The connection between increasing pericentric approach and increasing age is then explained if one supposes that star formation either took place, or perhaps began, at the centre of the galaxy sooner than in the outer parts—a conception that it seems reasonable to connect with the greater density at the centre.

Royal Greenwich Observatory,
Herstmonceux:
1957 October.

References

- Eggen, O. J., 1955a. *A.J.* **60**, 131; L.O.B. No. 532.
Eggen, O. J., 1955b. *A.J.* **60**, 401; L.O.B. No. 538.
Eggen, O. J., 1956a. *A.J.* **61**, 405; L.O.B. No. 547.
Eggen, O. J., 1956b. *A.J.* **61**, 462; L.O.B. No. 548.
Evans, D. H., Menzies, A., and Stoy, R. H., 1957. Unnumbered Cape Mimeogram.
Gleise, W., 1957. *Mitt. Heidelberg Astr. Rechen Inst.*, **8**.
Johnson, H. L., 1955. *Ann. D' Astroph.* **18**, 292.
Johnson, H. L. and Sandage, A. R., 1955. *Ap. J.* **121**, 616.
Kron, G. E., 1956. *Berkeley Symposium on Mathematics and Statistics*, **3**, 39.
Mumford, G. S., III, 1956. *A.J.* **61**, 213.
Woolley, R. v. d. R., 1958. *M.N.* **118**, 45, (referred to as Paper I).

STELLAR GROUPS. I. THE HYADES AND SIRIUS GROUPS

O. J. Eggen

(Communicated by the Astronomer Royal)

(Received 1957 November 27)

Summary

The accurate proper motions of the FK₃ and the available radial velocities have been used to establish the reality of an extended Hyades Group. The possible members of this group among the nearer stars are also discussed. The colour-luminosity array for the group is similar to that for two clusters, Hyades and Praesepe, included in it, except that stars of higher luminosity appear in the group at large than in clusters themselves. Also, 67 stars that appear to share the space motion of Sirius, here called the Sirius Group, present a colour-luminosity array that indicates, on the basis of the current theories of stellar evolution, that this group is probably younger than the Hyades Group.

Introduction.—As a result of many investigations, beginning with Richard Proctor (1869) nearly a century ago, the existence of at least two extended stellar streams has been firmly established in the literature. Part of the extensive literature concerning one—the Ursa Major stream—has been catalogued by Roman (1949); the other—the Taurus stream—was noted by Strömberg (1922) and later more fully discussed by Wilson (1932). In recent years (cf. Bok 1934, 1946) these two streams have been considered as resulting from the break-up, through encounters with field stars and the tidal forces of differential galactic rotation, of the Hyades and of the Ursa Major nucleus clusters, the smallness of the nuclear remnant of the latter being taken as indicating a greater age than that of the more compact Hyades nucleus of the Taurus stream.

The purpose of the present series of investigations is to determine (1) to what extent the well-determined space motions of certain stars, or groups of stars, might be shared, within certain limits, by other stars; and (2) with what degree of certainty the resulting "groups" of stars can be considered as physically significant. The present paper deals with those stars which appear to share the space motion of the Hyades cluster; for comparison purposes, the stars which share the motion of α Canis Majoris, here called the "Sirius Group", will also be discussed.

Hyades Group.—Undoubtedly the most convenient method of choosing stars with common motion would be an examination of the vector space motions. However, the observed radial velocities, ρ_o , the two components of the annual proper motion, $15\mu_\alpha \cos \delta$ and μ_δ , and the parallax, π , enter into these vectors in a complicated and irregular way, making any assessment of the spread to be allowed for observational inaccuracy difficult.

Since parallax is usually the greatest source of error in computing the vector motions, it seems advisable to adopt criteria for group membership which eliminate it by the following procedure. Although the tangential components

of velocity cannot be found without knowledge of the parallax, the ratio of the two tangential velocities, in right ascension and in declination, is equal to the ratio of the proper motions which can, of course, be found independently of the star's distance. This ratio gives θ_o , the position angle of the star's apparent motion from $\tan \theta_o = 15\mu_\alpha \cos \delta / \mu_\delta$, which may be compared with θ_e , the position angle of the group motion projected on to the tangential plane. The agreement between θ_o and θ_e , together with the agreement between the observed radial velocity and that computed from the radial component of the group motion, provide two criteria by which a star's membership in the group can be judged, without having recourse to the parallax.

Let (A, D) , computed from the radial velocity, proper motion and parallax of the defining star, or from the convergence of the proper motions of the defining cluster, be the direction of the apparent motion of the group. Then the observed direction of the proper motion, θ_o , of a suspected group member may be compared with the expected direction, computed from the following:

$$\cot \theta_e = \cos \delta \tan D \operatorname{cosec} (A - \alpha) - \sin \delta \cot (A - \alpha).$$

From a definitive discussion of the observed motions of the Hyades cluster members, van Bueren (1952) has found

$$A = 6^h 18^m.5 \pm 2^m.1 \text{ (mean error),}$$

$$D = 7^\circ 29' \pm 11' \text{ (mean error).}$$

The mean errors in the observed values of θ_o are equal to ϵ/μ , where ϵ represents the (equal) mean errors in $15\mu_\alpha \cos \delta$ and μ_δ , and μ is the total proper motion. Also, the "point" (A, D) has a dispersion, the size of which, for a particular star, will depend upon the angular distance, λ , from (A, D) . The size of this dispersion could be evaluated from the stated mean errors of A and D , but we have preferred to derive it from the Hyades stars of brightness comparable to the group members discussed below. Of the 56 Hyades stars brighter than visual magnitude 7.0, and considered to be "certain cluster members" by van Bueren, 46, or 80 per cent, satisfy the criterion $\theta_o - \theta_e \leq 2^\circ / \sin \lambda$, which is based on the observed position angles alone. Therefore, combining the errors in the observed and computed values of θ , we might call "candidates for group membership" those stars for which

$$\theta_o - \theta_e \leq (\epsilon^2/\mu^2 + 4/\sin^2 \lambda)^{1/2}. \quad (1)$$

However, since from practical considerations it is necessary to exclude very small and poorly determined values of μ , we impose the further *ad hoc* condition that $\epsilon/\mu \leq 2^\circ / \sin \lambda$. This condition then gives equation (1) the extreme values of $2^\circ / \sin \lambda$, when $\epsilon/\mu = 0$, and $2\sqrt{2}/\sin \lambda$, when $\epsilon/\mu = 2^\circ / \sin \lambda$. For simplicity then we will call candidates for membership those stars that meet the following requirement:

$$\theta_o - \theta_e \leq 2^\circ.8 / \sin \lambda. \quad (2)$$

This criterion passes 96 per cent of the "certain" members of the Hyades and, with the appropriate (A, D) , 90 per cent of the "certain" members of the Pleiades cluster that are brighter than visual magnitude 7.0. It should be emphasized that equation (2) merely represents a convenient criterion and, obviously, is not the result of mathematical rigour since it combines the empirically determined limit, $2^\circ / \sin \lambda$, with the more formally determined errors in the proper motions which, in the discussion below, are mean square errors,

Group members were then selected from the candidates for membership on the basis of the observed radial velocities. The velocity of the Hyades cluster relative to the Sun is $V = 43.95 \pm 0.6$ (mean error) km/sec (van Bueren 1952); the expected velocity for any group member is then $\rho_e = 43.95 \cos \lambda$. The observed radial velocities and their quality, Q , have been taken from the catalogue compiled by R. E. Wilson (1953) and if $\rho_o - \rho_e$ is less than, or equal to, 3, 4 or 5 km/sec for velocities of quality a , b or c , respectively, the star was considered to be a member of the group.

A convenient list of stars to search for possible members of the Hyades Group is the FK3 (Kopff 1937, 1938). After rejecting from further consideration all stars for which $\epsilon/\mu > 2^\circ/\sin \lambda$ and six known members of the Hyades cluster (van Bueren 1952) there remained 56 stars that satisfy the condition $\Delta\theta \sin \lambda \leq 2^\circ.8$ (class I). When the acceptance limits of the convergent point are doubled (class II), that is, when $2^\circ.8 > \Delta\theta \sin \lambda \leq 5^\circ.6$, 40 additional stars are admitted. The radial velocity criterion, described above, was then applied and the stars admitted to group membership are listed in Table I. The results may be summarized as follows.

Class	Candidates	Members	Field stars
I ($\Delta\theta \sin \lambda \leq 2^\circ.8$)	56	20	36
II ($2^\circ.8 > \Delta\theta \sin \lambda \leq 5^\circ.6$)	40	4	36.

It should be noted that if we increased the radial velocity limits to 5, 6 and 7 km/sec for stars of quality a , b and c , respectively, we would admit three additional members to class I and five to class II.

TABLE I

Proper motions and radial velocities of members of the Hyades Group

FK3	θ_o	$\Delta\theta \sin \lambda$	ρ_o	$\Delta\rho$	Q	μ
Class I	"	"	(km/sec)			"
48	98.7	-1.5	+ 7	-4	b	0.301
126	44.4	+1.1	+12	+3	a	.533
339	239.7	+2.1	+26	-3	a	.510
383	255.0	+1.5	+18	-2	b	.172
457	275.8	-1.7	- 4	-3	b	.160
485	282.0	+0.7	- 3	-1	b	.241
501	277.1	-0.7	-13	+1	b	.287
609	311.2	+1.1	+35	-1	b	.066
698	177.4	+2.2	-17	+2	a	.160
701	7.1	+2.5	-16	-3	c	.082
711	12.8	+1.3	-28	-1	a	.085
812	96.6	+1.4	+31	-2	a	.189
881	77.5	0.0	-11	-4	b	.194
1081	96.9	+0.7	+28	0	b	.234
1173	199.1	+2.4	+39	-3	a	.019
1609	85.2	+0.2	-10	+2	d	.045
1623	82.7	-0.2	- 7	0	b	.091
Ny	162.9	-0.7	+ 6	-3	d	.085
No	69.8	+1.3	+ 3	-1	a	.096
Sl	254.0	+1.8	- 9	-2	d	.082
Class II						
15	78.1	-5.0	- 5	-2	c	.176
250	192.6	+1.8	+33	-4	b	.118
476	268.1	-3.0	- 8	-1	b	.190
709	50.0	+3.2	-45	-2	c	0.057

The equal number of field stars in the two equal acceptance areas and the large ratio of class I to class II members is a strong indication of the reality of the group. This is, if satisfaction of the membership requirement was a matter of chance, we would expect a nearly equal ratio between members and field stars of classes I and II. A similar classification previously applied to a different selection of bright stars (Eggen 1958) yielded approximately the same ratios between members and field stars of classes I and II.

As a further check on the method used to segregate the group members we have applied the same test to the same stars in the FK3 but with a synthetic convergent point, $\delta = -90^\circ$; the "special" lists of 52 polar stars in the FK3 were omitted. This convergent point was chosen because (1) the computations are greatly simplified, since $\theta_c = 180^\circ$ and $\sin \lambda = \cos \delta$, and (2) it has no particular galactic significance. The candidates for membership in the synthetic group are as follows.

Class	Candidates
I	27
II	28

The number of "members" resulting from four assumed values of the group velocity relative to the Sun are as follows.

Class	km/sec			
	$V = 5$	10	20	50
I	2	4	2	2
II	4	2	2	1

It is noteworthy that even for a group with the high velocity relative to the Sun of 50 km/sec, that is, similar to the Hyades Group, five per cent of the candidates may accidentally be admitted as members and for smaller velocities, ten per cent might be expected.

The colours and luminosities computed from the group parallaxes are listed in Table II and plotted in Fig. 1, where the main sequence is shown with a half-width of $0^m.2$; the form of this "standard" main sequence was derived (Eggen 1955 *b*) from (a) the dwarfs of the Praesepe cluster with $(P - V)_E = +0^m.3$ to $+1^m.24$ and (b) the Pleiades cluster stars with $(P - V)_E = -0^m.2$ to $+0^m.3$, and the zero-point was obtained from the stars with parallaxes greater than $0''.2$. The class I members of the Hyades Group are represented with filled circles, the class II members with open circles. The known members of the Hyades cluster, brighter than visual magnitude $5^m.0$ (van Bueren 1952) are represented with crosses in the figure; the moduli of the individual cluster members are those given by van Bueren. Also, the ten brightest stars in the Praesepe cluster, whose membership in the group was discussed in a previous note (Eggen 1958), are indicated by plus signs.

The distribution in the colour-luminosity array of the brighter members of the clusters is very similar to that of the more widely scattered members of the group, although stars of both early and late type occur with higher luminosity in the group at large than within the clusters themselves.

The trigonometric parallaxes (Jenkins 1952) and the spectroscopic values determined at Mt Wilson (Adams *et al.* 1935), which were not used in the

method of selecting group members, are compared in Table IV with the values derived from the group motion. Theoretically we could exclude any accidental members as a result of this comparison but, keeping in mind the inherent errors of all three sources of parallax, in all cases where parallaxes are available for comparison the agreement is such that none of the members selected in Table I can definitely be eliminated on this basis.

TABLE II

Group parallaxes, colours and luminosities of Hyades Group stars

FK3	Name	V_E	$(P-V)_E$	Sp.	π_g	M_V
I.		m	m		"	m
48	δ Cas	2.70	+0.02	A5 V	0.0335	+0.32
126	κ Ret	4.66	+0.28	dF5	0.0590	+3.51
339	10 UMa	4.01	+0.30	F5 V	0.0725	+3.31A
383	λ UMa	3.46	-0.12	A2 IV	0.0210	+0.07
457	γ Crv	2.60	-0.23	B8 III	0.0175	-1.28
485	α CVn	2.89	-0.02	A0p	0.0260	-0.04
501	ζ Vir	3.38	-0.01	A3 V	0.0325	+0.94
609	γ Her	3.74	+0.18	A9 III	0.0110	-1.05
698	ζ Pav	3.96	+1.06	K0	0.0190	+0.35
701	HR 7013	6.0:	—	A3	0.0095	+0.9:
711	R Lyr	4.0:	+1.45	M5 III	0.0115	-0.7:
812	γ Cap	3.86	+0.22	F0p	0.0270	+1.02
881	ν Peg	4.38	+0.51	F8 IV	0.0210	+1.00
1081	47 Ari	5.8:	—	F0	0.0325	+3.4:
1173	ν Gem	4.00	-0.20	B7 IV	0.0095	-1.12
1609	95 Aqr	5.2:	—	A0	0.0050	-1.3:
1623	20 Psc	5.6:	—	K0	0.0100	+0.6:
N γ	HR 1616	6.5:	—	A5	0.0095	+1.4:
N0	HR 8748	4.70	+1.37	K4 III	0.0105	-0.20
SA	κ Oct	5.6:	—	A2	0.0090	+0.4:
II.						
15	λ' Phe	4.81	-0.10	A0 V	0.0160	+0.83
250	51 Aur	5.7:	—	K0	0.0240	+2.6:
476	γ Cen	2.14	-0.12	A0 III	0.0205	-1.30L
709	θ Ser A	4.59	+0.03	A5 V	0.0240	+1.49
	θ Ser B	4.99	+0.08	A5		+1.89

A Faint companion disregarded.

L Corrected for equal components.

Considering the reality of the Hyades Group as established, an attempt was made to pick out possible members among the nearest stars, and the convenient listing by Gliese (1957) of the stars that may be closer than 20 parsecs was examined for this purpose. These objects are, in general, fainter than those discussed above and the observed proper motions and radial velocities are therefore less accurately determined; only estimates of the proper motions of the faintest stars are available and the radial velocities have not been obtained for about 20 per cent. The 32 stars, and binary systems, selected as quite likely group members are given in Table III together with the following information:

No./Name: the number in the Yale parallax catalogue (Jenkins 1952) and the name or DM number of the star.

μ , θ_0 , Auth., $\Delta\theta\sin\lambda$: the observed proper motion, its position angle and source, and the normalized value of the position-angle residual.

ρ_c , ρ_0 : the computed and observed radial velocities. The observed values, the observatory abbreviations and the number of plates, were taken from the catalogue compiled by R. E. Wilson (1953); the designations C_1 (Evans, Menzies and Stoy 1957), Dy (Dyer 1954) and Sa (Sahade 1952) indicate determinations not included in that catalogue.

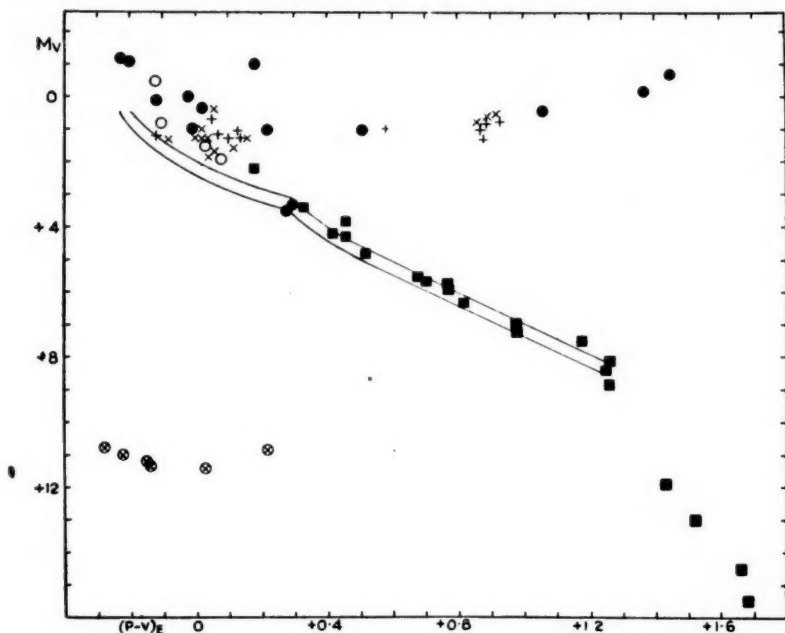


FIG. 1.—The colour-luminosity array for the Hyades Group. The filled circles represent the class I members from Table II, the open circles the class II members. The crosses and plus signs indicate the brightest members of the Hyades and Praesepe clusters, respectively. The possible members among the nearest stars are represented by filled squares and the five known white dwarf members of the Hyades cluster by crossed circles.

π_g : the group parallax computed from the relation $\pi_g = 4.74 \mu / 43.95 \sin \lambda$, V_E , $(P-V)_E$: the visual magnitude and colour. When a colour is listed, both it and the magnitude are photoelectric determinations on the $(P, V)_E$ -system (Eggen 1955a) or reduced to that system from several sources (Johnson and Morgan 1953; Johnson 1955; Evans, Menzies and Stoy 1957); when a colour is listed with a magnitude given only to one decimal, the listed values were both reduced from the red and infra-red magnitudes published by Kron (1956).

Sp, M_v : the spectral type, from several sources mostly on the Yerkes or Mt Wilson systems, and the absolute visual magnitude computed from the group parallax.

TABLE III

Possible members of the Hyades Group among the nearer stars

No./Name	θ_0	$\Delta\theta \sin \lambda$	Auth.	μ	ρ_c ρ_0 km/sec	π_g	V_R	$(P-V)_R$	Sp.	M_V
45	80°	4°	Cin 20	0.55	+ 3 +12W(3)	0.060	8.96	+1.26	dM0	+ 8.83
+40°45										
66	83	0	GC	0.647	- 2 +6W(3)	0.0725	8.0:	—	dK6	+ 7.3:
-27°108	84	1	Cape	0.671						
	86	3	Yale	0.671						
97	93	+9	GC	0.410	+ 2 +9Yk(90)	0.0445	5.18	+0.42	F8 V	+ 3.43*
13 C 24										
162	78	-2	GC	0.529	+ 3 +5W(3)	0.0565	7.11	+0.77	dG7	+ 5.87
-23°315	76	-4	Cape	0.516						
177	86	+5	GC	0.620	+ 3 -5W(3)	0.0670	7.13	+0.82	K3 V	+ 6.26
-31°325					+2McD(2)					
					+11C ₁ (6)					
257	74	0	GC	0.686	+ 3 +11L(12)	0.0740	4.91	+0.46	F8 V	+ 4.26
e Phe										
UV Cet	80	+3	Luyten	3.355	+12 +29W(4)	0.385	11.8	+1.68	dM6	+14.8*
350	100	+2	GC	0.823	+14 +4L(5)	0.0940	4.94	+0.52	G2 V	+ 4.81
+41°328					+5B(3)					
					+1W(6)					
					+2V(1)					
551	92	-2	GC	0.387	+16 +17L(3)	0.0460	5.42	+0.46	F9	+ 3.73
+18°339										
724	57	-3	GC	0.614	+28 +31W(4)	0.0870	8.39	+1.26	dM0	+ 8.09
-20°643	56	-4	Yale	0.634						
754	50	+4	Cape	0.514	+17 +22Sa(6)	0.0605	8.57	+1.18	K6	+ 7.48
-48°1011										
808	124	+8	Cin 20	0.42	+33 +38 Dy(2)	0.068	9.7:	—	K7	+ 8.4:
+25°613										
1010	145	0	Yale	0.55	+28 +36W(6)	0.077	8.66	+1.25	dM1	+ 8.19
+52°857										
1668	207	+3	Ross	1.03	+37 +52W(5)	0.204	11.5	+1.52	dM5	+13.0
Ross 986					-25McD(1)					
1864	320	-6	GC	0.314	+30 +29L(4)	0.0460	5.03	+0.33	F5 V	+ 3.34
-34°4036					+27C(4)					
					+27C ₁ (4)					
2117	244	-2	GC	0.537	+33 +26W(7)	0.0875	5.96	+0.77	dK0	+ 5.67
+28°1660					+28V(3)					
2256	281	+4	Grnwh.	0.52	+30 +27W(3)	0.076	7.4:	—	dK5	+ 6.8:
+6°2182										
2403	209	-4	Cape	0.27	+11 0C ₁ (4)	0.030	8.17	+0.68	G8 V	+ 5.51
-46°2953										
2480	280	+3	Luyten	0.68	+20 +21W(4)	0.082	12.5:	—	dM4	+12.1:
L1113-55										
2701	287	+4	GC	0.710	+ 2 +13C ₁ (4)	0.0765	7.77	+0.98	K5 V	+ 7.19
-43°7228	290	+6	Cape	0.703						
2841	276	-1	GC	0.146	+ 3 + 4W(4)	0.0160	6.18	+0.18	dA8	+ 2.20
+26°2329					+ 9V(10)					
2890	276	-2	Wolf	1.87	- 2 - 5W(6)	0.202	12.2	+1.66	M7	+13.8*
Wolf 424AB										
3101	270	-4	Ross	0.38	-15 -26Dy(1?)	0.044	9.3:	—	K5	+ 7.5:
3458	266	-5	Titus	1.21	-31 -30W(4)	0.184	10.56	+1.43	dM5	+11.89
-7°4003										
4049	347	-3	GC	0.345	- 8 + 2W(3)	0.0375	9.18	+0.98	dM0	+ 7.05
+71°851										
5076	94	0	GC	0.388	-33 -37W(4)	0.0630	7.1:	—	dK1	+ 6.1:
-14°5936										
5487	86	-9	Cape	0.391	-19 -21C ₁ (5)	0.0440	7.41	+0.705	G8 V	+ 5.63
-32°17191										

*Luminosity corrected for equal components before plotting in Fig. 1.

The colours and luminosities in Table III are represented in Fig. 1 with filled squares. Also, for completeness, the following known white dwarf members of the Hyades cluster are plotted in the figure as crossed circles:

Name	V	$(P-V)$	M_V
	m	m	
H-Z 4	14.47	+0.03:	+11.4
H-Z 7	14.18	-0.15:	+11.2
H-Z 9	13.95	+0.22:	+10.9
H-Z 14	13.83	-0.28:	+10.8
VR 7	14.29	-0.14:	+11.3
VR 16	14.02	-0.22:	+11.0

The magnitudes and colours were determined on the ($B-V$)-system by D. L. Harris (1957); the colours on the ($P-V$)_E-system are uncertain since the transformation equations used may not be applicable to white dwarfs. The luminosities have been derived from a mean modulus of $+3^m.03$ for the Hyades cluster (van Bueren 1952).

TABLE IV

Trigonometric, spectroscopic and group parallaxes of Hyades Group stars
(unit = $0''.001$)

Name	π_g	π_{tr}	$\pi_{gp}(w)$
+20°45	60	81M(7), 22 St(4)	72
-27°108	72	48C(7)	76
λ' Phe	16	18Y(10)	-
13 Cet	44	28M(5), 50Y(10), 64S(20), 75C(6)	46
-23°315	56	58Y(10), 53C(7)	48
-31°325	67	100C(8)	83
ν Phe	74	74Y(8), 76C(6)	-
δ Cas	34	25A(20), 60M(8), 10W(8)	52
<i>UV</i> Cet	385	385 (Gliese 1957)	-
+41°328	94	84A(20), 93M(6)	72
+18°339	56	53M(10)	-
74 Ari	32	30A(28)	30
-20°643	87	98C(6), 64Y(10), 65V(8), 40M(7)	110
ν Gem	10	8Y(10), 11M(8)	-
κ Ret	59	55Y(10), 47C(8)	-
-48°1011	60	72Y(12), 99C(7)	-
+25°613	68	85M(6)	-
+52 857	77	88V(12), 82M(7), 94Yk(7)	100
HR1616	10	-	-
51 Aur	24	-	-
Ross 986	46	68Y(12), 66C(7)	46
+28°1660	88	72A(16), 77M(7)	60
10 UMa	72	70A(16), 74M(8), 69S(20)	69
+6°2182	76	77M(6), 90V(10)	69
-42°2953	30	60C(6)	-
λ UMa	21	-12M(7)	-
L1113-55	82	65Yk(7)	-
-43°7228	76	70Y(12), 85C(6)	-
γ Crv	18	-	-
+26°2329	16	56M(8)	-
Wolf 424	202	218M(7), 215Y(5), 224Yk(8)	-
γ Cen	20	14Y(10), 18c(10)	-
α CVn	26	25A(20), 31M(4), 8Yk(8)	-
ζ Vir	32	38A(28), 38M(6), 22Y(12)	-
κ Oct	9	-	-
-7°3646	44	58M(8)	-
-7°4003	184	142M(8), 135Y(10), 173V(10), 144C(6)	-
γ Her	11	15A(16)	30
+71°851	38	60G(7)	-
-14°5936	63	54M(6), 48C(7)	55
γ Cap	27	14M(6), 30Y(10), 22C(7)	35
-32°17191	44	55C(7)	-
HR8748	10	0G(8)	10
ν Peg	21	36A(14), 8M(7)	44
95 Aqr	5	6A(20), 10Y(7)	-
20 Psc	10	-	10

The comparison between the group parallaxes, for the stars in Table IV, and the absolute trigonometric values (Jenkins 1952) and spectroscopic determinations made at Mt Wilson (Adams *et al.* 1935) is given in Table IV. The observatory abbreviations used to designate the source of the trigonometric values, and the weight of the determinations, in parentheses, are those assigned by Jenkins. In most cases the group parallax is within the range covered by the trigonometric and spectroscopic values although a few stars may be eliminated as group members when more accurate parallaxes, velocities and proper motions become available.

Sirius Group.—The well-determined space motion relative to the Sun of α Canis Majoris can be expressed as follows:

$$A = 20^h 44^m, \quad D = -42^\circ.7, \quad V = 18.4 \text{ km/sec}, \quad \pi = 0''.375.$$

This bright star has been included in most listings of members of the Ursa Major stream. This latter stream has often been considered an extension of the so-called Ursa Major nucleus cluster. However, although this "cluster" is only about 50 or 60 parsecs from the Sun, even the most extensive searches have not yielded more than a dozen members and it seems more likely that it is a local condensation, rather than the nucleus, of the stream. The difficulties peculiar to the determination of the convergent point of the motion of the Ursa Major stars have been extensively investigated by Brown (1950) and by Petrie and Moyls (1953). The numerous lists of possible members of the extended cluster have been collated by Roman (1949) and the collated list has been used to select members of what will here be called the "Sirius Group".

After eliminating 22 stars with proper motions less than $0''.02$ and 4 stars with no available radial velocity determination, values of θ_c and ρ_c , based on the convergent point and velocity given above for Sirius, were computed for the remaining 122 stars in Roman's list of "probable members of the Ursa Major stream". The following preliminary criteria for group membership were adopted: $(\theta_o - \theta_c) \sin \lambda < 10^\circ$; $\rho_o - \rho_c \leq 5, 6$ and 7 km/sec for velocities of quality a, b and c , respectively. The 58 accepted stars are listed in Table V; the rejected stars are in Table VI. Table V also includes seven stars, indicated by (§) following the luminosities in the last column, which were recovered from Roman's list of "stars probably not members of the Ursa Major stream"; most of these stars are south of -30° and were not observed by Roman. If similarly stringent criteria were applied to the values of $\theta_o - \theta_c$ listed by Roman, approximately the same selection of stars would result; a not surprising result since her tabulated values are based on $A = 20^h 28^m, D = -36^\circ.7, V = 17.0$ km/sec.

Although the proper motions for all except a half dozen stars in Table V are contained in the *General Catalogue* (Boss 1937), they are on the average much less accurately determined than those of the FK3 stars used in the discussion of the Hyades Group and none of the stars could be eliminated from group membership on the basis of the tabulated values of $\Delta\theta \sin \lambda$. The observed radial velocities and their quality, Q , have been taken from Wilson's catalogue (1953). Weighting values of quality a, b and c by 3, 2 and 1, respectively, the weighted mean value of $\Delta\rho$ is -0.1 km/sec and the average value without regard to sign is 3.4 km/sec. Although there do appear to be systematic runs to $\Delta\rho$ in localized areas—for example all of the Ursa Major stars have positive residuals and most of the Leo-Hydra stars negative residuals—the general agreement is satisfactory, especially since many of the stars have spectra that are difficult to measure.

TABLE V

Name	θ_0	$\Delta \theta \sin \lambda$	Members of the Sirius Group										M_V
			ρ_0	$\Delta \rho$	Q	μ	π_g	V_E	$(P-V)_E$	Sp			
			(km/sec)			"	"	m	m				
ϕ^2 Cet	226°	-1°	+ 8	-1	a	0.320	0.0930	5.20	+0.39	F8 V	+5.04		
27 Cet	233	-6	+12	+4	b	0.047	0.0135	6.13	+0.91	Ko III	+1.78		
HR 647	228	-5	- 8	0	b	0.087	0.0250	6.07	+0.28	F5 V	+3.06*		
HR 710	234	+5	+ 8	+4	c	0.074	0.0195	5.84	+0.02	A7p	+2.29		
ν Cet	231	+4	+ 5	+5	a	0.038	0.0100	4.86	+0.77	G5 III	-0.14		
γ Cet	224	-3	- 5	-4	b	0.203	0.0525	3.46	-0.01	A2 V	+2.06†		
								10.14	+1.22	K7 V	+8.74		
HR 1016	219	-8	+ 8	+5	b	0.033	0.0085	5.52	+0.79	G5 III	+0.16		
HR 1327	268	+1	-18	-4	a	0.027	0.0100	5.27	+0.715	G5 III	+0.27		
ξ Eri	221	-3	-10	-4	c	0.075	0.0205	5.17	-0.04	A2	+1.73		
2 Aur	249	+4	-16	-3	a	0.025	0.0090	4.77	+1.34	K3 III	-0.46		
β Eri	229	+8	- 8	-2	c	0.122	0.0335	2.78	0.00	A3 III	+0.40		
γ Lep	218	+4	-10	-5	a	0.470	0.1240	3.59	+0.36	F6 V	+4.05		
								6.18	+0.85	dK5	+6.64		
β Aur	265	+3	-18	-2	a	0.051	0.0260	1.90	-0.09	A2 IV	-1.03†		
δ Col	208	+2	- 3	+1	a	0.064	0.0170	3.76	+0.79	gG5	-0.09§		
α CMa	207	0	- 8	0	a	1.324	0.3750	-1.47	-0.125	A2 V	+1.40		
16 Lyn	259	-5	- 9	+6	c	0.020	0.0085	4.89	-0.09	A2 V	-0.46		
HR 3131	191	+1	-12	-3	c	0.048	0.0140	4.61	-0.03	A3 V	+0.34		
HR 3279	188	+3	- 8	0	c	0.022	0.0065	5.58	+0.67	G2 III(A)	-0.36†		
π' UMa	344	-4	-12	+5	c	0.088	0.0610	5.64	+0.52	Go V	+4.57		
HR 3512	174	-5	- 8	-3	b	0.049	0.0130	4.92	+0.81	G3	+0.49§		
α Vol	179	+2	+ 5	-1	b	0.104	0.0285	4.00	+0.03	A5 V	+1.28§†		
ν' Hya	157	-8	-14	-5	a	0.035	0.0110	4.14	+0.84	G5 III	-0.65		
34 Leo	137	-9	-16	-1	b	0.057	0.0260	6.44	+0.35	F6 V	+3.51		
ζ Leo	124	-7	-15	+1	b	0.023	0.0130	3.43	+0.19	Fo III	-1.00		
37 UMa	63	0	-12	+5	a	0.074	0.0500	5.14	+0.22	F1 V	+3.63		
HD 97686	42	+3	-21	-7	c	0.080	0.0325	7.32	+0.47	F8 V	+4.88		
β UMa	71	0	-12	+4	a	0.087	0.0520	2.36	-0.15	Ao V	+0.94		
61 Leo	158	+6	-14	-3	a	0.040	0.0120	4.55	+1.58	K5 III	-0.05§		
δ Leo	133	0	-21	-6	b	0.201	0.0845	2.57	+0.02	A4 V	+2.21		
τ Leo	135	+8	- 9	+2	a	0.025	0.0080	4.95	+0.91	G8 II	-0.53		
ξ CrI	138	-9	- 5	0	a	0.051	0.0130	4.63	+0.88	G8 III	+0.20		
γ UMa	88	0	-13	+3	a	0.084	0.0450	2.44	-0.125	Ao V	+0.71		
δ UMa	88	0	-13	+2	b	0.106	0.0475	3.29	-0.05	A3 V	+1.68		
HD 109011	93	-1	-13	+1	b	0.111	0.0465	8.12	+0.84	K2 V	+6.46		
HR 4803	142	-2	- 1	0	a	0.123	0.0315	5.45	+0.22	F2 V	+2.95		
29 Com	135	+3	- 7	+3	b	0.045	0.0135	5.70	-0.10	A2	+1.35		
HR 4867	93	+1	-12	+2	b	0.107	0.0430	5.85	+0.34	F6 V	+4.02		
41 Vir	123	-8	-10	-1	c	0.059	0.0175	6.25	+0.15	A7p	+2.47		
ϵ UMa	96	-1	- 9	+5	a	0.113	0.0445	1.78	-0.13	Aop	+0.03		
78 UMa	98	-1	-10	+4	b	0.115	0.0445	4.94	+0.25	F2 V	+3.19		
HD 115043	105	+3	- 9	+4	b	0.117	0.0440	6.83	+0.50	G2 V	+5.05		
γ Hya	127	-9	- 5	-5	a	0.086	0.0220	2.99	+0.80	G5 III	-0.30		
ζ UMa	103	-1	- 9	+4	a	0.127	0.0460	2.04	-0.10	A2 V	+0.35†		
80 UMa	101	-3	- 8	+5	a	0.121	0.0440	4.00	+0.04	A5 V	+2.22		
HR 5214	123	0	-12	-2	b	0.035	0.0110	6.65	-0.01	A5 III	+1.86		
HR 5373	134	+9	-10	-1	b	0.029	0.0085	6.35	-0.10	A2	+0.89		
HR 5473	123	-8	- 8	-5	b	0.062	0.0160	6.0:	—	A2	+2.0.§		
HR 5492	117	-3	- 6	+5	b	0.080	0.0260	6.25	+0.30	F2 III	+3.32		
45 Boo	134	+3	- 7	-3	b	0.255	0.0675	4.93	+0.32	F5 V	+4.08		
α CrB	129	-4	+ 2	+5	a	0.154	0.0405	2.22	-0.14	Ao V	+0.26		

TABLE V (continued)

Name	θ_0	$\Delta\theta \sin \lambda$	$\rho_0 \Delta\rho$ (km/sec)	Q	μ	π_g	V_E	$(P-V)_E$	Sp	M_V
					"	"	m	m		m
HR 5840	132	-2	+ 3 + 3	a	0.034	0.0085	6.01	+0.81	G5 III	+0.65
β Ser	130	-5	- 1 - 1	b	0.086	0.0220	3.66	-0.05	A2 IV	+0.37
							9.95	+0.90	dK3	+6.66
HD 151044	134	-4	0 + 5	c	0.170	0.0455	6.47	+0.44	F8 V	+4.76
HR 6917	153	-2	+ 8 + 5	a	0.028	0.0075	5.83	-0.06	A2 V	+0.21
5 Aql	158	+6	+19 + 7	c	0.025	0.0085	5.66	+0.05	A2	+0.30
59 Dra	159	-1	- 4 + 5	a	0.129	0.0385	5.12	+0.185	F2 V	+3.05
HR 7382	159	-6	0 - 1	b	0.031	0.0080	5.71	—	gG5	+0.23§
HR 7451	173	+6	+ 1 + 3	b	0.194	0.0500	5.72	+0.36	F8 V	+4.21
HR 8170	186	0	+ 1 - 1	a	0.208	0.0540	6.36	+0.44	F8 V	+5.02
76 Cyg	198	-8	+ 3 + 1	d	0.047	0.0125	6.10	-0.07	A2	+1.58
HR 8473	203	+5	- 3 + 5	b	0.026	0.0075	6.38	-0.175	A0	+0.76
γ PsA	236	-3	+16 0	b	0.042	0.0245	4.48	-0.14	A0 V	+1.42§
δ Aqr	207	-8	+18 + 4	b	0.047	0.0195	3.27	-0.06	A3 V	-0.28
4 And	210	+5	- 6 - 5	b	0.034	0.0095	5.33	+1.34	K5 III	+0.10
99 Aqr	224	-3	+16 + 2	a	0.078	0.0315	4.38	+1.41	K5 III	+1.88
λ Psc	223	+5	+12 + 3	b	0.199	0.0595	4.52	+0.08	A7 V	+3.39

* Companion disregarded.

† Not plotted in Fig. 2: Companion between $0^m.5$ and $2^m.5$ fainter.

‡ Luminosity corrected for equal companion before plotting in Fig. 2.

|| Indicated by a cross in Fig. 2.

§ Selected from Roman's list of "stars probably not members of the Ursa Major stream".

The values of π_g listed in Tables V and VI were computed from the relation $\pi_g = 4.74\mu/18.4 \sin \lambda$; the proper motions are uncorrected GC values except for a half-dozen taken from the Yale zone catalogues. The colours and magnitudes are by Eggen (1955a) and by Johnson and Knuckles (1957); when more than one determination was available, unweighted means were formed. The spectral types for a few stars are by Johnson and Morgan (1953) and the remainder are by Roman (1949).

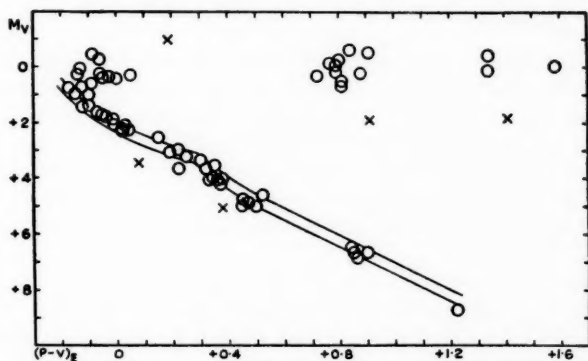


FIG. 2.—The members of the Sirius Group listed in Table V; the crosses indicate the five stars that stand out from the general run of the other members and may have been accidentally admitted to group membership.

TABLE VI

Stars included by Roman as "probable members of the Ursa Major stream" but rejected as members of the Sirius Group

Name	$\Delta\theta \sin \lambda$	$\Delta\rho$	Q	μ	π_g	Name	$\Delta\theta \sin \lambda$	$\Delta\rho$	Q	μ	π_g
σ And	25°	10	a	0.071	0.0185	8 Vir	5°	7	b	0.050	0.0135
η And	2	11	a	0.054	0.0140	τ Vir	16	5	b	0.030	0.0135
39 And	29	8	b	0.025	0.0065	κ Boo	13	6	a	0.064	0.0205
80 Psc	10	3	b	0.320	0.0850	HR 5343	0	10	c	0.055	0.0150
89 Psc	25	1	b	0.055	0.0145	18 Boo	21	2	a	0.110	0.0290
χ Cet	12	7	b	0.176	0.0475	ζ Boo	15	2	b	0.058	0.0150
HR 534	27	10	b	0.076	0.0195	ξ Boo	3	8	a	0.172	0.0450
HR 792	5	8	b	0.031	0.0080	8 Ser	17	4	b	0.080	0.0205
HR 875	10	15	c	0.050	0.0130	η Cr B	14	3	a	0.236	0.0625
HR 906	0	10	b	0.049	0.0170	HR 5830	17	5	b	0.158	0.0440
HR 919	30	14	b	0.152	0.0400	HR 5859	3	14	b	0.032	0.0085
HR 1046	9	12	b	0.044	0.0145	ω Ser	20	7	a	0.062	0.0160
HR 1448	16	0	b	0.022	0.0060	v CrB	10	4	c	0.030	0.0080
7 Cam	16	6	a	0.020	0.0080	ω Her	10	9	a	0.077	0.0200
38 Ori	17	1	c	0.036	0.0110	52 Her	19	3	a	0.066	0.0175
τ Aur	15	5	a	0.033	0.0155	56 Her	15	0	a	0.028	0.0070
λ' Ori	11	0	a	0.204	0.0780	α Oph	17	7	b	0.260	0.0710
42 Aur	15	8	c	0.042	0.0240	HR 6993	11	1	a	0.025	0.0080
RR Lyn	13	3	a	0.027	0.0155	11 Aql	16	7	a	0.126	0.0370
λ Gem	10	7	b	0.061	0.0290	16 Lyr	10	8	b	0.089	0.0230
9 Pup	2	8	a	0.345	0.1050	18 Sge	21	12	b	0.026	0.0075
9 Hya	1	9	b	0.094	0.0285	HR 7781	24	4	c	0.026	0.0070
18 UMa	13	3	b	0.078	0.0935	35 Cap	10	6	c	0.040	0.0275
21 LMi	17	0	a	0.053	0.0465	ρ Cyg	6	6	a	0.094	0.0240
ϵ Leo	18	3	a	0.188	0.0670	HR 8263	22	4	b	0.029	0.0110
α Crv	25	7	a	0.096	0.0250	HR 8407	15	1	b	0.038	0.0200
HR 4725	1	7	b	0.074	0.0255	32 Aqr	2	7	a	0.052	0.0190
HO 110463	3	7	b	0.128	0.0520	π Peg	18	2	b	0.027	0.0070
HR 4837	11	8	a	0.095	0.0260	66 Aqr	6	7	a	0.039	0.0180
HD 238179	10	20	c	0.096	0.0375	15 And	3	16	c	0.047	0.0120
HD 238208	8	29	c	0.108	0.0405	ψ Peg	20	7	a	0.049	0.0130
γ Hyd	10	5	a	0.086	0.0220						

The colours and luminosities are plotted in Fig. 2. Five stars, distinguished only by the fact that two fall well below the standard main sequence and the other three above it, in regions uncommon to the run of the rest of the group members, are indicated by crosses. It is possible that these five stars, and perhaps others not so distinguished, are accidental "members" of the group. The remaining stars form a compact main sequence with little dispersion for stars bluer than $+0^m.5$ and a compact group of yellow giants of spectral type near G5 and $M_V \sim 0$.

The colour-luminosity array constructed for these same stars, with luminosities derived from the group parallaxes computed by Roman, is nearly identical with Fig. 2, the only noticeable difference being that it exhibits roughly twice the dispersion in the main sequence. The scattering of yellow giants with $M_V \sim +1$ to $+2$ that were included in Roman's list of members of the Ursa Major stream have, except for the two indicated with crosses in Fig. 2, been excluded by the membership criteria employed here for the Sirius Group. Also, Roman included

nine stars with computed luminosities brighter than $M_V = -1$ but eliminated five of them on the basis of the spectroscopic parallaxes; the other four were eliminated here, two with $\mu < 0''.02$ and two, listed in Table VI, which did not meet the membership requirements for the Sirius Group.

TABLE VII

Group, trigonometric and spectroscopic parallaxes for members of the Sirius Group
(unit $0''.001$)

Name	π_g	π_{tr}	$\pi_{sp}(w)$
ϕ^3 Cet	93	72M(8), 48Y(12), 56C(7)	60
27 Cet	14	—	8
HR 647	25	45M(7), 11W(7), 35S(8)	—
HR 710	20	15Y(8)	—
ν Cet	10	6M(7), -8Y(12), -11C(8)	13
γ Cet	52	48A(28), 48M(8), 47Y(8), 45Yk(7)	40
HR 1016	8	—	10
HR 1327	10	—	13
ξ Eri	20	11A(28), 11M(8), -19Y(8), 12C(7)	—
2 Aur	9	—	11
β Eri	34	33A(28), 50M(8), 53Y(16)	63
γ Lep	124	145M(8), 100Y(12), 123C(10)	110
β Aur	26	39A(28), 27M(8)	63
δ Col	17	12Y(16)	—
α CMa	375	375 (Mean)	363
16 Lyn	8	7A(28)	—
HR 3131	14	14Y(12)	—
HR 3279	6	—	10
π' UMa	61	—	50
HR 3512	13	21Y(8)	—
α Vol	28	13Y(10)	—
ν' Hya	11	11M(10), 19Y(10)	17
34 Leo	26	—	—
ζ Leo	13	9A(20), 6M(8)	30
37 UMa	50	32A(12), 4M(7)	32
HD 94686	32	—	—
β UMa	52	46A(20), 26M(8)	46
61 Leo	12	24Y(10)	10
δ Leo	84	29A(28), 74M(8)	79
τ Leo	8	33A(20), 23Y(8)	9
ξ Crt	13	22Y(10)	14
γ UMa	45	26A(20), -1M(8)	—
δ UMa	48	49A(28), 64M(5)	—
HD 109011	46	—	—
HR 4803	32	30Y(10)	33
29 Com	14	—	—
HR 4867	43	37A(12), 41W(4)	27
41 Vir	18	—	16
ϵ UMa	44	6M(10)	—
78 UMa	44	29A(16)	24
HD 115043	44	45W(6)	—
γ Hya	22	18M(7), 29Y(8), 13C(7)	29
ζ UMa	46	39A(20), 32M(8)	38
80 UMa	44	38A(16), 30M(7)	—
HR 5214	11	—	—
HR 5373	8	—	—
HR 5473	16	—	—

TABLE VII (continued)

Name	π_g	π_{tr}	$\pi_{sp}(w)$
HR 5492	26	17A(28)	22
45 Boo	68	57A(16), 68M(6)	46
α CrB	40	37A(20), 57M(8)	79
HR 5840	8	—	7
β Ser	22	34A(16), 30M(8)	—
HD 151044	46	35A(28)	—
HR 6917	8	—	10
5 Aql	8	—	17
59 Dra	38	46A(28)	—
HR 7382	8	—	8
HR 7451	50	35A(20)	33
HR 8170	54	37A(28)	—
76 Cyg	12	14A(20), 6M(7)	—
HR 8473	8	—	—
γ PsA	24	36Y(8)	—
δ Aqr	20	32M(7), 42Y(12)	33
4 And	9	—	8
99 Aqr	32	—2Y(10)	8
λ Psc	60	30A(10), 15Y(10)	—

The group parallaxes given in Table VI are compared with the trigonometric and spectroscopic values in Table VII. The agreement for most of the stars is satisfactory; the agreement for at least two of the five stars indicated in Fig. 2 by crosses, is as unsatisfactory as any in the table.

Discussion.—The space motions of the Hyades and Sirius Groups, relative to the Sun, in U, V, W space are as follows (U ; $l=178^\circ$, $b=0^\circ$; V ; $l=58^\circ$, $b=0^\circ$; W ; $b=+90^\circ$):

	U	V	W	
Hyades	+40	-18	-2	km/sec
Sirius	-14	0	-12	km/sec.

The galactic orbits of the group members are, therefore, of type *A* for the Sirius Group and type *B* for the Hyades Group in the notation of a previous paper (Woolley and Eggen 1958); that is, the points of closest approach of the orbits to the galactic centre are about 200 (Sirius) and 600 (Hyades) parsecs closer to the centre than the present positions of the stars. Also, the colour-luminosity arrays for the two groups are similar to those derived previously (Woolley and Eggen 1958) for stars within 20 parsecs of the Sun and with galactic orbits of the same types.

An interesting aspect of the colour-luminosity arrays in Figs. 1 and 2 is their interpretation in the light of current theories of stellar evolution (Sandage 1954). Omitting for the moment the five stars indicated with crosses in Fig. 2, the array for the Sirius Group shows an absence of O- and B-type stars, an A-type main sequence similar to that of the Pleiades, and a sharply defined "break-away" from the main sequence at $M_V = +0^m.5$. The A-type stars in the Hyades Group, however, are above the main sequence and show considerably greater dispersion for a given colour. Also, the Hertzsprung gap is more marked in the Sirius Group with a large concentration of G5 giants on the red end of the gap; the composite spectra of HR 3279 in Table VI, G2 III + A, indicates that the components of this binary straddle the gap with the A-type star being the fainter.

The yellow giants of the Hyades Group show a greater spread in colour, although there is some concentration near a colour of $+0^m.9$, or spectral type Ko, due to the members of the Praesepe and Hyades clusters. From the evolutionary theory, therefore, these features indicate that the Sirius Group is younger than the Hyades Group.

The galactic distribution of the group members and the dynamics of the group motions will be included in a later discussion to be published by the author and R. v. d. R. Woolley.

I am greatly indebted to the Astronomer Royal for many stimulating discussions and for any cogency the mathematical arguments used here may have. The extensive computations were all made at least once by the author and repeated by Mr J. Alexander and Miss L. Mather of the Observatory computing section. Thanks are due to the machine section of the Nautical Almanac Office for subsidiary computational aid.

Royal Greenwich Observatory,
Herstmonceux Castle:
1957 November.

References

- Adams, W. S., Joy, A. H., Humason, M.L., and Brayton, A. M., 1935, *Ap. J.*, **81**, 187;
Mt. Wilson Contr. No. 511.
Bok, B. J., 1934, *Harvard Circular* No. 384.
Bok, B. J., 1946, *M.N.*, **106**, 61.
Boss, B., 1912, *A. J.*, **27**, 83.
Boss, B., 1937, *General Catalogue of 33342 Stars for the Epoch 1950*, Carnegie Inst. of Wash. Publ. No. 468.
Brown, A., 1950, *Ap. J.*, **112**, 225.
van Bueren, H. G., 1952, *B.A.N.*, **11**, 385.
Dyer, E. R., 1954, *A. J.*, **59**, 218.
Eddington, A. S., 1914, *Stellar Moments and the Structure of the Universe*, London.
Eggen, O. J., 1955a, *A. J.*, **60**, 131; *Lick Obs. Bull.* No. 532.
Eggen, O. J., 1955b, *A. J.*, **60**, 401; *Lick Obs. Bull.* No. 538.
Eggen, O. J., 1958, *Obs.*, **77**, 229.
Evans, D. S., Menzies, A. and Stoy, R. H., 1957, Unnumbered Cape Mimeogram.
Gliese, W., 1957, *Mitt. Astr. Rechen-Inst. Heidelberg*, 8.
Harris, D. L., 1957, *Ap. J.*, **124**, 665.
Jenkins, L., 1952, *General Catalogue of Trigonometric Stellar Parallaxes* (Yale University Obs.).
Petrie, R. M. and Moyls B. N., 1953, *M.N.*, **113**, 239.
Johnson, H. L., and Morgan, W. W., 1953, *Ap. J.*, **117**, 313; *McDonald Contr.* No. 216.
Johnson, H. L. and Knuckles, C. F., 1957, *Ap. J.*, **126**, 113.
Johnson, H. L., 1955, *Ann. d'Astroph.*, **18**, 292.
Kopff, A., 1937, *Veroff. Astron. Rechen-Inst. Berlin-Dahlem*, No. 54.
Kopff, A., 1938, *Abh. Preuss. Akad. Wiss. Berlin, Phys-Math. Kl.*, 3.
Kron, G. E., 1956, *Third Berkeley Symposium on Mathematics and Statistics*, 3, 39.
Proctor, R., 1869, *Proc. Roy. Soc.* **18**, 169.
Roman, N. G., 1949, *Ap. J.*, **110**, 205.
Sahade, J., 1952, *Ap. J.*, **117**, 234.
Sandage, A. R., 1954, Liège Symposium: *Les Processus Nucleaires dans les Astres*.
Stromberg, G., 1922, *Ap. J.*, **56**, 265; *Mt. Wilson Contr.* No. 245.
Wilson, R. E., 1932, *A. J.*, **42**, 49.
—1953, *General Catalogue of Stellar Radial Velocities*, Carnegie Inst. of Wash. Publ. No. 601.
Woolley, R. v. d. R. and Eggen, O. J., 1958, *M.N.*, **118**, 57.

A RE-EXAMINATION OF THE SPACE MOTIONS AND LUMINOSITIES OF THE STARS OF THE CASSIOPEIA-TAURUS GROUP BASED UPON NEW RADIAL VELOCITIES*

R. M. Petrie

(Received 1957 December 9)

Summary

Results are presented of an investigation of the motions of 49 stars composing the Cassiopeia-Taurus group. New radial velocities of 40 stars are given, based upon 668 spectrograms. Seven stars are found to vary in radial velocity. The new velocities are, on the average, 2 km/sec more negative than existing catalogue values. Spectroscopic absolute magnitudes of 46 stars are measured.

Proper motions are used to find the convergent point of the group and radial velocities then supply the stream motion and K -term. Correcting the observed motions for differential galactic rotation, the convergent point is at $A=97^\circ$, $D=-18^\circ$; the stream motion $S=23.9$ km/sec and the K -term is -1.2 km/sec. Including corrections for differential galactic rotation, the elements of the motion are $A=97^\circ$, $D=-15^\circ$, $S=20.1$ km/sec, $K=+0.4$ km/sec.

It is concluded that the stars are a sample of the general population in that they possess normal solar motion plus average random motion. This conclusion is confirmed in a general way by plots of the space motions after standard solar motion is removed. Furthermore the motions do not show an expansion of the stars from a common region.

The mean parallax deduced from the assumption of standard solar motion agrees exactly with the mean of the individual spectroscopic parallaxes.

Introduction.—The bright B stars in the Milky Way between Cassiopeia and Orion form a distinctive group with large proper motions approximately parallel in direction. The apparently common motion led Kapteyn (1), Eddington (2) and Boss (3) to suggest cluster motion for a number of the stars and this was followed by more detailed studies by Rasmuson (4) and by Smart and Ali (5). Rasmuson considered the stars to form a moving cluster, in the classical sense, but Smart and Ali decided that there existed little evidence to support that conclusion.

An extensive study of the motion of the group, augmented by some additional members, has been published recently by Blaauw (6). Having access to the new proper motions derived by Morgan (7) and the radial velocities of the new catalogue (8) his results, derived from the motions, should be more accurate than the earlier results. The space motion of the group is calculated from data for thirty-eight stars, and forty-nine stars were finally considered as probably qualifying for membership. After solving for the convergent point and stream

* Contributions from the Dominion Astrophysical Observatory, No. 61. Published by permission of the Deputy Minister, Department of Mines and Technical Surveys, Ottawa, Canada.

motion, Blaauw calculated parallaxes and absolute magnitudes for the individual stars and used these data in a calibration of the Yerkes luminosity classes of main-sequence stars of spectral types B2 and B3. He concluded that the motion showed a real divergence from standard solar motion and, from the appearance of a large K -term, that the stars had "a more or less related origin" and that the "expansion age" of the group is about 70×10^6 years.

The interest attached to Blaauw's results and the importance of this group of relatively nearby B stars as calibrating objects suggested that it would be worth while to strengthen the radial-velocity material with additional observations. The stars of this group generally exhibit spectra containing a few diffuse lines of hydrogen and helium and many spectrograms must be measured, therefore, to get a reliable mean velocity. The catalogue values in many cases are based upon a few plates only, from two or more observatories, without any test of the adopted wave-lengths having been applied, and they are, therefore, not homogeneous. Also, binary motion is indicated in a number of cases and this required further investigation.

It is essential that the best radial-velocity data be provided for a study of the motion of this nearby group. First, the numerical value of the stream motion comes entirely from the radial velocities and this, in turn, determines the absolute-magnitude system. Second, the radial velocities determine the K -term and the interpretation based upon it. And, finally, one finds it difficult to decide from the proper motions alone whether community of motion exists. More accurate radial velocities will assist in reaching a decision.

The above considerations led the writer to undertake a new determination of the radial velocities. At the same time the spectrograms could be measured spectrophotometrically to give the total absorption of $H\gamma$ and, consequently, spectroscopic absolute magnitudes. These could then be compared with the magnitudes derived from the motions to furnish a test of the absolute-magnitude system as set up at Victoria.

Radial velocities.—A substantial number of spectrograms was available at Victoria, these having been obtained in an earlier programme (9). It was decided to reduce the measures of these spectrograms anew, employing the wave-length system recently adopted for B-type spectra (10), and then to obtain additional spectra as required. A minimum of ten plates per star was set as adequate coverage.

Spectra were obtained with a variety of dispersions in the early stages of observing. This was systematized by deciding to use a single-prism instrument giving a linear dispersion, at $H\gamma$, of 51 Å/mm. A slit-width somewhat narrower than usual was used (0.038 mm) in order to minimize observational errors; this combined with the greater number of plates obtainable with lower dispersion compensates, it is hoped, for the sacrifice of scale on the spectrograms.

The spectrograms were measured, direct and reversed, using the projection comparator and employing the wave-lengths appropriate to the spectral class and dispersion. New radial velocities have been determined for forty stars out of the forty-nine. A total of 668 Victoria spectrograms was used in obtaining these new velocities. All spectrograms obtained since the early programme were measured by the writer. The new radial velocities are given with the probable errors, etc., in Table I, columns eight to ten. As far as possible only Victoria spectrograms have been allowed to enter into the new determinations

TABLE I
Radial velocities and spectroscopic absolute magnitudes

	H.D.	G.C.	m_V	Type	l	b	Radial velocity				Absolute magnitude			Remarks
							New velocity	n	Wt.	Catalogue value	$H\gamma$	n	M_{SP}	
1	221253	32683	4.89	B4	80°	- 2°	km/sec -13.4±1.0	173	1.0	km/sec -15.9	A 6.1	4	-1.3	Binary, several orbits
2	224559	33252	6.46	B3	82	-16	- 7.1±2.3	11	0.8	- 1.1	4.8	5	-2.0	Binary, range 77 km/sec, poor lines
3	829	228	6.57	B2	82	-26	- 9.8±0.8	10	1.0	- 9.0	5.2	4	-1.8	
4	1976	476	5.36	B4	86	-10	- 7.1±3.9	14	0.7	-12	6.0	4	-1.4	
5	3360	727	3.72	B2	88	- 8	+ 1.5±0.9	10	1.0	+ 2.1	5.0	4	-1.9	γ Cass.
6	3901	828	4.85	B3	90	-12	-13.3±3.1	12	0.7	- 8	5.3	4	-1.7	
7	4180	882	4.70	B5	90	-14	-16.9±1.9	12	0.9	- 8	5.2	4	-1.8	
8	5394	1117	2.25	B0	92	- 2	- 3.4±1.0	11	1.0	- 6.8	6.8	3	-1.0	ϕ Pers.
9	6300	1293	6.50	B4	93	-12	- 3.4±1.0	11	1.0	- 5.4	6.8	3	-1.0	
10	10516	2102	4.19	B0	99	-10	- 3.4±1.0	11	1.0	+ 0.8	6.8	3	-1.0	
11	11241	2241	5.49	B3	100	- 6	-10.9±2.3	12	0.8	- 3	5.0	3	-1.8	Two-spectrum binary, ϵ Pers.
12	11415	2289	3.44	B5	98	+ 2	- 8.4±0.5	13	1.0	- 8.1	5.6	10	-1.5	
13	16582	3192	4.04	B2	139	-52	- 8.4±0.5	13	1.0	+13.0	4.7	4	-2.1	
14	16908	3273	4.58	B3	120	-28	+ 6.0±1.9	10	0.9	+19	5.9	4	-1.4	γ Cass.
15	20336	3947	4.76	B2	106	+ 7	+13.5±1.8	10	0.9	+20	4.6	4	-2.2	
16	20756	4007	5.17	B5	132	-28	+12.4±1.6	12	0.9	+14	7.1	6	-0.9	
17	21803	4217	6.33	B2	118	- 9	+ 2.4±1.5	10	0.9	+ 3.7	4.1	4	-2.6	Two-spectrum binary, ϵ Pers.
18	23466	4505	5.36	B3	149	-36	+16.3±2.5	14	0.8	+13	6.6	3	-1.0	
19	23793	4568	5.03	B4	145	-32	+14.5±1.0	25	1.0	+18.9	7.2	2	-0.8	
20	24760	4759	2.06	B1	124	-10	+ 2.2±2.1	15	0.9	- 1	3.6	10	-3.0	Two-spectrum binary, ϵ Pers.
21	25340	4828	5.25	B6	160	-36	+19.5±1.7	12	0.9	+16	7.7	3	-0.8	
22	25558	4870	5.33	B3	153	-32	+ 9.6±1.1	13	1.0	+12.1	7.0	3	-0.9	
23	25940	4967	4.03	B3	122	- 2	- 1.2±2.6	11	0.8	+ 3.0	4.3	3	-2.4	Spect. Binary, range 26 km/sec.
24	26912	5134	4.32	B3	152	-28	-14.9±2.2	8	0.8	+18.2	5.5	3	-1.5	
25	27192	5207	5.54	B2	120	+ 1	-15.8±2.0	10	0.9	-18	4.0	3	-2.7	
26	29763	5716	4.33	B3	144	-13	-15.8±2.0	10	0.9	+14.6	7.7	4	-0.6	Spect. Binary, range 71 km/sec.
27	30211	5796	4.18	B5	168	-28	+10.5±2.1	10	0.9	+ 7	5.8	3	-1.5	
28	32630	6226	3.28	B5	133	+ 2	+ 6.7±1.5	9	0.9	+ 7.4	7.0	3	-0.9	
29	32990	6267	5.50	B3	147	- 8	+15.2±0.7	36	1.0	+16.2	4.7	2	-2.1	Spect. Binary, range 63 km/sec.
30	32991	6263	5.95	B3	150	-10	+20.4±2.7	13	0.8	+25	4.1	3	-2.6	
31	34233	6478	6.23	B4	120	+12	+ 6.7±5.1	12	0.5	- 3	7.3	3	-0.8	
32	34759	6556	5.12	B4	134	+ 4	+21.1±4.9	9	0.4	+ 5	7.8	3	-0.7	Spect. Binary, range 55 km/sec.
33	35671	6714	5.31	B4	155	- 8	+16.4±2.3	12	0.8	+19	7.2	3	-0.9	
34	35708	6723	4.83	B3	151	- 6	+ 8.2±1.4	10	0.9	+14.4	5.7	3	-1.5	
35	36267	6813	4.32	B4	166	-14	+18.2±2.1	10	0.9	+21	7.8	3	-0.7	Spect. Binary, range 71 km/sec.
36	36819	6916	5.28	B3	151	- 4	+23.3±1.9	10	0.9	+22.6	5.8	3	-1.4	
37	37202	6985	3.00	B2p	154	- 4	+23.3±1.9	10	0.9	+24.3	3.5	10	-3.2	
38	37367	7026	6.00	B3	146	0	+19.6±2.9	14	0.8	+30	4.9	3	-2.0	Spect. Binary, range 63 km/sec.
39	37438	7047	5.00	B3	150	- 2	+ 4.6±1.3	10	0.9	+14.8	6.1	3	-1.2	
40	37711	7094	4.87	B3	158	- 6	+21.1±1.7	10	0.9	+21	6.1	3	-1.3	
41	37967	7148	6.06	B3	152	- 2	+16.4±1.8	13	0.9	+19.1	5.9	3	-1.5	Spect. Binary, range 20 km/sec.
42	38622	7249	5.20	B3	161	- 6	+31.0±1.2	13	1.0	+28.3	5.3	3	-1.7	
43	39698	7436	5.89	B2	156	- 2	+31.0±1.2	13	1.0	+ 7.2	4.7	2	-2.1	
44	41753	7772	4.40	B2	162	- 1	+19.8±1.0	47	1.0	+22.1	6.2	4	-1.2	Spect. Binary, range 20 km/sec.
45	42545	7891	4.92	B3	162	0	+12.5±2.9	12	0.8	+22	7.8	2	-0.7	
46	42560	7889	4.35	B4	164	- 1	+12.5±2.9	12	0.5	+24	6.6	2	-1.0	
47	44700	8227	6.25	B4	174	- 3	+29.6±1.5	10	0.9	+29	6.6	4	-1.0	Spect. Binary, range 20 km/sec.
48	120315	18643	1.91	B3	65	+66	-10.7±1.2	16	1.0	-10.9	5.9	3	-1.3	
49	158427	23708	2.97	B3	308	-10	-10.7±1.2	16	0.5	- 2	5.9	3	-1.3	

so that one can rely upon the homogeneity of the results and their freedom from systematic wave-length errors. There are several exceptions, however, as follows.

(a) For H.D. 5394 (γ Cass) and H.D. 10516 (ϕ Pers), giving emission spectra with very poor lines and variable velocity, it was thought best to adopt the catalogue values which are based upon long series of spectrograms.

(b) The spectroscopic binaries, H.D. 32990, 37202, 39698, 41753, and 221253 have been observed at Victoria and orbital elements have been determined. The values of V_0 so found have been adopted. The velocities of H.D. 41753 and H.D. 221253 are recent determinations and have not yet been published.

(c) The spectroscopic binary H.D. 29763 was observed at Ottawa by Parker (11). The systematic velocity, as published, has been used.

(d) Victoria observations are lacking for H.D. 16908, 42560, and 158427. Catalogue values have been adopted for these stars.

The diffuse appearance of the spectral lines makes it difficult to decide which stars are variable in velocity although it is of obvious importance to determine this when considering absolute magnitudes. Fortunately, for each star several plates were taken in rapid succession, usually on more than one occasion, and we can then estimate the average error, η , of a single observation. This represents the scatter and probable error produced by errors of measurement and guiding, and may be compared with the "external" probable error, r_0 , as deduced from the whole series of observations. When the external error is at least three times the internal error this fact was taken to indicate variability. The numerical values of $(r_0/\sqrt{n})/\eta$ are given in Table I, column sixteen, r_0 being the probable error of the mean in column eight. Where the numbers in column sixteen exceed 2.5 the star is called a binary unless a fortuitously small value of η indicated that the criterion should not be trusted.

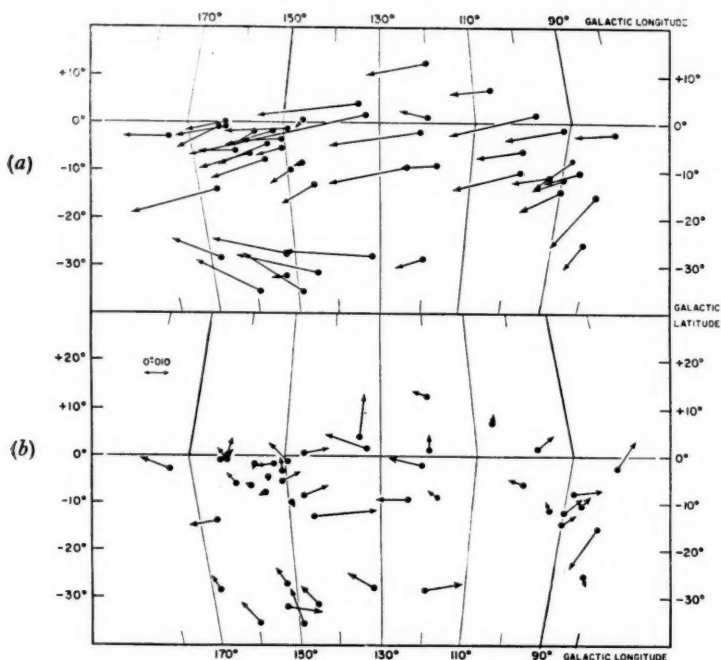
The following stars, according to this criterion, are to be regarded as variable in velocity: H.D. 1976, 30211, 32991, 34233, 37367 and 44700. In addition the binary nature of ϵ Pers (H.D. 24760) is definitely confirmed since two spectra are seen plainly upon two high-dispersion plates (11.0 Å/mm at H γ) obtained by Miss A. B. Underhill. The components are approximately equal in intensity. On the other hand our results remove from the binary category H.D. 23466, previously announced as showing two spectra. A re-examination of the early plates does not give convincing evidence of duplicity.

Among the 49 stars in Table I we thus find twelve to be variable in velocity. This high percentage agrees with the incidence of binaries among the B stars generally.

The radial velocities in Table I are, on the average, about 2 km/sec more negative than the catalogue values. Excluding binaries, the mean difference is -2.0 ± 0.5 km/sec from 18 stars in precision categories *a* and *b*, while for 14 stars in the less precise divisions *c* and *d* the mean difference is -2.4 ± 1.2 km/sec.

Two results of interest may be deduced at once from the radial velocities. If we subtract standard solar motion from the values in Table I the weighted mean residual velocity is $+1.4 \pm 0.7$ km/sec, while the average value of the residual motion, without regard to sign, is 5.6 km/sec. One may conclude that the *K*-term in a solar-motion solution will be small and, important in its implications, the peculiar motion in radial velocity does not differ materially from that for B stars generally (12).

Proper motions.—Proper motions of the stars of the Cassiopeia–Taurus group appear in a list published recently by Morgan (7). The motions are on the N30 system, and are of high accuracy, and being relatively large they lend themselves well to a determination of a convergent point. The published values were corrected for errors in the precessional constants, as recommended by Morgan, and then transformed to galactic coordinate components. The Lund tables (13) were used in making these, and other, transformations. Corrections for differential galactic rotation were computed for application to the proper motions employing numerical values $A = +0''.0040$ per year per parsec and $B = -0''.0015$ per year per parsec.



¹ *Proper motions of the Cassiopeia–Taurus stars*

FIG. 1.—Proper motions, in galactic coordinates, plotted against position on the sky. In the upper half (a) the observed motions are plotted; in the lower half (b) they are plotted after the removal of standard solar motion.

The observed proper motions, after being corrected by the relatively small effects described above, are plotted in Fig. 1 (a). They give a strong impression of common motion and this has undoubtedly suggested the idea of a moving group. The proper motions are dominated by the solar motion which overrides other effects because the stars are close to us. To demonstrate this the motions of Fig. 1 (a) have had removed from them standard solar motion and were then plotted in Fig. 1 (b). One no longer recognizes easily a community of motion among the individual stars and it appears to be questionable whether

the interpretations made by Rasmuson, Blaauw and others can be maintained. If there does not exist common space motion among the stars then the solutions for convergent point and stream motion give only the solar motion for this particular sample of stars. It follows that we can determine a mean parallax from the proper motions but not unbiased individual parallaxes and absolute magnitudes. An attempt will be made to decide for or against community of motion, apart from solar motion, after the solutions have been performed.

Spectroscopic absolute magnitudes.—The new spectrograms, being calibrated, allowed one to measure the absorption at $H\gamma$ and so to obtain spectroscopic absolute magnitudes. These data are given in columns twelve to fourteen of Table I. Three or four plates of each star were measured in order to obtain a reliable mean equivalent width at $H\gamma$; the absolute magnitudes then follow from the calibration derived by the writer (14). This calibration has recently been tested and found to be satisfactory (15). We may hence adopt the spectroscopic distances for the computation of galactic-rotation corrections to the radial velocities and for the calculation of space motions of the individual stars. Or we may, alternatively, use the observed motions as an additional test of the absolute-magnitude system.

Convergent.—The first task is to calculate the convergent point from the directions of the individual proper motions. Following Blaauw, this was done using thirty-seven stars originally considered to be members of the stream. In order to be able to make a close comparison with Blaauw's results we followed his grouping into six normal places. Solutions were made with, and without, corrections for differential galactic rotation.

TABLE II

Subgroups and representation of solutions for the convergent point

Subgroup	Number	Wt.	Coefficient		Final $\theta_0 - \theta_c$	
			of dL	of dB	Solution I	Solution II
2	9	3.8	+0.157	+1.019	+0.24	+0.62
3	2	0.9	+0.462	+0.981	-1.49	-1.87
4	4	3.1	-0.036	+1.045	+1.33	+2.18
5	6	2.6	+0.773	+1.201	-2.97	-3.93
6	8	3.5	-0.125	+1.457	+2.27	+3.64
7	8	1.5	-0.154	+1.429	+2.40	+3.82

Blaauw employed a graphical method to determine the convergent but it was decided here to adopt an objective analytical solution which gives also the formal probable errors. The method developed by Moys (16) and the writer (17) was used wherein a preliminary trial convergent is adjusted by a least-squares solution of the residuals in the position angles of the proper motions.

The analytical method works well in this particular case if we use galactic coordinates. The equation of condition transformed to this system is,

$$\sin^2 \theta \operatorname{cosec} (L-l) [\cos b \tan B \cot (L-l) - \sin b \operatorname{cosec} (L-l)] dL \\ - [\sin^2 \theta \operatorname{cosec} (L-l) \cos b \sec^2 B] dB = \theta_0 - \theta_c$$

where $\theta_0 - \theta_c$ is the residual in position angle calculated from a preliminary convergent L, B ; and l, b are the galactic coordinates of a star. In order to

minimize biasing the solution, coefficients of dL and dB were computed for each star and mean values found for the normal points instead of using trigonometric functions of the mean coordinates. Weights were assigned inversely proportional to the squares of $\delta\mu/\mu$ where μ is the total proper motion and $\delta\mu$ is the probable error in one coordinate as tabulated by Morgan (7).

Six normal places were formed from 37 stars as mentioned above. Table II gives a representation of the solution, corrections for differential galactic rotation are excluded in Solution I and applied in Solution II. Values obtained for the convergent are included in Table IV.

Stream motion and K-term.—A determination of the convergent point enables us to solve for the stream motion, and for a K -term, from the radial velocities. Here we use the well-known formula

$$\rho = K + S \cos \lambda$$

where ρ is the observed radial velocity, S is the stream motion, and λ the angular distance of the star from the convergent. Stars were grouped into six normal points as before and mean values of $\cos \lambda$ were computed for each group. Weights were applied here inversely as $\epsilon^2 + 25$, where ϵ is the probable error in the radial velocity as given in Table I and a dispersion of ± 7.5 km/sec is assumed to represent the peculiar motion in radial velocity. Table III gives the groupings and representation of the solutions made, as before, with and without galactic rotation corrections.

The numerical results from the solutions are brought together in Table IV; these may be compared with the values given by Blaauw (6) in his Table III.

TABLE III

Subgroups and representation of solutions for stream motion

Subgroup	Number	Wt.	Solution I		Solution II	
			$\overline{\cos \lambda}$	$\overline{\rho_0 - \rho_c}$ km/sec	$\overline{\cos \lambda}$	$\overline{\rho_0 - \rho_c}$ km/sec
2	9	8.2	-0.188	+0.4	-0.149	+0.2
3	2	1.8	+0.405	+0.7	+0.434	+1.9
4	4	3.0	+0.390	-2.9	+0.427	-2.4
5	6	5.4	+0.733	-2.2	+0.750	-2.2
6	8	7.3	+0.777	+0.9	+0.802	+0.6
7	8	6.8	+0.735	+1.6	+0.763	+1.4

TABLE IV

Kinematical properties

	Solution I (Corrections for galactic rotation omitted).	Solution II (Corrections for galactic rotation applied).
Longitude of convergent	194.6 ± 2.0	192.2 ± 2.9
Latitude of convergent	-10.9 ± 0.6	-10.2 ± 0.9
Right ascension of convergent	97.4 ± 1.1	97.0 ± 1.6
Declination of convergent	-17.8 ± 1.7	-15.4 ± 2.6
Stream motion	23.9 ± 1.3 km/sec	20.1 ± 1.2 km/sec
K -term	-1.2 ± 0.8 km/sec	$+0.4 \pm 0.8$ km/sec

We note first that the position of the convergent point is essentially the same whether we use Blaauw's, or Petrie's, solutions. For example, Solution I shows a difference in longitude of $6^\circ \pm 3^\circ.6$ and the latitude difference is $1^\circ \pm 0^\circ.8$. Recalling that Blaauw used a graphical method to fix the convergent while the present results come from a least-squares solution of the residuals in position angle we may conclude that the agreement is quite satisfactory and we may take it that the convergent point is close to the average of our values, i.e. $L=198^\circ$, $B=-11^\circ$ if we adopt Solution I, and at 195° , -11° if Solution II is used.

The convergent is about 15° away from the standard solar antapex with an estimated probable error of about one-fifth the difference, the departure being mostly in declination. The small sample used here and its restriction to a small area on the sky would suggest differences of the order of that found. Furthermore solar motion solutions often differ a good deal among themselves even when one uses a large number of stars scattered over most of the sky. It is concluded therefore that the convergents of Table IV do not signify a departure from random motion plus solar motion and give no strong evidence of real community of motion among the stars of this group.

Table IV shows excellent agreement with Blaauw in the stream motion but a definite discrepancy in the K -term. The difference is caused, at least in part, by the different radial-velocity material. The very large K -term found by Blaauw disposed him to reject Solution II and to conclude that the group had a motion distinctly different from the field stars. This led to the supposition that the group is expanding from an initially small volume of space with an associated "expansion age" of 50×10^6 years.

Our results do not confirm the above interpretation. The K -term is small in both solutions, not differing significantly from zero. Solution II shows almost ideal solar motion, i.e. a stream velocity of 20 km/sec and a zero K -term. There is no evidence that we have anything but a small sample of B stars with random peculiar motions.

The above conclusion is verified and illustrated in a general way by Fig. 2, where the positions and motions in the galactic plane are shown, after removal of standard solar motion. An inspection of the distribution of the stars and of their motion vectors indicates that the case for common motion is very weak. In more detail the frequency distribution of the direction of motion in the galactic plane is shown in Fig. 3. The dispersion in direction produced by observational errors in the proper motions and radial velocities is found to be $\pm 16^\circ$. A normal error curve corresponding to this value is drawn on Fig. 3. It is plain that the observed distribution given by the plotted points is much too flat to correspond to a preferred direction of the space motion. Whatever turns out to be the explanation of the observed distribution and its maximum at 200° it is definitely not a single preferred direction "smeared" by accidental error.

The distribution of the sizes of the motions in Fig. 2 is also in favour of random motion. The dispersion in velocity in one coordinate, corrected for observational error, is found to be ± 6.4 km/sec. This value is characteristic for the random motion of stars of class B.

The velocities in Fig. 2 have been analysed further to see whether they give evidence of expansion of the stars away from a region within the group, or external to it. Fig. 4 shows the ξ -velocities plotted against X and the η -velocities plotted

against Y . The X -axis points toward $l=0^\circ$ and the Y -axis toward $l=90^\circ$; ξ and η are the linear velocities parallel to the X and Y coordinates respectively. An expansion of the group would appear as a variation of ξ with X and a variation of η with Y . It is evident from Fig. 4 that the ξ and η values are not correlated with X and Y and therefore there is no expansion of the group.

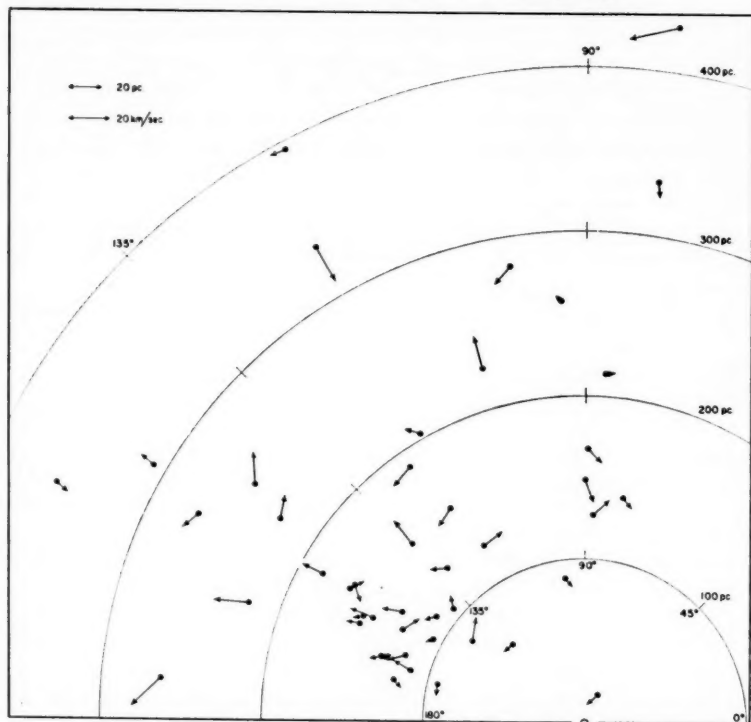


FIG. 2.—Positions and motions of the individual stars projected on to the galactic plane.

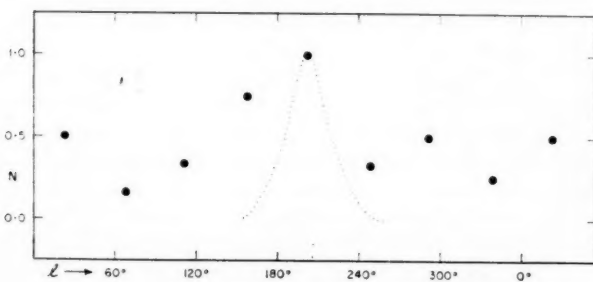


FIG. 3.—Frequency distribution of the direction of the motions.

Absolute magnitudes.—The stars studied here are valuable in testing spectroscopic absolute magnitudes because they are among the nearest of the B stars. Blaauw made use of this fact to propose a calibration of some of the Yerkes

No.
lumi
strea
para
not p
mean
case
Ther
error
lumi
only
25 p

Fi

Tal
stel
app
is t
spe
mo

wh
join
the

luminosity classes based upon the motions. He points out that the large stream motion, relative to the peculiar motions, allows one to compute individual parallaxes and absolute magnitudes. If we are dealing with a sample of stars not possessing a common space motion we can, strictly speaking, derive only the mean parallax but Blaauw's procedure is approximately correct even in that case because of the large value of the parallactic component of the proper motion. There is however a bias in the system caused by the distribution of observational error and random motion, and the reciprocal relation between parallax and luminosity. This danger was recognized by Blaauw who used in his calibration only those stars for which the proportional error in the parallax was less than 25 per cent.

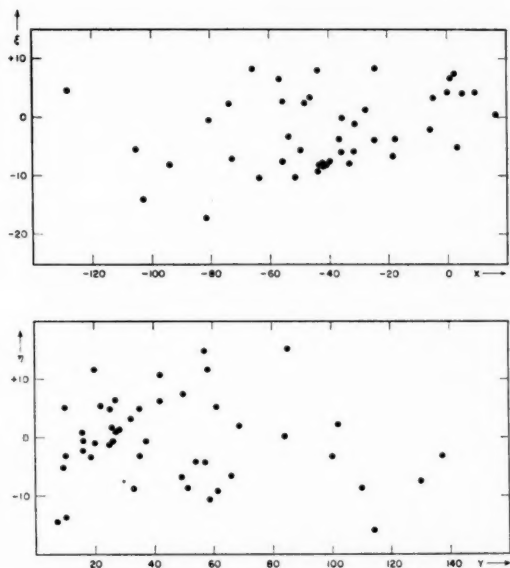


FIG. 4.—The upper plot gives the motion parallel to the X -axis plotted against X ; the lower the motion parallel to the Y -axis plotted against Y .

Spectroscopic absolute magnitudes have been measured for the stars of Table I as described above. The apparent magnitudes were freed from interstellar extinction and were corrected for duplicity either by applying the correction appropriate to a known Δm or by adding 0.1 mag. where the only information is that the velocity is variable. The corrected distance moduli then give the spectroscopic parallaxes which are to be compared with those derived from the motions.

The computed parallaxes follow, of course, from

$$\pi = \frac{4.74 v}{S \sin \lambda},$$

where in this case v is the component of proper motion along the great circle joining the star and convergent point, λ is the angular distance from the star to the convergent, and S is the stream velocity. Blaauw preferred the values given

by Solution I but this choice is permitted only if the group has some kind of common origin so that differential galactic rotation has not yet established itself in the observed motions.

Individual parallaxes were computed for both sets of elements given in Table IV, above, and the conventional mean parallax was computed using standard solar motion and the formula

$$\pi = \frac{4.74}{V_0} \frac{\sum v \sin \lambda}{\sum \sin^2 \lambda}.$$

The mean of the computed individual parallaxes, and the mean parallax, are compared with the mean of the spectroscopic parallaxes in Table V which lists also the mean values of the absolute magnitude differences for Solutions I and II.

TABLE V

Comparison of calculated and spectroscopic parallaxes

	Calculated parallax	Spectroscopic parallax	$\overline{M_{sp}-M_c}$
Solution I	0.0062	0.0065	+0.32 ± 0.11
Solution II	0.0076	0.0065	-0.12 ± 0.12
Mean parallax	0.0064	0.0065	+0.02 ± 0.24

There is a bias in the mean values of $M_{sp}-M_c$ calculated from Solutions I and II. Its value depends upon the size of the relative errors in the parallaxes and upon the distribution of the parallaxes themselves. The bias for an average error, ϵ , in the true parallax, π , is, with sufficient accuracy, $-1.1(\epsilon/\pi)^2$ and we may estimate the effect upon our results by estimating the average error and using the observed frequency distribution of the parallaxes. It should, perhaps, be specially noted that the range of distances for the stars is considerable, from about 20 to over 400 parsecs (see Fig. 2). The error ϵ originates largely in the errors in the proper motion and the stream motion as follows:

$$\left(\frac{\epsilon}{\pi}\right)^2 = \left(\frac{\delta v}{v}\right)^2 + \left(\frac{\delta S}{S}\right)^2.$$

The value of ϵ is estimated to be $\pm 0''.0012$ and we finally arrive at a value of the bias of -0.07 mag. The corrected values are then:

Solution I, $\overline{M_{sp}-M_c} = +0.25 \pm 0.11$, Solution II, $\overline{M_{sp}-M_c} = -0.19 \pm 0.12$,

Mean parallax, $\overline{M_{sp}-M_c} = +0.02 \pm 0.24$.

The above estimate of the bias may be too small for it does not allow for the possible accidental occurrence of one or two large negative values of ϵ . All solutions agree essentially with the system of spectroscopic absolute magnitudes and the agreement is exact for the mean parallax solution which is the one to be preferred according to the analysis of the motions given in the preceding sections. This same confirmation of the spectroscopic parallaxes of the nearby B stars was obtained recently from proper motion studies of stars more widely distributed over the sky (15).

The absolute magnitudes found by Blaauw from the Cassiopeia-Taurus group were not corrected for the several cases of stellar duplicity. Making the necessary corrections we find the following comparison:

Class	Spect.-Blaauw	No.
B2, B3 IV	0.0 ± 0.2	7
B2 V	$+0.5 \pm 0.2$	12
B3 V	$+0.7 \pm 0.2$	15
B5 V	-0.2 ± 0.2	6

giving a mean difference of $+0.38 \pm 0.13$. This difference is practically identical with that found in Solution I of this paper as given in Table V. The absolute magnitudes derived from the Cassiopeia-Taurus stars then depend upon whether we interpret the group as possessing a community of motion or consider them as a sample of B stars of the general population.

It is believed that the mean parallax solution based upon standard solar motion, galactic rotation, and peculiar motion is the correct interpretation of the motions. Therefore we retain confidence in the Victoria system of spectroscopic absolute magnitudes recognizing that they would require a correction of about -0.2 mag. if the group should indeed be an expanding association of rather recent origin.

The writer is indebted to Mr D. H. Andrews for substantial assistance with the computations carried out during the work.

*Dominion Astrophysical Observatory,
Victoria, B.C.:*

1957, November.

References

- (1) J. C. Kapteyn, *Trans. I., Solar Union*, **3**, 215, 1910.
- (2) A. S. Eddington, *M.N.*, **71**, 43, 1910.
- (3) B. Boss, *A. J.*, **28**, 15, 1913.
- (4) N. H. Rasmuson, *Lund Medd.*, Series II, No. 26, 1921.
- (5) W. M. Smart and A. Ali, *M.N.*, **100**, 560, 1940.
- (6) A. Blaauw, *Ap. J.*, **123**, 408, 1956.
- (7) H. R. Morgan, *A. J.*, **61**, 90, 1956.
- (8) R. E. Wilson, *P. Carnegie Inst. Washington*, No. 601, 1953.
- (9) J. S. Plaskett and J. A. Pearce, *P. Dom. Ap. O.*, **5**, 1, 1930.
- (10) R. M. Petrie, *P. Dom. Ap. O.*, **9**, 297, 1953.
- (11) *Report Chief Ast. Can.*, **1**, 166, 1910.
- (12) W. M. Smart and H. E. Green, *M.N.*, **96**, 471, 1936.
- (13) *Lund Ann.*, No. 3, 1932.
- (14) R. M. Petrie, *P. Dom. Ap. O.*, **9**, 251, 1953.
- (15) R. M. Petrie and B. N. Moyls, *P. Dom. Ap. O.*, **10**, 287, 1956.
- (16) R. M. Petrie and B. N. Moyls, *M.N.*, **113**, 239, 1953; *Contr. Dom. Ap. O.*, No. 31.
- (17) R. M. Petrie, *P. Dom. Ap. O.*, **8**, 117, 1949.

SPECTROPHOTOMETRIC MEASUREMENTS OF EARLY-TYPE STARS *

IV. RESULTS FOR STARS OF TYPES O6-Bo

R. Wilson

Summary

Measures are given of the equivalent widths of thirty-five lines in the visible region of the spectra of sixteen stars of types O6-Bo. These equivalent widths are derived by integrating the unsmoothed measures of intensity between specific wave-length limits and therefore include, in addition to the main line, the effect of any blend lines. The method of blend analysis is described and blending contributions are tabulated for all lines. The subsequent discussion of the results is made for the blend-free equivalent widths.

The variation of line strength with spectral type and luminosity is investigated, incorporating the Edinburgh B1 results (references II and III) so as to embrace the range O6-B1 in spectral type. Three luminosity criteria are introduced which are relatively insensitive to temperature. This is done by forming the ratios of the strengths of spectral lines which are differently sensitive to luminosity but which are produced by the same ion. The three criteria are defined by $\text{He I } [4472 + (4144 + 4388)/2]/\text{He I } (5876 + 6678)$; $\text{He II } 4686/\text{He II } (4200 + 4542 + 5412)$ and $\text{C III } 5696/\text{C III } 4647-51$. Absolute magnitudes are derived from the strength of $\text{H}\gamma$ by using Petrie's ($\text{H}\gamma$, M_V) calibration (reference 19). This calibration is only applicable to spectral types O9 and later and curves relating the luminosity criteria in terms of absolute magnitude are derived for the later spectral subtypes. The early O stars, for which spectroscopic absolute magnitudes have not yet been derived, are of particular interest and the fit of the measures of five such stars (O6-O8) into the general scheme shown by the later subtypes, was examined. This was most conveniently done by reading off the late O star calibration curves, the absolute magnitudes corresponding to the values of the luminosity criteria (including $\text{H}\gamma$) in the early O stars. Good agreement is shown by the values of "absolute magnitude" thus obtained and is taken to mean that the four luminosity criteria are governed by one general parameter — the effective surface gravity (or electron pressure). This is correlated with absolute magnitude in the later O stars but the relation must change or disappear in the early O stars. The results are consistent with the idea that the atmospheres of the early O stars become mechanically unstable. One of the stars investigated (λ Cep) is an Of star and thus the Of and "normal" O stars can be placed into a continuous two parameter sequence.

Measures are made of the emission features due to $\text{He II } 4686$, $\text{N III } 4634-2$ and $\text{C III } 5696$, whose strengths show a strong luminosity progression. The presence of these lines in emission is the characteristic feature of Of stars, and $\text{He II } 4686$ and $\text{N III } 4634-42$ have been detected here as late as O9.5 (in the supergiant α Cam) and $\text{C III } 5696$ as late as Bo (in the supergiant ϵ Orion). In general, the profiles of the emission features seem to be composite in nature, comprising a central, relatively sharp emission line superimposed on a faint but very extensive emission band. The detection of this broad emission is believed to be new and is accomplished by means of a precise method of interpolating the continuum between regions of continuous spectrum. The extent of the emission features is of the same order as observed in Wolf-Rayet stars and probably indicates a common mechanism. An analysis of the profiles on Beal's ejection hypothesis gave ejection velocities of the order of 1500 km/sec.

* The full text of this paper appears in *Publications of the Royal Observatory, Edinburgh*, 2, No. 3, 1958.

SPECTROPHOTOMETRIC MEASUREMENTS OF EARLY-TYPE STARS *

V. RESULTS AND DISCUSSION FOR 20 STARS OF MK TYPE B2

*H. E. Butler and H. Seddon**Summary*

Measures of the equivalent widths of 69 absorption and emission lines and bands have been measured in the spectra of 20 stars of MK type B2. Every possible effort has been made to eliminate systematic errors. The methods used, which are almost entirely numerical and free from subjective estimates, are described. The results obtained are strictly comparable with those in previous papers in the series. Where appropriate, allowances for blends have been made, the methods used being described.

A quantitative measure ϕ_L , similar to that used in earlier papers in this series is derived for all 20 stars, this measure being based chiefly on the strengths of N II, O II and Si III absorption lines. Comparison with other results shows that ϕ_L is closely correlated with luminosity and that it is in some ways superior to the equivalent width of H γ as a measure of luminosity, in particular when it is applied to dwarf stars with emission characteristics. Certain luminosity-sensitive relations between the strengths of lines of neutral Helium are shown to be correlated with ϕ_L and also with the strength of the Balmer line H γ . A smooth trend towards emission with increasing luminosity is shown for H α and H β in the normal stars. At any one luminosity, mean wing profiles for H α , H β and H γ are shown to have the same profiles within the limits of experimental error. In addition to Mg II 4481 previously reported, the absorption lines of Si II and C II are found to be relatively insensitive to luminosity. Behaviour of individual lines with luminosity throughout the measured spectrum is described.

Emission phenomena in four B2 dwarfs are examined, and it is shown that when emission occurs in H α , real or incipient emission may also occur in any of He I, He II, Fe II, Mg II and C II. It is shown that N II, O II and Si III and therefore ϕ_L are not affected by emission and thus ϕ_L as an indicator of luminosity for these stars is not affected. By use of ϕ_L , an emission profile of H γ in ν Cygni is obtained. Some comparisons are made between these stars and ϕ Persei.

The stars treated here divide conveniently into four groups—supergiant, giant, dwarf and dwarf with Balmer emission. In the Atlas at the end of the paper are given mean spectra of the supergiant, dwarf and emission dwarf stars for wavelength regions 4125–4977 and 5620–6780 Å. They are presented so that comparisons can conveniently be made between supergiant and dwarf and between the two types of dwarf stars. These spectra, though of smaller resolution than might be desirable have high accuracy in intensity, the standard error of the individual plotted point being 0.5 per cent.

Measures are given of numerous interstellar lines and bands, together with a profile of the band at 4430 Å. The relationship between interstellar line absorption and distance modulus is given, and would appear to place all three stars of class Ia beyond the absorption associated with our galactic spiral arm. Although their distance moduli extend to 2600 parsecs there is no indication of the increase in absorption which might be expected in a further spiral arm. An absorption band centred on 4890 Å, similar in shape to that at 6180 Å (which was reported earlier from this Observatory), and to that at 4430 Å, has been detected. No measures of this band can be given yet.

* The full text of this paper appears in *Publications of the Royal Observatory, Edinburgh*, 2, No. 4, 1958.

КОЛИЧЕСТВЕННЫЙ АНАЛИЗ ЗВЕЗДНОГО СПЕКТРА

Лекция имени Георга Дарвина, прочитанная Альбрехтом Унсёльд

РЕЗЮМЕ ЦОДЛИННЫХ ДОКЛАДОВ, В ПЕРЕВОДЕ НА РУССКИЙ ЯЗЫК

ПОЛЗУЧЕСТЬ ГОРНЫХ ПОРОД, ТРЕНИЕ ПРИЛИВНЫХ ВОЛН И ЭЛЛИПТИЧНОСТЬ ЛУНЫ

Х. Джекффрис

Согласно закону ползучести при продолжительном, постоянном напряжении, предложенному К. Ломницем, смещение возрастает со временем согласно формуле $\log(at)$, где a постоянная. Обнаружено, что это правило не покрывает одновременно резкость сейсмических импульсов, ни затухания при изменении широты, но что последние могут быть учтены законом, в котором ползучесть возрастает в зависимости от времени согласно формуле $t^{0.17}$. Измененный закон свободно объясняет вращение Меркурия и спутников Земли и Марса. Он не противоречит существованию излишних эллиптичностей Луны.

КОНТУРЫ ХРОМОСФЕРНЫХ ЛИНИЙ $H\alpha$ И D_3 , ПОЛУЧЕННЫЕ ПРИ ПОМОЩИ ИНТЕРФЕРОМЕТРИЧЕСКИХ НАБЛЮДЕНИЙ

С. В. М. Клюб

Пять снимков хромосферных линий D_3 и $H\alpha$, находящихся в виде групп интерференционных полос, анализируются методом Трэнора (16). Этот анализ указывает на то, что для низших 3000 км хромосферы контур D_3 не изменяется систематически с высотой (при нормированных интенсивностях), а ширина контура $H\alpha$ убывает от 1,15 Å при 200 км до 0,795 Å при 3200 км. Поэтому делается вывод, что расширение линии $H\alpha$ происходит частично за счет самопоглощения и описывается метод устранения влияния этого эффекта. Предполагая, что эмиссия $H\alpha$ и D_3 обусловлена в значительной степени одними и теми же зонами хромосферы, делается вывод, сравнивая получающиеся Доплеровские контуры гелия и водорода, что величина турбулентной скорости около 16 км/сек. и, несмотря на то, что температуру нельзя определить точно, она вероятно выше температуры фотосферы.

ФОТОГРАФИЧЕСКОЕ ОПРЕДЕЛЕНИЕ ЗВЕЗДНЫХ ПАРАЛЛАКСОВ КАПШТАДТСКОЙ ОБСЕРВАТОРИЕЙ

Дж. Б. Г. Тэрнер

Даны определенные впервые, относительные параллаксы 18ти звезд, в том числе 11ти не рассматривавшихся прежде в Капштадте, а также собственные, относительные движения в склонении 40ми звезд. Данные касающиеся относительных параллакс и собственных движений этих последних, в своем прямом восхождении, были опубликованы прежде.

МОДЕЛИ ЗВЕЗД ГЛАВНОЙ ПОСЛЕДОВАТЕЛЬНОСТИ

Джойс М. Блэклер

Рассчитаны модели однородных звезд главной последовательности методом Хэзелтрова и Хойля (1), с содержанием водорода от 76 % до 99 % по массе. Рассмотрены также ранние стадии эволюции моделей с исходным содержанием водорода в 85 %, а в заключение, модель Солнца с исходным содержанием водорода в 76,2 %.

О РАСПРЕДЕЛЕНИИ СКОРОСТЕЙ 743 ЗВЕЗД РАСПОЛОЖЕННЫХ НА РАССТОЯНИЯХ ДО 20 ПАРСЕК ОТ СОЛНЦА

Р. ф. д. Р. Вулл

Скорости 743 звезд из каталога Глизе (Gliese), расположенных на расстояниях до 20 парсек от Солнца, проанализированы с различных точек зрения. Среднее движение этих звезд по отношению к Солнцу оказалось равным: $u_0 = +11$ км/сек (в направлении на центр Галактики), $v_0 = -17$ км/сек (в направлении тангенциальном к центру Галактики) и $w_0 = -7$ км/сек (в направлении перпендикулярном к галактической плоскости; к северу от нее). Это соответствует скорости 21,4 км/сек в направлении противоположном AR 18h 13m, склонение $= +30^\circ, 5$. Средние скорости по v в координате показывают слабую корреляцию со спектральным типом. Для спектральных типов М и К средняя тангенциальная скорость больше, чем это следовало бы при случайном отборе наблюдательного материала. Распределение тангенциальных скоростей весьма далеко от Гауссова, что указывает на селекцию наблюдательного материала, для звезд данных типов, по большим собственным движениям. Исследуемые звезды были сгруппированы по эксцентриситетам их галактических орбит. Для групп звезд с малыми эксцентриситетами вертекс эллипсоида скоростей не отличается от направления на галактический центр. Величина $(B-A)/A$, образованная из постоянных Оорта A и B , оказалась равной 3,1. Дисперсия скоростей перпендикулярных к галактической плоскости показывает ясную корреляцию с эксцентриситетами галактических орбит (большим дисперсиям соответствуют большие эксцентриситеты). Дисперсия в $(w-w_0)$ остается постоянной если группировать звезды по их массам, что означает полное отсутствие равномерного распределения энергии.

ДИАГРАММЫ ЦВЕТ-СВЕТИМОСТЬ ДЛЯ БЛИЗКИХ К СОЛНЦУ ЗВЕЗД

Р. ф. д. Р. Вулл и О. Дж. Эгген

Диаграммы цвет-светимость были построены для звезд взятых из каталога Глизе (Gliese), расположенных на расстояниях до 20 парсек от Солнца и имеющих по крайней мере два независимых определения тригонометрического параллакса. Звезды были классифицированы согласно степени их приближения к галактическому центру. Оказалось что имеет место правильная зависимость между этой характеристикой и характером диаграммы цвет-светимость. Звезды класса А—с примерно круговыми галактическими орбитами образуют сравнительно «молодую» диаграмму цвет-светимости, как у Плеяд. Звезды крайнего класса Е+, орбиты звезд которого глубоко проникают в сторону галактического центра, образуют диаграмму аналогичную «очень старому» скоплению М 67.

ГРУППЫ ЗВЕЗД. I. ГИАДЫ И ГРУППА СИРИУСА

О. Дж. Эгген

Точные, собственные движения звезд, зарегистрированных в каталоге FK3, и наблюдаемые радиальные скорости, были применены для определения существования растянутой группы Гиад. Рассмотрены также ближайшие звезды, могущие принадлежать этой группе. Диаграмма цвета-светимости этой группы подобна диаграммам двух составляющих ее скоплений: Гиад и Ясел, за исключением некоторых отдельных звезд, находящихся в группе, большей светимости, чем звезды в самих скоплениях. В добавок, 67 звезд, так называемой группы Сириуса, движение которых в пространстве представляется подобным движению Сириуса, дают место диаграмме цвета-светимости, указывающей, базируясь на современные теории эволюции звезд, на то, что эта группа вероятно моложе группы Гиад.

ПЕРЕСМОТР ДВИЖЕНИЙ В ПРОСТРАНСТВЕ И СВЕТИМОСТЕЙ ЗВЕЗД
ГРУППЫ КАССИОПЕИ-ТЕЛЬЦА НА ОСНОВАНИИ
НОВЫХ ВЕЛИЧИН РАДИАЛЬНЫХ СОСТАВЛЯЮЩИХ СКОРОСТЕЙ ЗВЕЗД.

Р. М. Петри

Даны результаты исследования движений 49 звезд, составляющих группу Кассиопеи-Тельца. Получены новые величины радиальных составляющих скоростей 40 звезд по 668 спектрограммам. Оказывается, что семь звезд обладают переменными радиальными скоростями. Новые скорости в среднем на 2 км/сек более отрицательны, чем величины внесенные в каталоги. Измерены абсолютные спектроскопические величины 46 звезд.

При помощи собственных движений найдена вершина сходимости группы, после чего определены, при помощи радиальных скоростей, движение потока и термин K . Наблюдаемые движения поправляются, учитывая дифференциальное вращение галактики. Без этой поправки вершина сходимости определяется: $A=97^\circ$, $D=-18^\circ$, скорость потока $S=23,9$ км/сек, а термин $K=-1,2$ км/сек. С поправкой: $A=97^\circ$, $D=-15^\circ$, $S=20,1$ км/сек, $K=+0,4$ км/сек.

Делается вывод, что эти звезды являются образцом вселенной, в том смысле, что их движения состоят из нормального солнечного движения и своего среднего произвольного движения. Этот вывод закрепляется общим образом графиками, на которые нанесены движения в пространстве, исключив нормальное солнечное движение. Кроме того, движения не свидетельствуют о расширении зоны расположения этих звезд.

Средний параллакс выводится из предположения, что нормальное солнечное движение точно согласуется со средним движением по спектроскопическим параллаксам отдельных звезд.